2014

Structural Health Monitoring Using Novel Sensing Technologies And Data Analysis Methods

Seyedmasoud Malekzadeh
University of Central Florida

STRUCTURAL HEALTH MONITORING USING NOVEL SENSING TECHNOLOGIES AND DATA ANALYSIS METHODS

by

MASOUD MALEKZADEH
B.S. University of Tabriz, 2006
M.Sc. Amirkabir University of Technology, 2009

A dissertation submitted in partial fulfillment of the requirements
for the degree of Doctor of Philosophy
in the Department of Civil, Environmental and Construction Engineering
in the College of Engineering and Computer Science
at the University of Central Florida
Orlando, Florida

Spring Term
2014

Major Professor: F. Necati Catbas

ABSTRACT

The main objective of this research is to explore, investigate and develop the new data analysis techniques along with novel sensing technologies for structural health monitoring applications. The study has three main parts. First, a systematic comparative evaluation of some of the most common and promising methods is carried out along with a combined method proposed in this study for mitigating drawbacks of some of the techniques. Secondly, non-parametric methods are evaluated on a real life movable bridge. Finally, a hybrid approach for non-parametric and parametric method is proposed and demonstrated for more in depth understanding of the structural performance.

In view of that, it is shown in the literature that four efficient non-parametric algorithms including, Cross Correlation Analysis (CCA), Robust Regression Analysis (RRA), Moving Cross Correlation Analysis (MCCA) and Moving Principal Component Analysis (MPCA) have shown promise with respect to the conducted numerical studies. As a result, these methods are selected for further systematic and comparative evaluation using experimental data. A comprehensive experimental test is designed utilizing Fiber Bragg Grating (FBG) sensors simulating some of the most critical and common damage scenarios on a unique experimental structure in the laboratory. Subsequently the SHM data, that is generated and collected under different damage scenarios, are employed for comparative study of the selected techniques based on critical criteria such as detectability, time to detection, effect of noise, computational time and size of the window. The observations indicate that while MPCA has the best detectability, it does not perform very reliable results in terms of time to detection. As a result, a machine-learning based algorithm is explored that not only reduces the associated delay with MPCA but further

improves the detectability performance. Accordingly, the MPCA and MCCA are combined to introduce an improved algorithm named MPCA-CCA. The new algorithm is evaluated through both experimental and real-life studies. It is realized that while the methods identified above have failed to detect the simulated damage on a movable bridge, the MPCA-CCA algorithm successfully identified the induced damage.

An investigative study for automated data processing method is developed using non-parametric data analysis methods for real-time condition maintenance monitoring of critical mechanical components of a movable bridge. A maintenance condition index is defined for identifying and tracking the critical maintenance issues. The efficiency of the maintenance condition index is then investigated and demonstrated against some of the corresponding maintenance problems that have been visually and independently identified for the bridge.

Finally, a hybrid data interpretation framework is designed taking advantage of the benefits of both parametric and non-parametric approaches and mitigating their shortcomings. The proposed approach can then be employed not only to detect the damage but also to assess the identified abnormal behavior. This approach is also employed for optimized sensor number and locations on the structure.

To My Family

ACKNOWLEDGMENTS

First and foremost, I would like to express my thanks and my deepest gratitude to Dr. F. Necati Çatbaş; for his guidance as well as his friendship throughout this study. He has made this whole experience possible and enjoyable. None of this would have been possible without his mentorship and help.

I would also like to thank to the members of my dissertation committee, Dr. Hae-Bum Yun, Dr. George Atia, Dr. Mustafa Gul, Dr. Omer Tatari, Dr. Faissal Moslehy and Mr. Rudy Werlink for their time and feedback.

I would like to thank to the current and former members of our research team, Dr. Ricardo Zaurin, Burak Gokce, Tung Khuc and Tom Terrell for their collaboration and help. I also would like to thank my friends for their support during this study. Finally, I would like to thank Marzieh, who has been one of the biggest supports during the most difficult times of this study.

And last, but most certainly not the least, I would like to express my deepest love and gratitude to my family; I cannot thank them enough for their love and support.

TABLE OF CONTENTS

LIST of FIGURES

LIST OF TABLES

CHAPTER ONE: INTRODUCTION

1.1. Introduction

As a result of advances in sensing and information technologies, Structural Health Monitoring (SHM) is rapidly developing as a multi-disciplinary technology solution for condition assessment and performance evaluation of civil infrastructures of infrastructure systems, particularly bridges [1-2]. Several studies report that about a quarter of the bridges are either structurally deficient or functionally obsolete in the United States [3]. Accordingly, $17 billion in annual investments is required to substantially enhance current bridge conditions.

As a consequence, there is an unavoidable and continuously increasing demand for monitoring the behavior of existing structures over time [4]. SHM can be considered as a promising technology for effective and efficient management of different structures such as bridges, buildings, airplanes [5-7]. Steps for SHM implementations are summarized and illustrated in Figure 1. In comparison to all civil structures, bridges have always been classified as critical strategic lifeline structures due to serving crucial role in transportation networks.

Consequently, bridges have received a significant amount of attention in terms of condition evaluation and assessment by utilizing SHM. Pursuing this intention, a number of investigations have been designed and devoted to investigate SHM of bridge structures [8-12]. It is fairly clear, as also shown in Figure 1, that the first two stages of SHM are fundamental and critical phases in order to accomplish the predefined decision-making objectives.

The first stage, referred to as monitoring and measurement, highly relies on having a properly designed and well-distributed network of sensors to generate useful data. In other

words, the major goal of the first stage is to turn a structure into a smart and sensible structure. This mission can be achieved by employing advanced precise measurement devices including superior sensors and data acquisition systems such as optical sensors.

In particular, Fiber Bragg Grating (FBG) sensors are popular alternatives to the traditional sensors in terms of several aspects, such as spatial resolution, durability, stability and immunity to electrical noise [13-17]. FBG strain sensors hold a great deal of potential for civil structural health monitoring [18-23]. Having a well-distributed network of sensor provides the opportunity of measuring desired structural parameters over critical areas along the monitored structure; however processing this data and extracting the useful information is still a challenging step and tackled at so called signal processing stage of Figure 1.

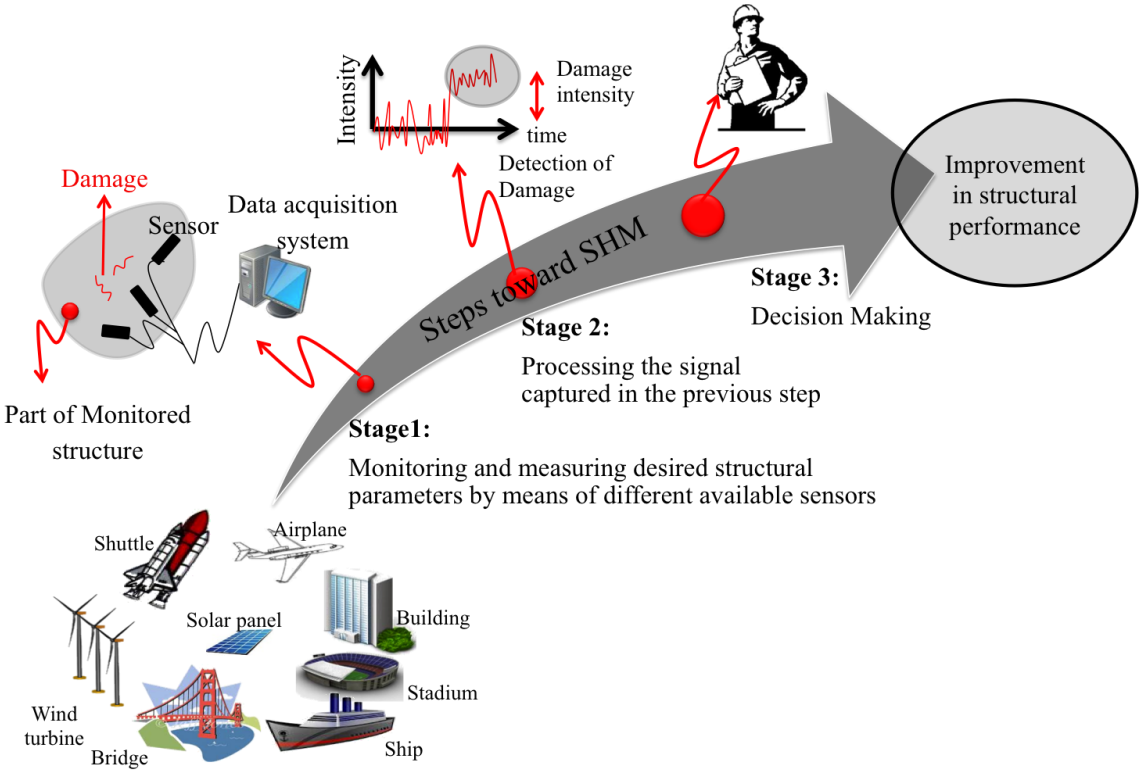

Figure 1: Simplified representation of stages involved in SHM process

Basically, the processing, analysis and interpretation within the concept of SHM fall into two main classes: parametric (also known as model-based) methods and non-parametric (also known as model-free or data-driven) methods [24].

These methodologies follow specific procedures and are applicable in distinct contexts. These interpretation methods will be preferred over each other based on desired objectives. If the objective is to provide a better physical conceptualization or developing a prediction model, then parametric methods may be better alternatives while dependency on behaviour model is the main downside associated with this type of algorithm [25-28].

Alternatively, non-parametric methods, (also called model-free approaches or data driven methods) are superior for non-parametric the circumstances in which creating a behavioral model is either time consuming or expensive, and this aspect is considered as the leading advantage of nonparametric methods over parametric ones [27-28].

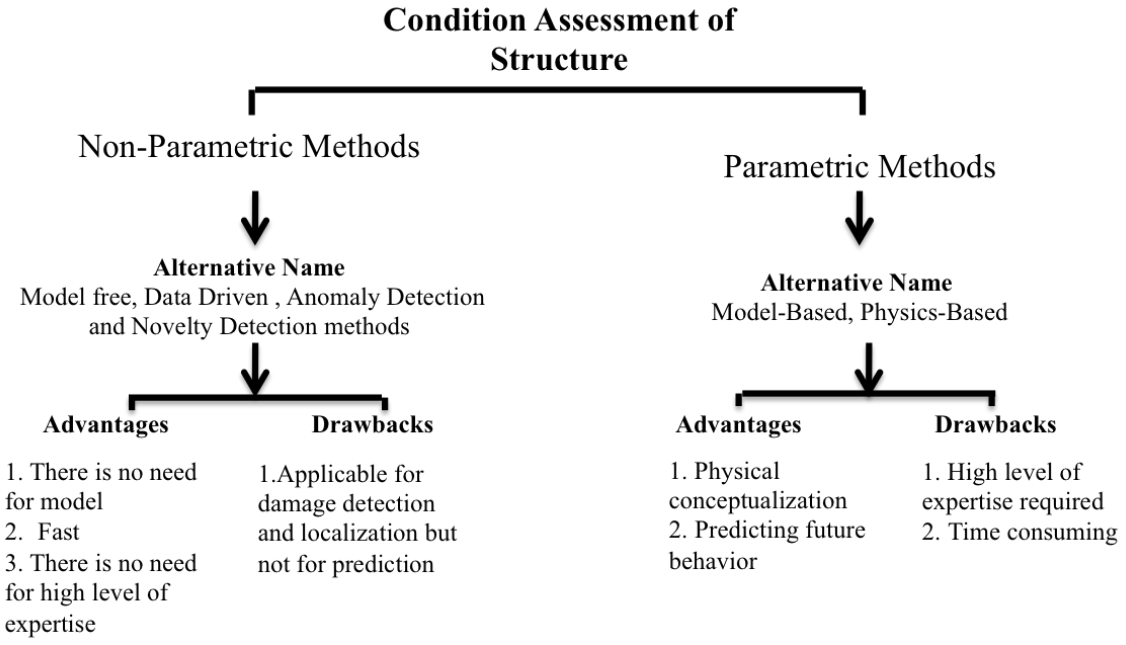

Figure 2: Comparison of parametric and nonparametric approach

Indeed, model-free approaches are free of geometrical and material information. Also, interpreting a finite element model is not needed for these methods. The main shortcoming of these approaches is that having a predictive model based on existing data driven methods is not possible. The flowchart presented in Figure 2 sheds light on the critical aspects of parametric and non-parametric damage detection algorithms.

The model based, and model free approaches are discussed separately and in more details through the following sections.

1.2. Data Interpretation Approaches

Long term monitoring of real-life structures, particularly large and complex ones, requires dealing with high dimension data sets, captured from different types of sensors. Having a large civil structure heavily instrumented with several sensors is eventually ends up with a huge amount of data that, however, has not any value without being really well interpreted. There are two distinct approaches toward an interpretation of SHM data so-called parametric and non-parametric methods.

The selection of one method over another one stands on the expected objectives from the data interpretation. The parametric is preferred in the cases that conceptualization and prediction are of the main concerns. Non-parametric techniques, on the contrary, are considered as an appropriate alternative when prediction is not a matter of interest and also developing a mathematical model of structure is either expensive or time consuming. Each of these approaches is discussed in further details throughout the following sections.

1.2.1. Parametric Data Analysis Approach

There are some responses or attributes of structure that can be measured by means of sensors such as strain, displacement, acceleration, etc. In most of the cases, however, these types of responses are not directly carrying the sort of information that can be beneficial for identifying the healthy status of structure. Instead, other responses are of interest such as load carrying, capacity, reliability index and, etc. The solution to this challenge is referred as structural identification. In fact, the parametric structural identification techniques can be viewed as translation of "raw" measured parameters into "actionable" information.

Since the 1970's, there has been a significant amount of research carried out in this field [29-46]. The identified model, or candidate models, makes the data conceptualization much more feasible. Likewise, behavioral simulation under critical operational and environmental loading condition is facilitated by taking advantage of this updated model. Furthermore, these models can be employed to explicitly diagnose the root reason of detected abnormal behavior as well as identifying the impact of such changes on the entire performance of structure.

In addition to diagnosis, prognosis of structural health as well as remaining life of structures is possible through the parametric approach. Model-based structural identification is often described in six fundamental steps [1, 30]:

- Observation and conceptualization
- A prior modeling (developing of first generation of FE model)
- Controlled experimentation
- Processing and interpolation of data
- Model correlation
- Utilization of model for simulations

Readers are referred to papers for more detail information on each step.

1.2.2. Non-Parametric Data Analysis Approach

Alternatively, non-parametric approaches are superior in the circumstances in which creating a behavioral model is either time consuming or expensive, and this aspect is considered as the leading advantage of nonparametric methods over parametric ones [27-28]. Indeed, model-free approaches are free of geometrical and material information. Also, interpreting a finite element model is not needed for these methods. Unlike parametric approaches, through the data-driven techniques, a statistical model are generated based on the signal itself, and any change can be detected explicitly by only continuously evaluating this model. Dealing with this statistical model is much more convenient and in most of the cases is preferred to a complex mechanical model. Moreover, tracking the abnormal behaviors from statistical models turns the nonparametric techniques into a well-suited approach for long term monitoring of civil structure.

It was not until early 1990s that researchers have started exploring the efficiency of nonparametric methods for system identification and subsequently SHM applications. Some of the most well-known data-driven methods are summarized as follow:

- Artificial Neural Networks (ANNs) [47-49].
- Wavelet decomposition [50-53].
- Auto-regressive moving average vector (ARMAV) models [54-56].
- State space models, and empirical mode decomposition (EMD) in conjunction with the Hilbert- Huang Transform [57-60].
- Instance based method [61].
- Correlation anomaly scores analysis [62].
- Principal Component Analysis (PCA) [63].

- Moving principal component analysis (MPCA) and robust regression analysis (RRA) [63-65].

However, the main inadequacies associated with this approach are lacking prediction capability as well as the absence of the physical conceptualization. The extensive application of data-driven techniques in SHM is somewhat negatively affected by the aforementioned deficiencies.

1.3. Local and Global Monitoring

The SHM objectives can be, generally, pursued through two distinct strategies data collection: static and dynamic monitoring. In this text, dynamic monitoring refers to identifying dynamic properties for global condition evaluation by means of input -output testing. There have been significant amount of investigations focused on vibration based structural health monitoring. A comprehensive summary of these studies can be found in the report prepared by S.W. Doebling et.al. [36]. Despite the vast amount of research being conducted in this area, the applicability of dynamic monitoring is restricted, particularly for large complex civil structure. It has been proven that, particularly in the case of complex structures, even a severe damage may result in a minor alteration of the natural frequencies [66-70].

Furthermore, the proficiency of this strategy, dynamic monitoring, is seriously threatened by the presence of noise in the data [71-73]. In other words, the occurrence of damage can be masked by presence of noise in the data [73]. Therefore, for the long-term monitoring of complex structures, which is the case for many of the civil structures, dynamic monitoring is not the most reliable approach. Alternatively, localized change or damage can be identified through

the static monitoring by comparing the predictive model, or candidate models, with the static structural responses, including strain, displacement, etc.

However, as it was discussed before, creating a model is both expensive and time consuming. In addition, regardless of time and expenses, specifically in the case of complex structures, this model may not accurately reflect the behavior of structure. Even by taking benefits of multiple model approach, there is not still any assurance, due to difficulties and uncertainties involved in the procedure, that the damage can be identified accurately. To address these issues, long term monitoring is required to produce reliable information. In fact, the roles of the models are replaced by long period of data captured from critical locations of structure. Monitoring a real-life structure for a long period of time was not practical, due to the lack of reliable and low cost sensors, only until recently.

Due to significant advances in the field of sensor technology, the main challenge in front of long-term structural health monitoring is to interpret the vast amount of data effectively, timely yielding meaningful information. By decreasing the cost of both reliable sensors and data-acquisition systems, the amount of structures that are monitored is vastly growing and this subsequently results in a great amount of measurements in different formats. Therefore, a properly developed non-parametric algorithm, which can process this vast information and extract the most informative features, is one of the most important SHM concerns.

1.4. Objective and Scope

As it was presented throughout the previous sections, despite the great amount of research devoted to the field of SHM and in particular data interpretation, still a lot more research to be

done, especially for long term monitoring of structures. There are still some difficulties against the widespread acceptance of SHM, particularly for civil structures. As it was discussed earlier, the sensing issues are not considered as very critical challenges anymore, thanks to vast improvement of sensing technologies in the past decade. However, inferring the deep meaning of massive data for long-term monitoring of large and complex civil structures is one of the most critical difficulties that the SHM is facing. The challenge of damage identification and localization for long term monitoring has been investigated recently [63-65]. To the best knowledge of the author, there are only limited comparative studies that investigate the performance of non-parametric algorithms using SHM data from both experimental and real-life studies.

Exploring and developing new data analysis techniques along with novel sensing technologies for structural health monitoring are the main objectives of this study. Therefore three parts have been designed for this study, as follow:

1) A systematic comparative evaluation of some of the most common and promising methods is carried out along with a combined method proposed in this study for mitigating drawbacks of some of the techniques.
2) Non-parametric methods are evaluated on a rea-life movable bridge using data from both structural and mechanical components.
3) A hybrid data interpretation approach is proposed and demonstrated for more in depth understanding of the structural performance.

Therefore in order to meet the objectives of this study eight chapters are designed for this dissertation. These chapters are discussed in more details throughout the following section.

1.5. Organization of the Dissertation

The organization of the dissertation as follow:

In chapter 2, sensing technologies for SHM with a special emphasis on Fiber Optic Sensing (FOS) are discussed. In addition, an in-house developed FBG system is introduced in this chapter. Different types of FOS are reviewed including FBG, BOTDA and BOTDR. An experimental bridge model is instrumented and monitored with point type FOS (FBG) as well as distributed FOS (BOTDA/BOTDR).

In chapter 3, some of the most efficient non-parametric techniques which have shown promising results, in particular with regard to civil infrastructure, are selected through an extensive literature review. The procedure and basic behind the selected algorithms including Cross Correlation Analysis (CCA), Robust Regression Analysis (RRA), Moving Cross Correlation Analysis (MCCA), and Moving Principal Component Analysis (MPCA) are discussed in detail.

Chapter 4 is designed to explore the efficiency of the selected algorithm utilizing the SHM data from a unique experimental structure named as 4-Span Bridges. Several critical and common damage scenarios are simulated on the 4-Span Bridge and the corresponding SHM data are collected using the in-house developed FBG system. The data is then implemented to test the performance of the selected algorithms.

Chapter 5 is dedicated to design and introduce a new machine-learning algorithm through which some of the associated disadvantages of existing algorithms are being covered. The newly developed algorithm (MPCA-CCA) is designed based on combining the MPCA and CCA analysis. The main objective is to reduce the corresponding delay associated with MPCA and

also further improve the detectability potential. The performance of the MPCA-CCA is evaluated using the SHM data from the laboratory study as well as the real-life SHM data from a unique structure. Moreover, the proposed algorithm is compared against some of the selected algorithms utilizing new identified critical criteria including, detectability, time to detection, computational time, effect of noise and window size (amount of required data sets for training phase).

In chapter 6, an investigative study for automated data processing method is developed using non-parametric data analysis methods for real-time condition maintenance monitoring of critical mechanical components of a movable bridge. A maintenance condition index is defined for identifying and tracking the critical maintenance issues. The efficiency of the maintenance condition index is then investigated and demonstrated against some of the corresponding maintenance problems that have been visually and independently identified for the bridge.

Chapter 7 is dedicated to develop a hybrid data interpretation framework for automated and continuous performance assessment of infrastructure. The framework is developed by integrating the parametric and non-parametric approaches. The critical damage scenarios are identified and simulated on the FEM model of a given infrastructure and the corresponding responses are predicted through Monte-Carlo simulation technique. The responses are subsequently analyzed by MPCA algorithm to extract the sensitive features. The hypothesis testing is implemented to learn to underlying distribution of performance sensitive feature under individual damage scenarios. Afterward, the supervised damage classification algorithm can be employed for processing the live-SHM data and classifying the possible abnormal behavior. The proposed algorithm can be further used to identify the optimized amounts of sensors and the corresponding locations.

Finally, Chapter 8 provides the summary and presents the conclusions after theoretical and applied studies are given in the dissertation. General comments about the methodologies described in this study are reviewed along with recommendations and possible directions for future research.

CHAPTER TWO: SENSING TECHNOLOGIES FOR SHM: EMPHASIS ON FIBER OPTIC SENSORS (FOS)

2.1. Introduction

The fundamental idea of structural health monitoring stands on the hypothesis that perturbations in a structural system can be identified from local or global monitoring. The confirmation of this hypothesis is highly dependent on the sensing technology for structural health monitoring.

However, the structural properties or responses of interest are, in most cases, impossible to be intuitively measured. Some of the responses correspond to the structural performance, such as reliability index, load carrying capacity or remaining life of the structure cannot be measured directly by means of a sensor. In order to deal with this issue, the most sensitive and relevant physical quantities to the response of interest can be identified through a preliminary sensitivity analysis. Followed by identification of these physical quantities, appropriate sensors are to be determined for the monitoring purpose.

A number of different types of sensors are used for SHM. Among all of the different technologies, Fiber Optic Sensors (FOS) have gained great attention during the recent decade. The reason is that the conventional sensors have suffered from major deficiencies including sensitivity to electrical noise, heavy cabling labor, etc. Inappropriately, noise and outliers are very common challenges in dealing with civil structures and accordingly this, in particular, sensitivity to noise, makes the implementation of conventional sensors even more restricted for civil SHM applications.

Inspired by this, an in-house developed FBG system was assembled in the UCF Structural Lab. In order to explore the development of low-cost fiber optic interrogator, use of FBGs and promising practical non-parametric methods in a comparative fashion for commonly experienced bridge problems, studies have been carried out in an integrated manner as a step towards holistic SHM implementation on highway bridges. Therefore, this chapter is devoted to shed light on the special in-house developed FBG system as well as different types of FOSs.

2.2. Fiber Optic Sensor (FOS)

The sensor technology has been dominated by electrical based sensors for decades. However, there are several features in which conventional sensors need significant improvements including sensitivity to electrical noise, heavy cabling labor, etc. Due to these deficiencies, a significant amount of effort has been devoted by researchers worldwide to the improvement of traditional sensors. Hence, these efforts resulted in a new generation of sensors, so called optical fiber technology.

The most superior aspects of optical fiber, in comparison to electrical-based sensors, are switching from electricity and copper wire to light and optical fiber, respectively. Eventually, these benefits turn the FOS into one of the most attractive sensors for SHM applications. Due to the integrated implementation of special FOS-network with non-parametric data analysis this chapter is dedicated to explore this type of sensor in more detail.

Generally, there are two individual categories of optical sensors available for distinct applications. The first category named as point type of sensor and the most famous optical sensor in this category is Fiber Bragg Grating (FBG). The distributed types of sensors are considered as

the second category, including Brillouin Optical Time Domain Analysis (BOTDA) and Brillouin Optical Time Domain Reflectometry (BOTDR) [74]. In the following sections, first a summary of optical sensors application for SHM is presented and eventually different types of FOS are discussed in more detail.

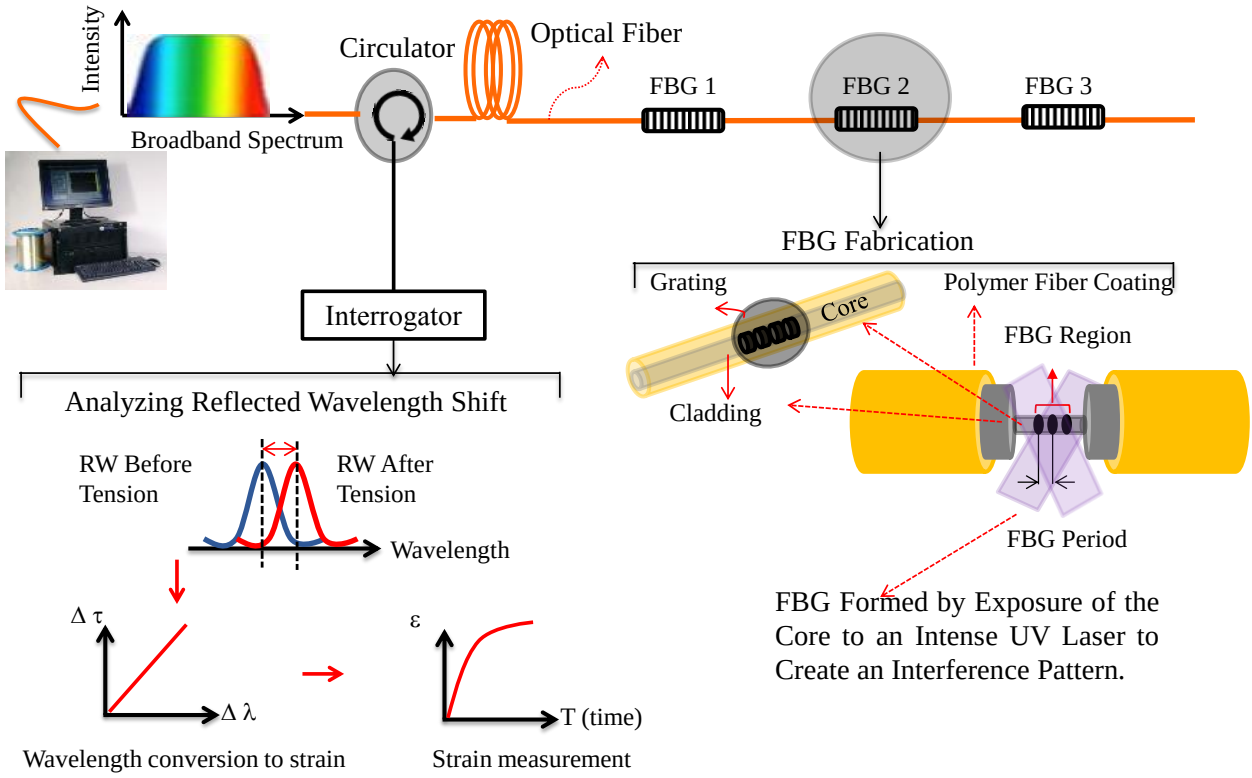

Figure 3: Measurement principal of Fiber Bragg Grating (FBG) sensor

2.3. Application of Optical Sensors in SHM Applications

Optical sensors are gaining attention particularly in the field of structural health monitoring. In this section a short summary of their applications in the SHM is presented. One the most interesting features of the FOS is that it can be embedded within the structure. Giles et.al (1999) explored the application of embedded fiber optic sensor for monitoring of composite

structures [74]. The findings confirmed that the distributed fiber optic sensors are able to monitor strain as well as impact within the structure. Seim et.al (1999) implemented the FBG strain sensors for monitoring of a historical bridge [75]. The data from the bridge was used to validate finite element models and eventually predict the performance of this historical bridge. The application of FBG for fatigue and crack monitoring is considered as another attractive implementation of FBG sensors [76].

The results show that FBG can be successfully applied for crack and delamination monitoring. Monitoring and detecting transverse cracks within FRP structures are investigated by Takeda et.al (1999) [77]. From the experiments, the authors concluded that the presence of cracks near the sensors resulted in a nonlinear reduction in the optical power transmitted. Exploring the ability of optical waveguide sensors for strain measurement up to 2000 microstrain is conducted by Gregory et al (1999) [78]. The fiber optic sensor has been also applied for composite bridge deck monitoring [79]. Kwon et al (2000) study the use of fiber optics for detecting damage in reinforced concrete beams [80]. A procedure for long term monitoring of structures using SOFO deformation sensors is proposed by LIoret and his colleague [81].

Farhad Ansari et.al (2009) investigated some of the most common issues associated with FOSs including strain transfer mechanism sensor packaging, sensor placement in construction environment, and reliability and survivability of the sensors [82]. The application of three individual FOS including: fiber Bragg grating sensor, Brillouin OTDR(optical time domain reflectometry) and Raman OTDR in structural health monitoring has been explored by Dr.Il Bum Kwon et al (2012) [83]. The SOFO system is a fiber optic measurement system based on low coherence interferometry. It was introduced by SMARTEC and is widely used for structural health monitoring. Important issues like temperature insensitivity and long- term stability of

SOFO system is investigated and it is shown that SOFO has reliable measurement system for long-term applications [84].

These are just a few selected applications of optical fiber sensors in the field of SHM. In the following sections more details are presented in term of sensing mechanism and principal of optical sensors.

2.3.1. In-house Developed FBG System

The basic working principle of FOS and FBG sensors is reflection and filtration of different wavelengths of light; this concept is presented in Figure 4. A conventional FBG sensor system is composed of a broadband light source, FBGs, a wavelength interrogator, and system software, as shown in Figure 3. When broadband light is launched into an FBG, the reflection occurs at the FBG. Some light, of which wavelength satisfies Bragg condition of Equation (1), is reflected, and the others passes the grating.

$$\lambda_B = 2n_e\Lambda \quad (1)$$

Where λ_B is the Bragg wavelength, n_e is the effective refractive index, and Λ is the grating period. When strain is induced in an FBG, the Bragg wavelength is expected to have a proportional shift. The strain can be easily determined by analyzing the change of the wavelength. According to this principle, FBG sensors can sense the grating period change due to strain variation, and they can measure strain without the influence from noise and light intensity perturbation.

The wavelength shift is proportional to strain, and absolute strain can be measured.

$$\frac{\Delta\lambda_B}{\lambda_B} = \{1 - \frac{{n_e}^2}{2}[\rho_{12} - \upsilon(\rho_{11} + \rho_{12})]\}\varepsilon \quad (2)$$

Where ρ_{ij} are the silica photo-elastic tensor components and υ is the Poisson's ratio.

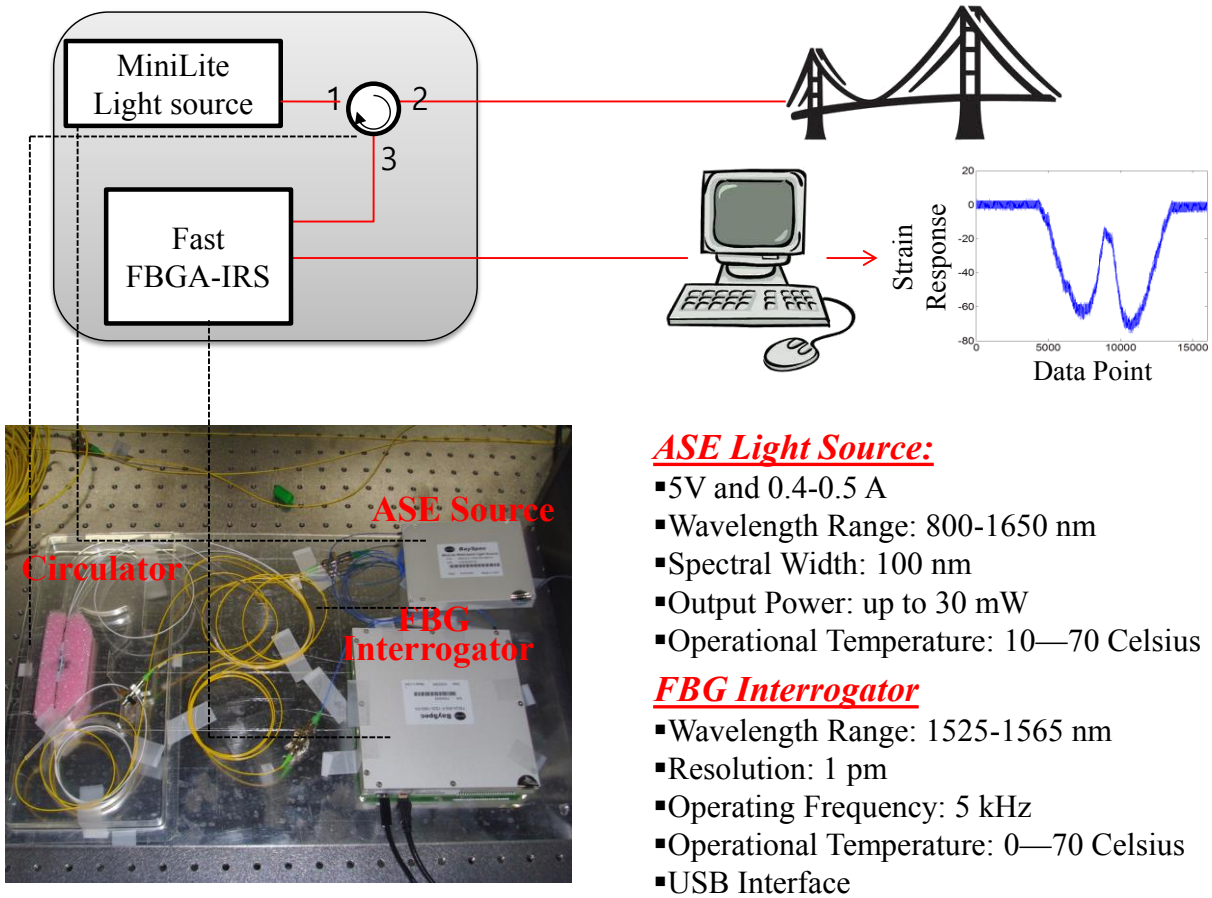

Figure 4: In-house developed FBG system

In order to construct an FBG sensor system, three major elements are needed:

1) The power source which has to have a voltage about 5V and 0.4-0.5 A to insure the optical light source is working fine.

2) A minilite light source (ASE source) which has a wavelength range of 800-1650 nm, spectral width of 100 nm, output power: up to 30 mW and it is operating temperature between 10-70 oC (50-158 oF).
3) The most important part, the FBG interrogator has a wavelength range of 1525-1565 nm, resolution about 1 pm, operating frequency around 5 kHz and interface with USB 2.0 and it requires the operating temperature between 0-70 oC (32-158 oF) and the last one is the circulator, which is to making sure the reflected wavelength is going back to the FBG interrogator and the interrogator is going to send the data directly to the computer to do analysis, The system picture and components are shown in Figure 4.

2.4. Methods for Bragg Grating

The structure of the FBG can vary as a consequence of modification of grating period or refractive index. Based on these modifications and subsequently various types of FBG structures, multiple types of Bragg Grating exist. Since detailed information about various methods of Bragg grating is beyond the scope of this report, only the titles of these methods are presented here **[**21**]**.

1) Uniform Fiber Bragg Grating
2) Chirped Fiber Bragg Grating
3) Tilted Fiber Bragg Grating
4) Superstructure Fiber Bragg Grating

The above addressed types of Bragg Grating consequently result in different fiber optic structures as shown in Figure 5.

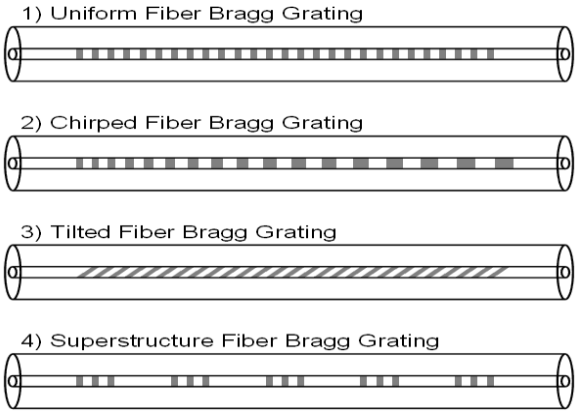

Figure 5: Structure of Fiber in different Bragg Grating [21]

2.5. Distributed Fiber Optic Sensor

The Brilliouin Optical Time Domain Reflectometry (BOTDR) and Brillouin Optical Time Domain Analysis (BOTDA) are two distinct optical fiber systems with which strain and temperature can be measured along an arbitrary location of fiber. In fact, these types of distributed optical sensors can be considered as significant development in sensing technology. There is a perfect analogy between human nerve system and distributed fiber-optic sensors.

The human nerve system, functions as a sensing network of the body structure while optical distributed sensors are serving as a nerve system for a structure. Having the ability to sense strain or temperature at any arbitrary location along the fiber makes these sensors one of the most attractive alternatives to the traditional sensors. The following sections are dedicated to shed some light on the principal mechanism of these advanced systems.

2.5.1. Measurement Principal of Optical Time Domain Reflectometry (BOTDR)

The principal measurement of BOTDR stands on the interaction between light waves that are launched from light source through the fiber line and acoustic phonons. As a consequence of this interaction, Brillouin scattered is generated and broadcasts in the reverse direction of the original light waves. The Brillouin frequency is sensitive to any applied external load, including strain and temperature. Therefore, the strain and temperature variation can be calculated by monitoring any shift in Brillouin frequency. In other words, any shift in Brillouin frequency (ν_B) is in proportion to the strain caused either by external load or temperature variation and this can be computed by the following Equation:

$$\nu_B(\varepsilon) = \nu_B(0) + \frac{d\nu_B(\varepsilon)}{d_\varepsilon}\varepsilon \quad (3)$$

Where the coefficient $\frac{d\nu_B(\varepsilon)}{d_\varepsilon}$ is approximately given by:

$$\frac{d\nu_B(\varepsilon)}{d_\varepsilon} = 0.5\ GHZ\ (\%Strain) \quad (4)$$

The distance (Z) between the location of system (light source) and the position that induced strain has taken place can be identified through the following Equation:

$$Z = \frac{cT}{2n} \quad (5)$$

Where C is light velocity in a vacuum and n is the refractive index for optical fiber. Figure 6 exhibits the measurement principle of BOTDR.

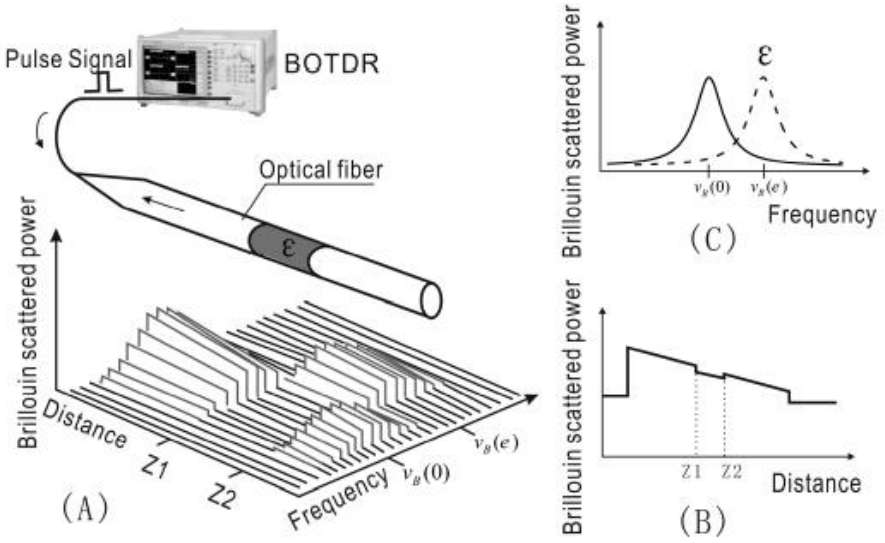

Figure 6: BODTR measurement principle [74]

2.5.2. Measurement principle of Optical Time Domain Analysis (BOTDA)

The BOTDA out-performs the BOTDR system in terms of spatial resolution. In fact, BOTDA was developed to compensate for spatial resolution issue corresponded to BOTDR system. Unlike BOTDR system, which is functioning with only one laser source, the BOTDA requires two individual laser sources: a pulse laser (pump laser) source and a continuous laser source. The functionality of BOTDA is established on the idea of stimulating the Brillouin back scattering. Basically, the intention of having two distinct laser sources is to stimulate Brillouin back scattering. When the frequency difference between the two lasers is equal the Brillouin frequency shift, the back Brillouin is stimulated. The Brillouin frequency shift, similar to BOTDR, is derived from this Equation:

$$\nu_B(T, \varepsilon) = C_\varepsilon \varepsilon + C_T T \quad (6)$$

Where C_ε and C_T are the strain and temperature coefficients, respectively.

2.6. Concluding Remarks

The in-house developed FBG system is utilized to collect the data from an experimental structure known as UCF 4-Span Bridge. The collected data by means FOSs (both FBG and BOTDA) are used to integrate the implementation of FOSs and non-parametric methods. Different damage scenarios are simulated on the UCF 4-Span Bridge and the generated data are captured with 12 individual FBG sensors as well as BOTDA system. Consequently the data are fed into the selective non-parametric algorithms to explore the efficiency of both in-house FBG and also non-parametric methods. The results will be discussed in more details in Chapters 3 and 4.

CHAPTER THREE: REVIEW OF SOME NON-PARAMETRIC TECHNIQUES

3.1. Introduction

Long term monitoring of real-life structures, particularly large and complex ones, requires dealing with high dimension data sets, captured from different types of sensors. Having a large civil structure heavily instrumented with several sensors eventually ends up with a huge amount of data which should be well interpreted and utilized in timely manner. There are mainly two distinct approaches toward an interpretation of SHM data parametric and non-parametric methods.

The selection of one approach over another one stands on the expected objectives from data interpretation. There are recognized hierarchy levels for change/damage detection procedure that can be divided into following steps [85]:

Level 1. (Detection.) The damage detection algorithm should be capable of timely raising the alarm after any damage taken place.

Level 2. (Localization.) The location of the damage is informed by the algorithm.

Level 3. (Assessment.) The information is provided about the severity and extension of the occurred damage.

Level 4. (Prediction.) The information is provided about the future performance of structure, e.g. estimation of remaining life.

Although there are some major deficiencies associated with the parametric approach for data interpretation, all the damage detection levels are achievable. However, due to some issues,

such as time, expense, level of expertise, etc., it may not be the perfect solution to data interpretation or damage identification of structure. The dependency on the physical model can be avoided by taking advantage of non-parametric techniques. The non-parametric techniques generally fall into two main categories: supervised and unsupervised learning. The former requires having some knowledge of damage conditions so that the algorithm can be trained. This feature makes this type of algorithm less effective for at least civil structure applications due to the fact that having access to experimental data from a damaged structure in most of the cases is almost impossible.

The latter, unsupervised, can be implemented to the data not containing example from the damage structure. In fact, the unsupervised learning algorithms develop a baseline structure upon the training data and consequently, any significant deviation from that baseline is considered as abnormal behavior. However, this approach has some inherent limitations that make its application restricted as well. Basically, the applications of unsupervised based data driven technique are restricted to level 1 (detection) and in some cases level 2 (localization).

There are several strategies proposed by different researchers as data-driven techniques for damage identification. These methods can be summarized as follows:

1) Auto-regressive methods [55-57].
2) Fourier analyses [87].
3) Wavelet methods [51-56].
4) Robust regression [63-65].
5) Correlation analysis [62][88].
6) Instance-based methods [61][89].

7) Moving principal component analysis [62-64].

However, in the field of localized long term monitoring, the problem of damage detection and localization has more recently been faced than global monitoring [62-64]. A comparative study, including the existing algorithms indicates that moving correlation analysis (MCCA); moving principal components analysis (MPCA) and robust regression analysis (RRA) have the greatest deal of potential in compare to other techniques.

For that reason, this chapter is started with a brief outline of CCA, MCCA, MPCA and RRA. Finally, this chapter will be concluded with a summary of a comparison between these techniques.

3.2. Selective Data-Driven Techniques

3.2.1. Cross Correlation Analysis (CCA)

One of the most preliminary objectives followed by SHM is timely detection and localization of any possible anomaly behavior and subsequently making appropriate decision in order to mitigate any potential detrimental effect on the structure. For that reason, properly developed change/damage detection algorithms should be designed and employed along sensor network. Herein, Cross Correlation Analysis (CCA) is presented and evaluated with the FBG data.

The methodology is based on comparing the correlation matrices for the baseline and damaged cases. The cross correlation coefficients of the strain data at one location and all other locations are calculated to create a row of the cross-correlation matrix. Then, the same procedure is repeated for all of the sensors and a full cross-correlation coefficient matrix is created. After

obtaining these matrices for baseline and damaged conditions, they are compared to detect and locate the damage. When comparing two signal pairs, the correlation can be obtained using the following formula:

$$\rho_{ij}(t) = \frac{\sum_{k=1}^{n}(S_i(t_k)-\mu_i)(S_j(t_k)-\mu_j)}{\sqrt{\sum_{k=1}^{n}(S_i(t_k)-\mu_i)^2}\sqrt{\sum_{k}^{n}(S_j(t_k)-\mu_j)^2}} \quad (7)$$

Where ρ_{ij} is the correlation between the sensors *i* and *j*, n is the total number of time observations during the monitoring duration, $S_i(t_k)$ and $S_j(t_k)$ are the values of the sensors *i* and *j* at time t_k, and, μ_i, μ_j are the mean values of the sensors *i* and *j*.

Baseline correlation matrices are generated based on the data captured from undamaged structure. For each baseline data set, a baseline correlation matrix, which consists of the correlation of individual pairs of sensors, is generated. Baseline correlation matrix is an *n*x*n* matrix where *n* refers to number of sensors existing on monitored structure. Each row (or column) in the matrix is presenting the correlation of a sensor with the rest of sensors. Creating the baseline matrix, the state of structure prior to damage occurrence is characterized.

The same steps should be taken for data sets measured from damaged (or unknown state) structure to obtain the new matrices. Afterwards, these two sets of matrices are compared in order to obtain damage location matrices (Equation 8). Steps toward CCA are presented in Figure 7.

Damage Location Matrix = (*Damaged Matrix*)-(*Baseline Matrix*) (8)

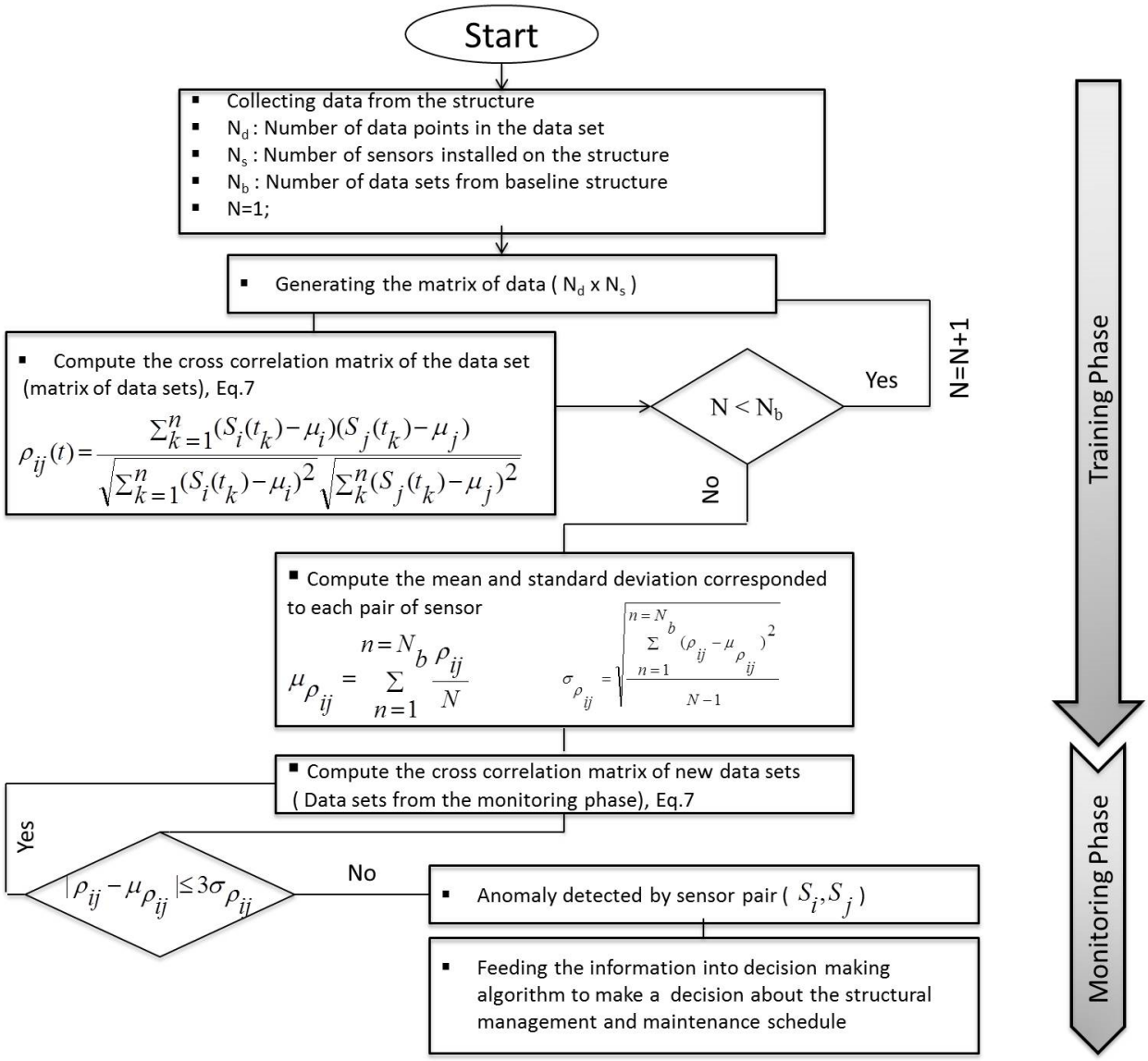

Figure 7: Sequential steps for detection algorithm based on Cross Correlation Analysis (CCA)

3.2.2. Robust Regression Analysis (RRA)

In order to mitigate some of the drawbacks associated with traditional regression methods, robust regression method has been utilized [90-91]. Traditional regression methods are based on least square estimation and sensitive to their underlying assumption such as a normal distribution of errors in the observed responses. On the other hand, robust regression works by

assigning a weight to each data point. Weighting is done automatically and iteratively using a process called iteratively reweighted least squares. In the first iteration, each point is assigned equal weight and model coefficients are estimated using ordinary least squares. At subsequent iterations, weights are recomputed so that points farther from model predictions in the previous iteration are given lower weight.

Model coefficients are then recomputed using weighted least squares. The process continues until the values of the coefficient estimates converge within a specified tolerance. As a result these methods are highly non-robust to outliers. Application of RRA for damage detection is discussed in the next section.

RRA damage detection algorithm consists of two main steps, preliminary correlation analysis and robust regression analysis. A matrix of data should be generated by inserting the time history of data from each sensor into individual columns. Once the matrix is created, it should be divided into two segments, called training and monitoring phases. The training phase is intended for developing a baseline, confidence interval, based on normal condition, while monitoring phase is set for long term monitoring.

A correlation analysis is performed for training phase in order to find sensor pairs with high correlation.

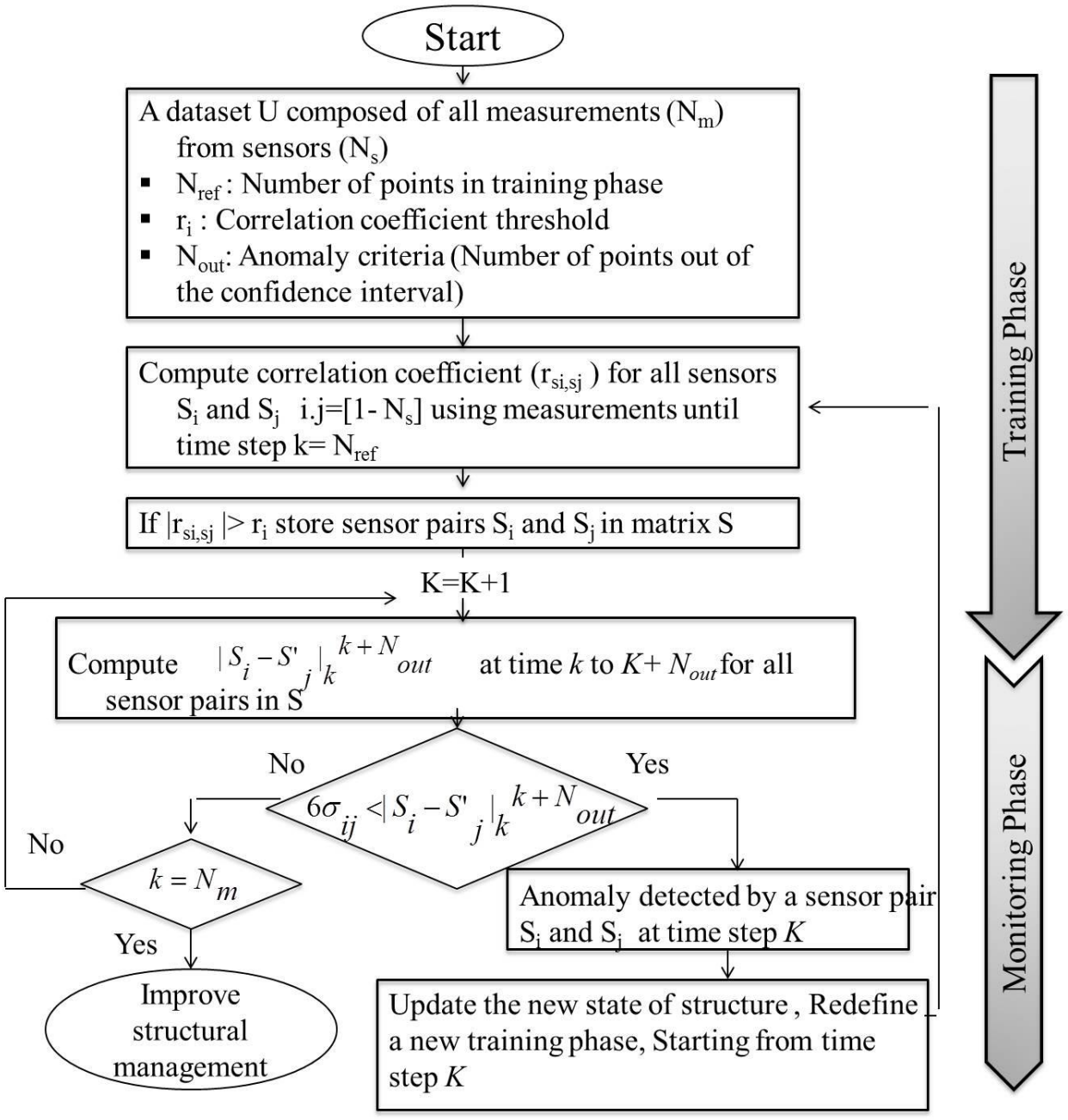

Figure 8: Sequential steps for detection algorithm based on Robust Regression Analysis (RRA)

After conducting the correlation analysis in the training phase, sensor pairs should be stored in a new matrix called matrix of highly correlated sesnors. In other words, the RRA algorithm identify sensor pairs that have high correlation, above the threshold, in the training

phase and then by arranging those in a new matrix, the study is focused on these pairs. Next in order, correlations of these pairs are tracked during monitoring phase in order to detect any abnormal behaviour. The steps are shown in Figure 8.

3.2.3. Moving Cross Correlation Analysis (MCCA)

Moving Cross Correlation Analysis (MCCA) was developed as a promising upgraded version of CCA adapted for long term SHM. A key parameter of MCCA is the size of the moving window N_w. This parameter should be sufficiently large so that it is not influenced by variations in measurements due to environmental effects and small enough to provide rapid anomaly detection. The same matrix of data structure is developed and CCA is conducted for each individual window. Therefore, performing CCA for each moving window, correlation coefficient value is computed as correlation of sensor “i” and “j”.

For detecting any possible abnormal behavior, the matrix of data is separated unequally into two segments as training and monitoring segments. The baseline behavior for each pair of sensors, sensors “i” and “j”, are defined by the confidence interval developed based on correlation coefficients obtained in the training phase. In the following step, the generated confidence intervals in training phase are considered as damage criteria for each pair of sensor throughout the monitoring phase. In other words, if the observed correlation coefficients for a given sensor “i” and “j” in monitoring phase exceed the confidence interval for the same sensors in training phase, then it can be claimed that possible abnormal, behavior exists in the structure. The entire process is summarized in Figure 9.

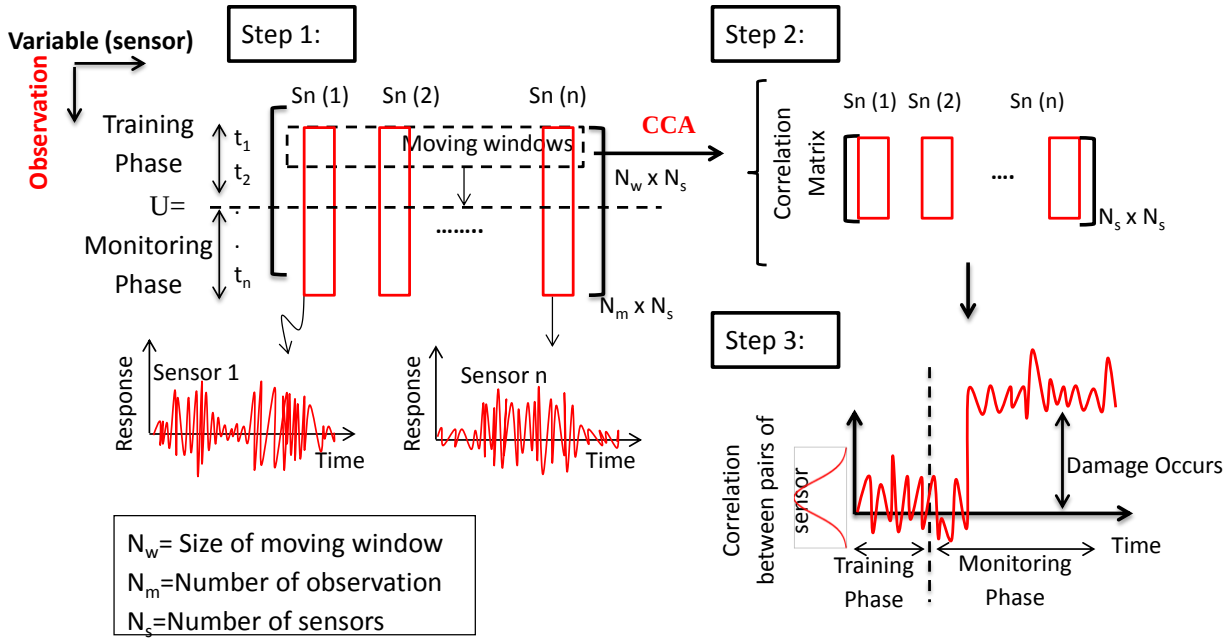

Figure 9: Procedure for Moving Cross Correlation Analysis (MCCA)

3.2.4. Principal Component Analysis (PCA)

Long term monitoring of real life, large and complex structures requires dealing with multi-modal large data sets captured from different type of sensors. Therefore, efficient data analysis methods should be employed to deal with large sets of data and to evaluate the condition of the monitored structure by means of detecting any change that can be attributed to damage or change in operational conditions. In many cases, high dimensional parametric data analysis methods may not only be complicated but also time consuming. In addition, the interpretation of the results may be challenging.

In contrast, multivariate dimensionality reduction techniques are desirable methods for SHM to avoid such disadvantages. Principal Component Analysis (PCA) is one the most powerful techniques for reducing a complex data set to fewer dimensions. PCA is used for feature extraction from high dimensional data to reveal the most informative underlining patterns

in fewer dimensions. PCA can be referred as a projection/transformation method to turn a set of observations of possibly correlated variables, variable space, into sets of independent variables termed as principal components, principal space. The schematic presentation of this projection is demonstrated in Figure 10. In fact, PCA can be considered as a projection technique in which the observations are projected from a high dimensional space named as original space (Figure 10) into a less dimensional space so called principal component space.

This projection should be performed in such a way that the new coordinates would be laid in the directions in which the original data has the most variance so that this transformation does not end up with losing important information. In order to achieve this goal, the optimized plane in original space should be identified in a way that projection of observations can be performed with the minimum possible residual value and consequently minimum possible loss of information; these procedures are illustrated in Figure 10. The steps towards PCA analysis are explained in more details in the following sections.

3.2.4.1. Constructing and Scaling Sensor Network Measurement Data for PCA

The preliminary step for PCA is generating a main matrix by inserting time history of each variable (sensor) as illustrated in the following matrix:

$$\begin{pmatrix} M_{t_{1^1}} & \cdots & M_{t_{1^n}} \\ \vdots & \ddots & \vdots \\ M_{t_{m^1}} & \cdots & M_{t_{m^n}} \end{pmatrix} \quad (9)$$

where the number of rows indicates the number of observations while the number of columns specifies the number of measured variables (sensors). In other words, $M_{t_{m^n}}$ represents

the n^{th} observation collected at time t_m. There are different desired structural data that are collected through the SHM procedure including, strain, acceleration, displacement data etc. However, each of these parameters or measured variables has its own scale and magnitudes and as a result should be scaled before applying PCA or any other multivariate techniques. So as to solve this issue, several methods are recommended in the literature for scaling experimental data. The most popular technique among all others, which is also implemented in this study, is autoscaling. Each variable (column) should be scaled in such a way that the distribution follows the standard Gaussian distribution. The following procedures have to be taken for performing the autoscale method.

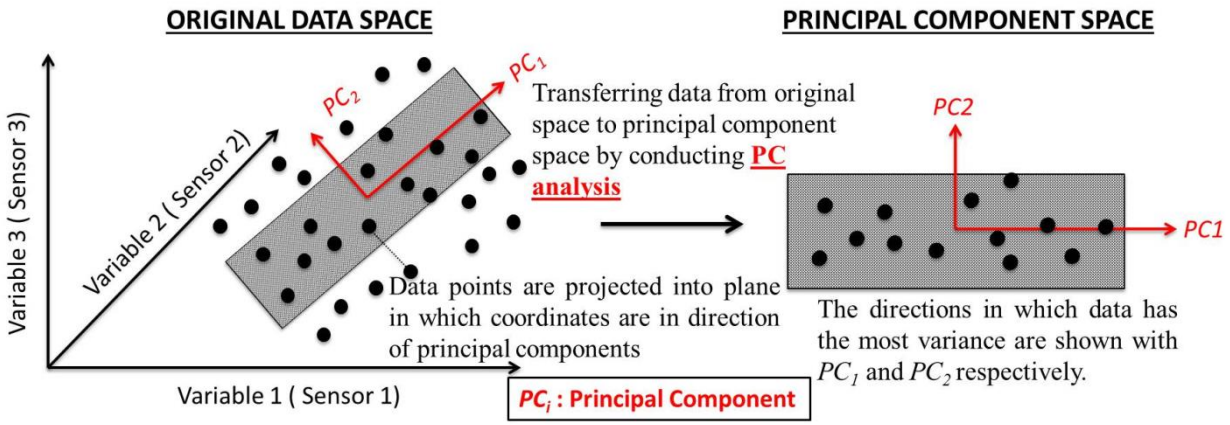

Figure 10: Schematic demonstration of principal component analysis

$$\mu_{t_{ij}} = \frac{1}{m} \sum_{t_i=t_0}^{t_i=t_{end}} M_{t_{ij}} \qquad (10)$$

$$\sigma^2{}_{t_{ij}} = \frac{1}{m-1} \sum_{t_i=t_0}^{t_i=t_{end}} (M_{t_{ij}} - \mu_{t_{ij}})^2 \qquad (11)$$

Where $\mu_{t_{ij}}$ and $\sigma^2{}_{t_{ij}}$ are mean and variance respectively, corresponding to variable j (sensor j). It should be also noted that *m* is the number of rows, which represent the number of observations. Therefore, the scaled variables are derived from the succeeding Equation.

$$\overline{M}_{t_{ij}} = \frac{M_{t_{ij}} - \mu_{t_{ij}}}{\sigma^2{}_{t_{ij}}} \quad (12)$$

3.2.4.2. Covariance Matrix and Extraction of Eigenvectors and Eigenvalues

Having a scaled data matrix, as it was discussed in details throughout previous sections, the covariance matrix is derived based on the following Equation:

$$C_M = \frac{1}{m-1}\bar{M}^T\bar{M} \quad (13)$$

where $\bar{M}$ denotes the scaled matrix achieved in section 3.2.4.1. The principal components of the original matrix can be found by extracting the eigenvectors and eigenvalues of the scaled matrix, which should satisfy the Equation 14:

$$(C_M - \lambda_i I)\psi_i = 0 \Longrightarrow i = 1, \dots, n \quad (14)$$

where $\psi_i$and λ_i are referred as eigenvectors and eigenvalues of the scaled matrix. *I* also denotes nxn identity matrix. In fact, the eigenvectors are laid in the directions in which the original data has the most variances. Typically, the first few components contain the most of the variance, and the rest is just corresponded to noise measurements. Due to this fact, in most cases, the first few principal components are only taken into account.

3.2.5. Moving Principal Component Analysis (PCA)

Real life employment of SHM involves dealing with large amount of multivariate data. Only a small portion of abnormal data, in comparison to overall data, is available at the time when damage occurs. For detecting the changes in data sets effectively, the classical PCA should be improved to make it more practical for long term SHM data analysis. By means of PCA, the damage can be detectable only when the principal components (eigenvectors) are influenced by abnormal behavior. Subsequently, eigenvectors are subjected to change only if certain amount of abnormal data are captured and possibly affected the overall structure of data. This feature makes PCA less effective for long term SHM implementation. Moving principal component analysis (MPCA) was proposed to address this challenge [62-64]. Basically, MPCA computes the PCA within moving windows with a constant size. MPCA procedures applied in this study can be summarized in five different steps, which are presented here. Moreover, Figure 11 gives details of MPCA algorithm designed for long term SHM applications.

Step 1: A data matrix should be generated by sorting the time history data from each sensor, or variable, into individual columns. Once the matrix is created, it should be divided into two segments, called training and monitoring phases. The training phase is intended for developing a baseline, confidence interval, based on normal condition, while monitoring phase is set for long term monitoring. The fixed moving windows should be well-defined. In fact, determining the window size precisely is one of the most critical issues in MPCA. The reader is referred to section 5.4.5 of this study for further information on window size.

Step 2: PCA should be conducted for each window individually and results should be stored. Score matrix and coefficient matrix for each window should be calculated. The size of

score matrix is identical to the moving window whereas the number of rows for coefficient matrix is equal to number of sensors and the number of columns is identical to the number of principal components. The score matrix is representative of projected observations in the new coordinate system known as principal component coordinate and as a result the number of rows, observations, is equal to the amount of observations inside the fixed moving window. Alternatively, the coefficient matrix presents individual variables in terms of principal components. This step should be repeated for each window.

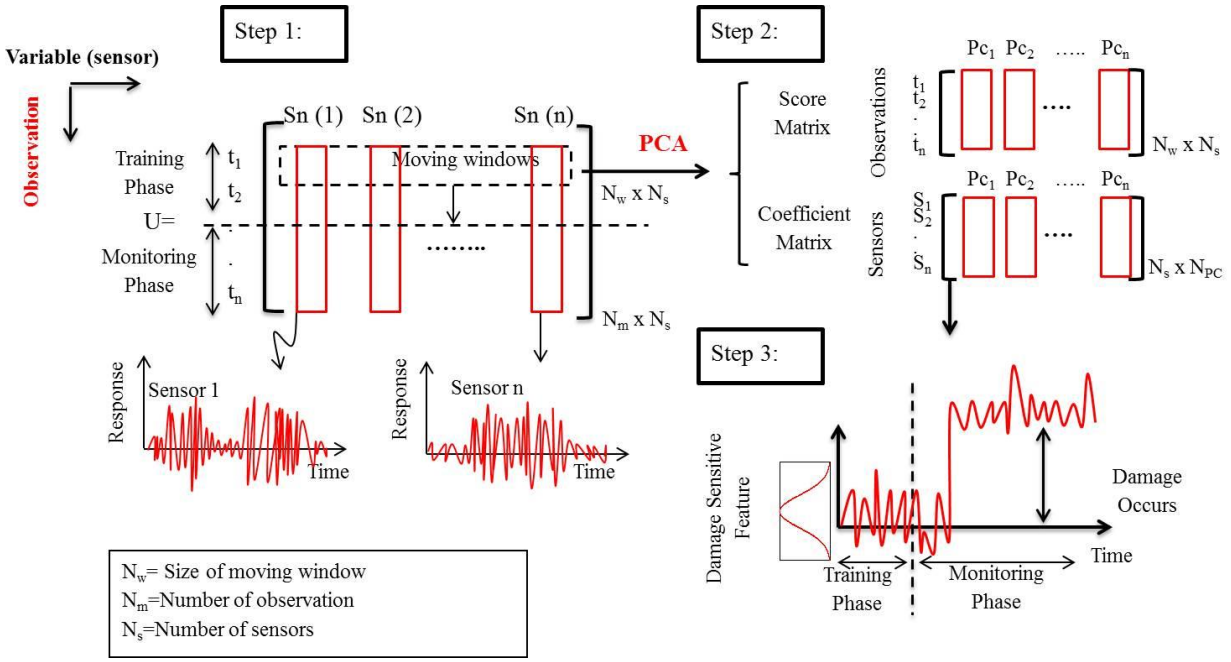

Figure 11: Procedure for Moving Principal Component Analysis (MPCA)

Step 3: A sensitive damage index should be selected in this step based on PCA outputs. Different entries of the first eigenvector are considered as individual damage indices.

In most cases the most variance is covered by the first few components. Therefore, the assumption is that, if any damage occurred in structure it should affect the data and consequently variance of data and should be detected by the first few components. It should be mentioned that

D_{si} are calculated for each windows along the time and consequently these values are plotted against time as shown in Figure 11 and Step 3. As a final point, the confidence interval developed in the training phase should be considered as a benchmark (baseline) for detecting any possible damage sing the rest of the data.

3.3. Comparative Evaluation of Selective Non-parametric Methods

This section is dedicated to present an outline of three comparative studies of non-parametric techniques that have been implemented to numerically simulated long-term data of two distinct structural cases. It should be also noticed that although these studies are very useful in terms of evaluation different non-parametric methods, all results are only extracted based on the numerically simulated data and a simple structure (a simple beam). Therefore, as it will be discussed in Chapter 5, evaluating non-parametric methods based on data extracted from real-life structure is one of the proposed objectives for this study. Each study is reviewed and summarized in individual section below.

3.3.1. First Study: Model-free Data Interpretation for Continued Monitoring of Complex Structures

In the first study [62], five different non-parametric techniques, including continuous wavelet transform (CWT), short term Fourier transform (STFT), Instance-based method (IBM), Moving principal component analysis (MPCA) and Moving cross correlation analysis (MCCA) are compared to each other. A finite- element model of a beam is used to simulate the different level of damage. Subsequently, all the aforementioned techniques are evaluated in terms of detecting and localizing different level of damage. Total number of 12 ‘virtual’ strain sensors, 6

at the lower surface and 6 at the upper surface, were located to 'virtually' collect the data from the numerically simulated beam. The temperature variations, including both daily and seasonal variation are simulated in the FE model. As a result, the effect of temperature variations can be viewed in the time series captured from each sensor. Considering results obtained from each technique, it is realized that the performance of MPCA and MCCA for long term structural health monitoring are better in comparison to the other three techniques. Results of the comparative study between the proposed algorithms (MPCA and MCCA) and other techniques are summarized in Figure 12.

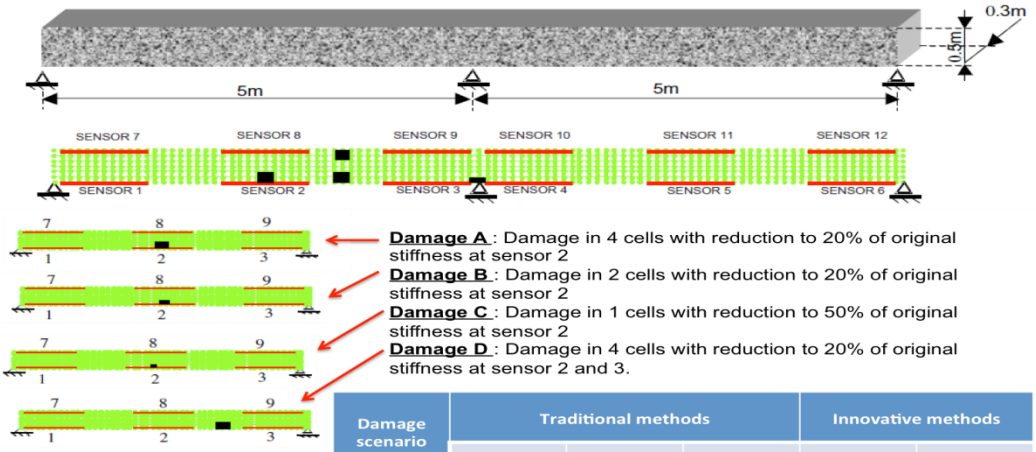

Damage scenario	Traditional methods			Innovative methods	
	CWT	SFTF	DTS	MPCA	MCCA
A	D	D	D	D	D
B	D	D	D	D	D
C	ND	ND	ND	D	ND
D	ND	ND	ND	D	D

Figure 12: Summary of the first study (Model-free data interpretation for continued monitoring of complex structures) [64]

3.3.2. Second Study: Methodologies for Model-free Data Interpretation of Civil Engineering Structures

In the second study [64], ten different non-parametric (model-free) techniques are evaluated based on most common issues associated with the long-term data from civil structures including noise, outlier and missing data. The load history and the numerical model are as the same as the first study. Fifteen cases of variations in daily temperature, traffic loading and sensor noise were used in this comparison.

The following methods were compared:

- Auto Regressive with Moving Average (ARMA)
- Box-Jenkins (BJ)
- Seasonal ARIMA
- Discrete Wavelet Transform (DWT)
- Wavelet Packet Transform (WPT)
- Robust Regression Analysis (RRA)
- Instance Based Method (IBM)
- Short-term Fourier Transform (SFT)
- Correlation Anomaly Scores Analysis

All ten techniques were able to detect damage in the absence of noise and outlier while in presence of those issues only few remain effective for detection. This is very important finding since noise and outlier are common issues in data measured from civil structures. The following conclusions are results of the second study [63-64]:

1) The MPCA and RRA are effective in detecting and localizing abnormal behavior.
2) In the case that data contains noise, only MPCA and wavelet packet transform have shown promising results. The performance of MPCA is even better than wavelet

packet transform since it can distinguish between temporary and permanent anomalies.

3) RRA has the advantage of being insensitive to outlier and missing data while it is not as efficient as MPCA and WPT in terms of detectability.
4) MPCA can also be adapted to situations when measurements are missing completely and when a single measurement is missing.

3.3.3. Third Study: Evaluating Two Model-free Data Interpretation methods for Measurements that are Influenced by Temperature

In the third study, a numerically simulated steel-truss railway bridge is used to generate data for the sake of comparing MPCA and RRA in term of 'time to detection' and 'detectability' [63].

Time to detection: 100%- minimum detectable damage level

Detectability: Time to damage detection is the time interval from the moment when damage occurs to the one when damage is detected.

Different levels of damage as well sensor locations are employed to investigate the efficiency of MPCA and RRA for long-term monitoring of complex structure. The results from this study are as below:

- Removing seasonal effect decreases the detectability of MPCA
- MPCA performed better than RRA in terms detectability
- RRA outperformed MPCA regarding to time to detection
- Decrease in traffic loading increase detectability of both MPCA and RRA

- Removing seasonal effect has a small influence of detectability of RRA

As it can be concluded from these three comparative studies, MPCA is a promising technique for long term monitoring of civil structure. However, the effectiveness of this method has only been explored in a few studies with real experimental data. Based on previous studies CCA, RRA, MPCA and MCCA are selected for experimental investigation in this study.

CHAPTER FOUR: PRILIMINARY EXPERIMENTAL STUDIES FOR IMPLEMENTATION AND DEMONSTRATION

4.1. Introduction

The purpose of this chapter is to experimentally explore the proficiency of some of the most reliable data driven techniques including cross correlation analysis (CCA), robust regression analysis (RRA), moving cross correlation analysis (MCCA) and moving principal component analysis (MPCA). As it was explained earlier, the reason for conducting this study is to explore the limitations associated with each technique by taking advantages of experimental data and also several common and critical damage scenarios. Moreover, the efficiency of in-house-developed FBG system is investigated along with different damage detection algorithms. A specially designed 4-span highway bridge model in the laboratory is considered as test structure. This unique four span bridge model is phenomenologically representative of common highway bridges in terms of its local and global response as well as its structural components and characteristics such as the deck, girders, composite action, boundary conditions etc. A number of damage conditions are simulated on the bridge model based on the feedback from bridge engineers from four different States' Departments of Transportation. SHM data generated under operating traffic loading on the model bridge are analyzed to evaluate the efficiency of the above-mentioned algorithms for the purpose of bridge monitoring implementations. In order to explore the development of low-cost fiber optic interrogator, use of FBGs and promising practical non-parametric methods in a comparative fashion for commonly experienced bridge problems, the research team carried out this study in an integrated manner as a first step towards holistic SHM implementation on highway bridges.

4.2. Structural Configuration

For the evaluation of using the non-parametric algorithms along with FBG sensors, several experiments with a laboratory bridge model (UCF 4-span Bridge Model) were designed and conducted by considering five common damage scenarios. The structure consists of two 120 cm (3.93 ft) approach (end) spans and two 304.8 cm (10 ft) main spans with a 3.18 mm (0.12 in) thick, 120 cm (3.93 ft) wide steel deck supported by two HSS 25x25x3 girders separated 60.96 cm (2 ft) from each other. Using the 4-span bridge model in the UCF structural laboratory (Figure 13) it is feasible to simulate and test a variety of damage scenarios that are commonly observed in bridge type structures [91].

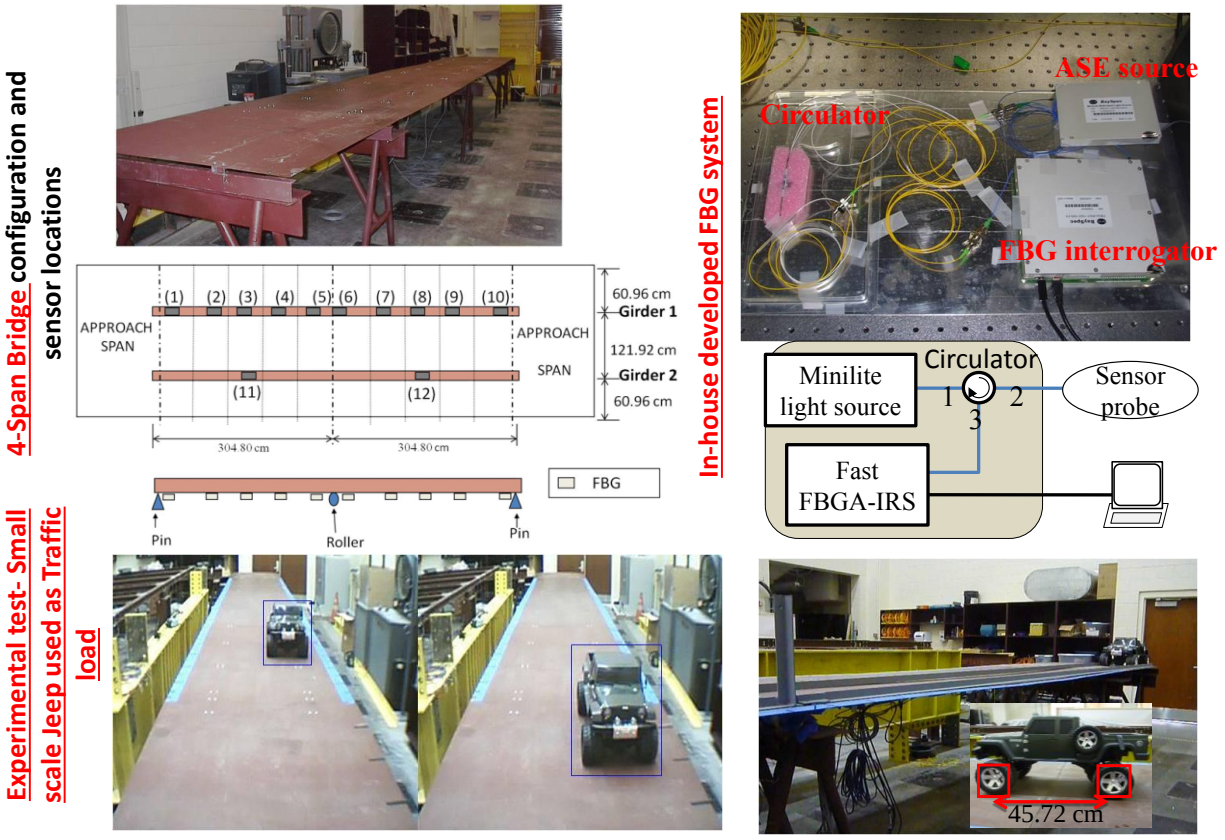

Figure 13: UCF-4 Span Bridge used for experimental test

It is possible to simulate common boundary conditions, including roller, pin, and fixed support. In addition to these, the bolts connecting the girders and deck can be loosened or removed at different locations to modify the stiffness of the system and to simulate damage. In other words, the first feature provides the opportunity to simulate the global damage scenarios, while the second one is desirable for local damage simulations.

It should be pointed out that even though the structure is not a scaled down model of a specific bridge, its responses are representative of typical values for medium-span bridges. Radio controlled vehicles (15.7 kg) (34.62 Ib) were crawled over the deck of the 4-span bridge to simulate traffic data on the bridge structure as seen in Figure 13.

4.3. Damage Scenarios

Based on the discussions with the Department of Transportation (DOT) engineers, several critical and common damage scenarios were identified and simulated on the 4-span bridge model. A crucial type of damage observed in bridges is alterations in boundary conditions. These types of alterations may cause stress redistributions and in most cases it may result in additional load in different elements.

Therefore, three cases were devoted to this type of damage using the advantage of the ability to shift from pinned to fixed or roller condition and vice versa. Missing bolts and section stiffness reductions are also observed in existing bridges. Fourth and fifth damage cases simulate the loss of connectivity between the girder and the deck generating localized stiffness reduction. The damage scenarios implemented in this study and also locations of sensors are summarized in Table 1 and Figure 14.

Table 1: The implemented damage scenarios for comparative study

Global Damage Scenarios			Local Damage Scenarios	
Case 1: Fixing the first bearing	Case 2: Fixing the first two bearings	Case 3: Fixing the middle bearings	Case 4: Removing 4 bolts close to middle bearing	Case 5: Removing 8 bolts on both side of middle bearing

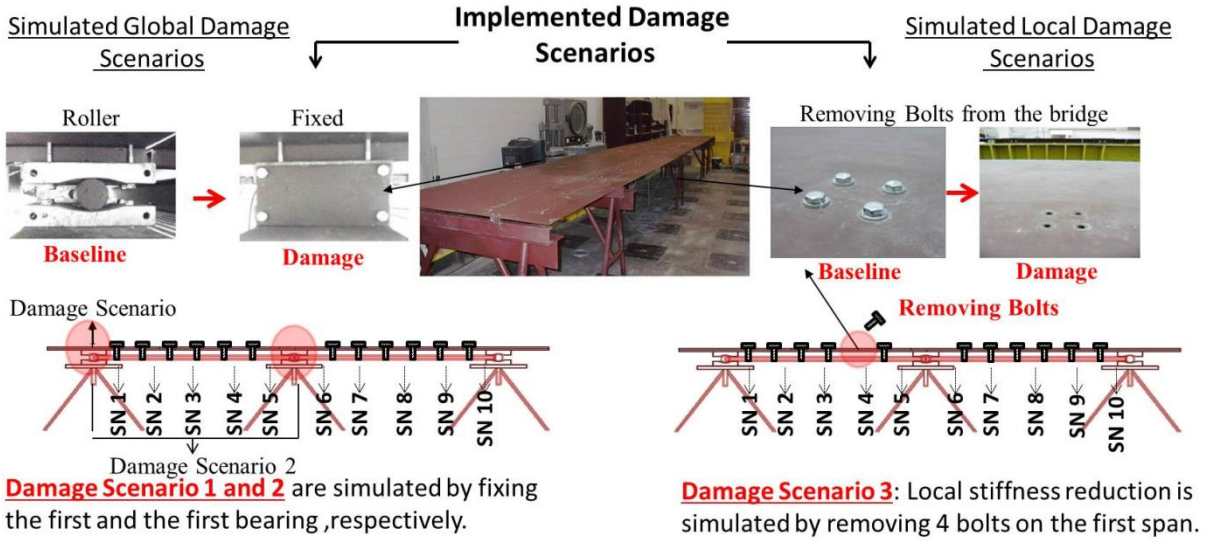

Figure 14: The implement the damage scenarios (local and global)

4.4. Damage Assessment (RRA and CCA)

Each of these algorithms, CCA and RRA, has its own advantages and drawbacks. Therefore, the algorithms should be preferred based on monitoring constraints and missions. RRA and CCA are both developed based on correlation between measurements. However, the process for each algorithm is different. Regarding to RRA, all the measurements with high correlation are selected and subsequently robust regression analysis is conducted on these

selective measurements. On the other hands, CCA is directly based on correlation between all the measurements. It is worth noting that, for CCA, measurement data is compared through the data set, which contains a window of specific amounts of measurements. For RRA, however, the procedure is performed for every measurement.

The comparative study between RRA and CCA is conducted based on three different criteria, which includes: damage detectability, time to detection and required computational time. Damage detectability is the ability of algorithm to detect different types of damage scenarios. The period of time between the moment that the damage occurs and the moment that the damage is detected by an algorithm is called time to detection. Finally, the demanded total amount of time for each algorithm to be performed is called the computational time. A 2D perspective of damage location matrix is carefully chosen as diagnostic plot for CCA while three-dimensional graphs are preferred for the case of RRA. Regarding CCA, it is possible to merge altogether corresponding results in one figure as damage location matrix.

However, since RRA is dealing with several different sensor pairs and also two different phases, training and monitoring phase, only selected results are presented. In other words, for the sake of brevity, responses associated with sensor 1, 5 and 10, which are chosen based on their locations, are presented here. In fact, these sensors are nominated due to their location on bridge. Sensors 1, 5 and 10 are the closest sensors to the first, second and third boundary condition respectively. In other words, possible changes over available boundary conditions would be expected to alter the response of selected sensors and as a consequence should be observable through the figures provided in the next section.

It should also be mentioned that, S_{ij} at time (t) denotes the difference (error) between exact value (strain) of sensor i at time (t) and estimated value based on regression model and corresponding value of sensor j. It is apparent that any possible dramatic changes in this error should be considered as an indication of abnormal behaviour in the particular sensor and consequently near the corresponding location. In the following sections these algorithms are compared based on above-mentioned criteria and through individual damage scenarios.

4.5. Global Assessment (RRA and CCA)

4.5.1. First Damage Scenario (Fixing the First Boundary Condition)

The detectability of CCA and RRA methods are put to the test by fixing the first bearing on the 4-span bridge model. The corresponding results of CCA and RRA are shown in Figure 15 and Figure 16 respectively. It is observed from Figure 15 that damage location matrix has values mostly close to zero, shown with dark color, except that values for sensors that are close to the damage locations. In other words, all arrays in each individual column of damage location matrix are close to zero except for the columns corresponding to the sensors with abnormal behavior due to damage.

As mentioned previously, each individual column in the damage location matrix corresponds to one particular sensor on the structure. Consequently, in pursuance of detecting damage location on the bridge model, each column should be investigated to determine if the sensor shows any abnormal behavior due to damage.

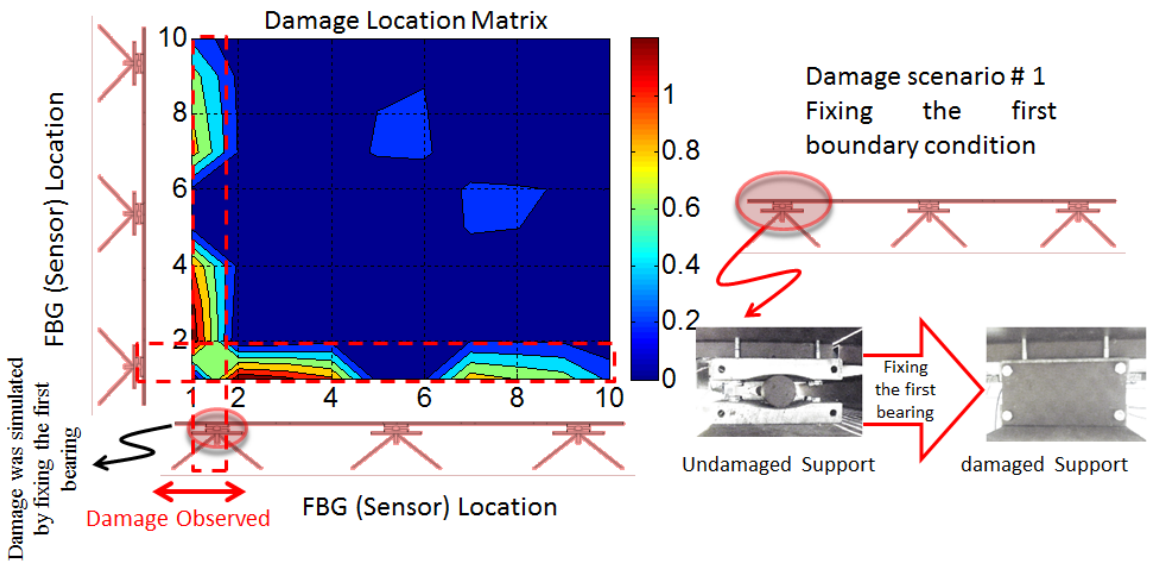

Figure 15: Damage location matrix corresponding to damage scenario 1

It should be also pointed out that the color bar range changes from one figure to another. Based on observation Figure 15, it is evident that, the correlations of sensor 1 and 2 with the other sensors have experienced dramatic change due to this damage scenario, fixing the first bearing. In effect, sensors 1 and 2, express the most, and only, abnormal behavior among all other sensors and this confirm the efficiency of CCA algorithm in detecting irregular behavior due to this scenario.

RRA results are presented in individual 3D graphs, shown in Figure 16. This graph illustrates the time history of error in estimating the value of corresponding sensors based on robust regression model generated in training phase. S_{12}, error in estimating value of sensor 1 based on value of sensor 2 by means of robust regression model. The calculated error is almost constant before damage occurred (t=600sec) and after that a dramatic shift occurred due to damage. The same behavior but with less intensity is observed for S_{13} and S_{14}, while for S_{18} and S_{19} there are not any significant changes observed. This reveals the fact that fixing the first

bearing makes the robust regression model, generated in the training phase, less effective in predicting responses of sensors located close to the damage location.

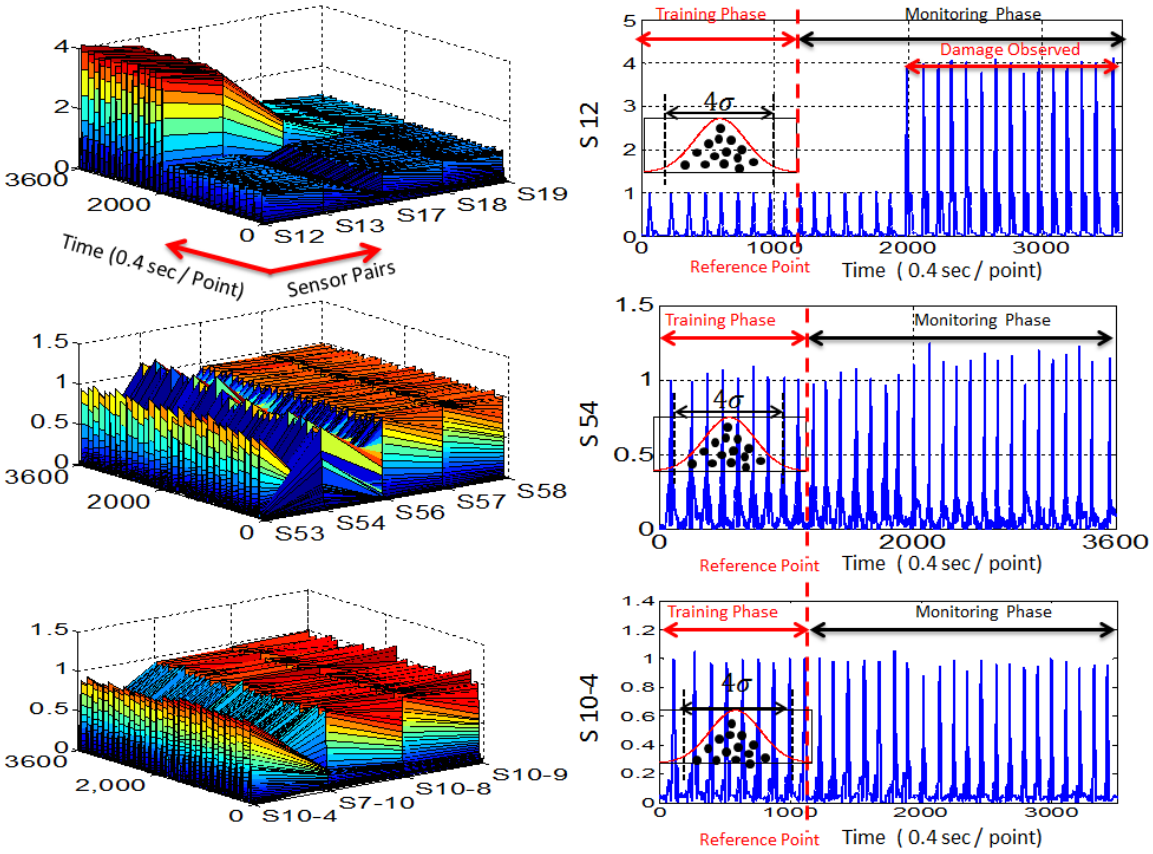

Figure 16: Robust Regression Analysis (RRA) corresponding to damage scenario 1

On the contrary, this mathematical model stays effective for sensors away from damage location and as a result there is not noteworthy shift observed in the time history of error associated with these sensors. A confidence interval will develop based on the computed error prior to the reference point (t=200 sec). In fact, the training phase is separated from the monitoring phase by the reference point. Another important observation is that CCA is failed to detect damage adjacent to sensor 3 and 4 while RRA detects abnormal behavior from measurements of these sensors.

4.5.2. Second Damage Scenario (Fixing the First Two Boundary Conditions)

The second simulated scenario is fixing the first two bearings on the 4- span bridge. The corresponding results are shown in Figure 17 and Figure 18. These results show that, fixing the second, middle, bearings spreads out the damage from being detected by sensors 1 and 2 to sensor 3, 4, 5 and 6.

However, the most intensive alteration is still observed by sensor 1 and 2, similar to scenario 1. Significant changes are also experienced by sensors 5 and 6, located next to damage location, while sensor 3 and 4, which are placed in the middle of the first span; exhibit less alteration caused by this scenario. However, there is not significant damage to be sensed over the second span where sensors 7, 8, 9 and 10 are positioned. Similar results are observed from Figure 18 which shows the RRA.

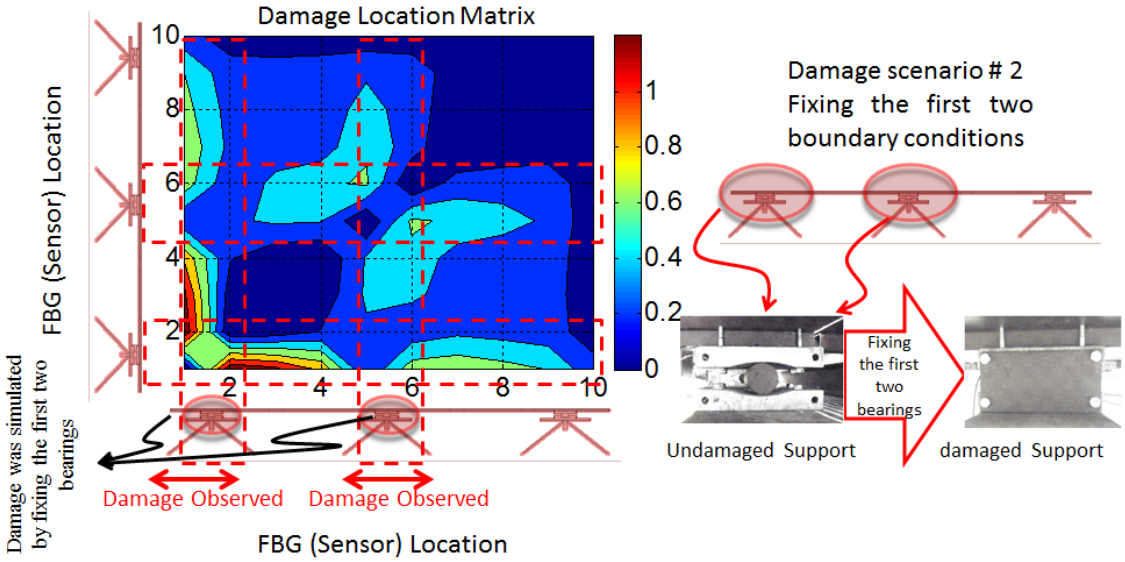

Figure 17: Damage location matrix corresponding to damage scenario 2

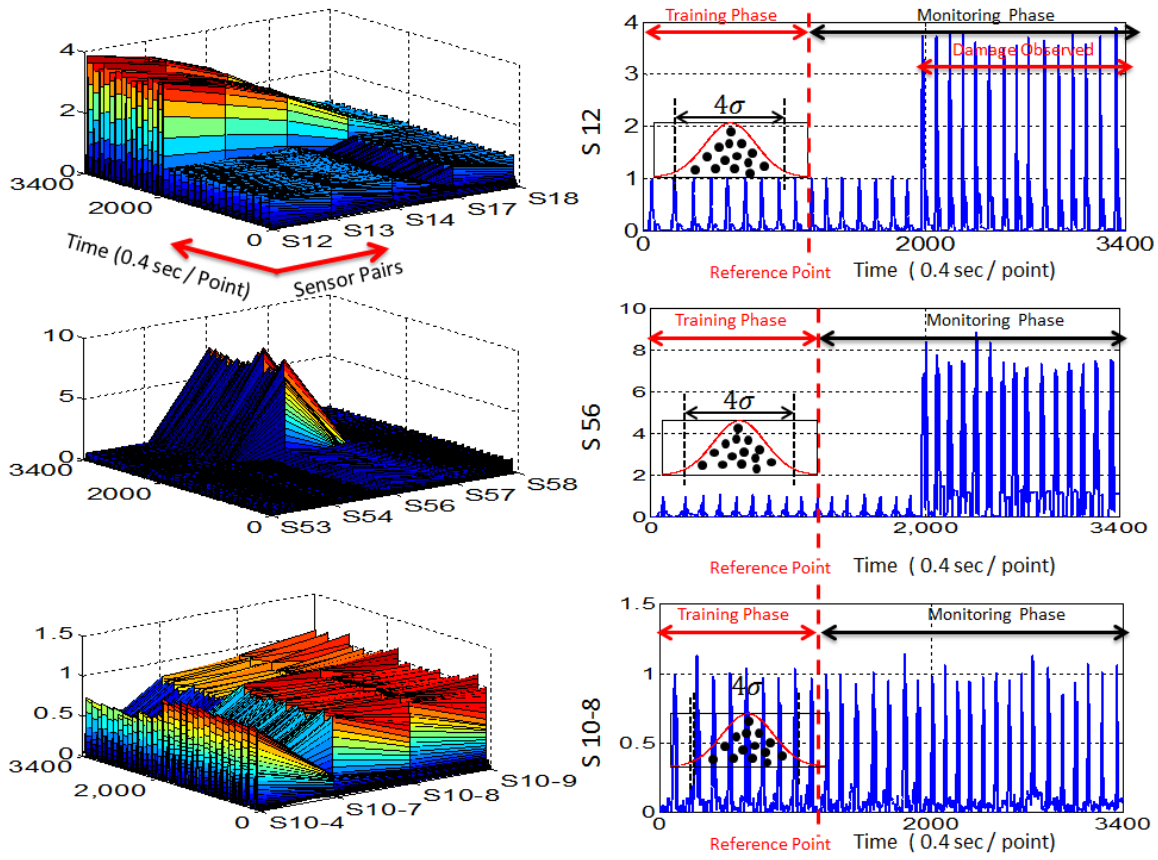

Figure 18: Robust Regression Analysis (RRA) corresponding to damage scenario 2

4.5.3. Third Damage Scenario (Fixing the Middle Boundary Condition)

The third damage scenario is conducted by just exchanging the middle boundary condition from roller to fixed bearing. The CCA and RRA results are demonstrated in Figure 19 and Figure 20 respectively. Based on CCA results, and as opposed to the first two scenarios, sensor 1 and 2 are not experiencing significant alterations due to this scenario. The reason is obviously because of reverting the first boundary condition from fixed back to roller state. Therefore, the damage is just concentered around the middle bearing where the sensors 4 and 6 are positioned. Figure 19, illustrates that the correlation of sensors 5 and 6, as expected, with other sensors have changed meaningfully.

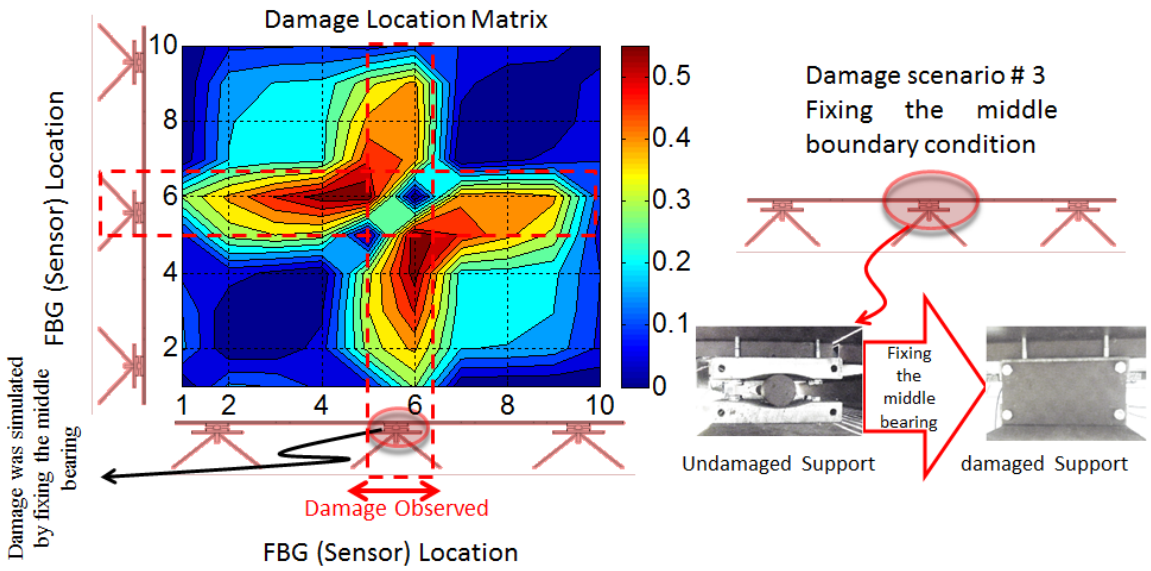

Figure 19: Damage location matrix corresponding to damage scenario 3

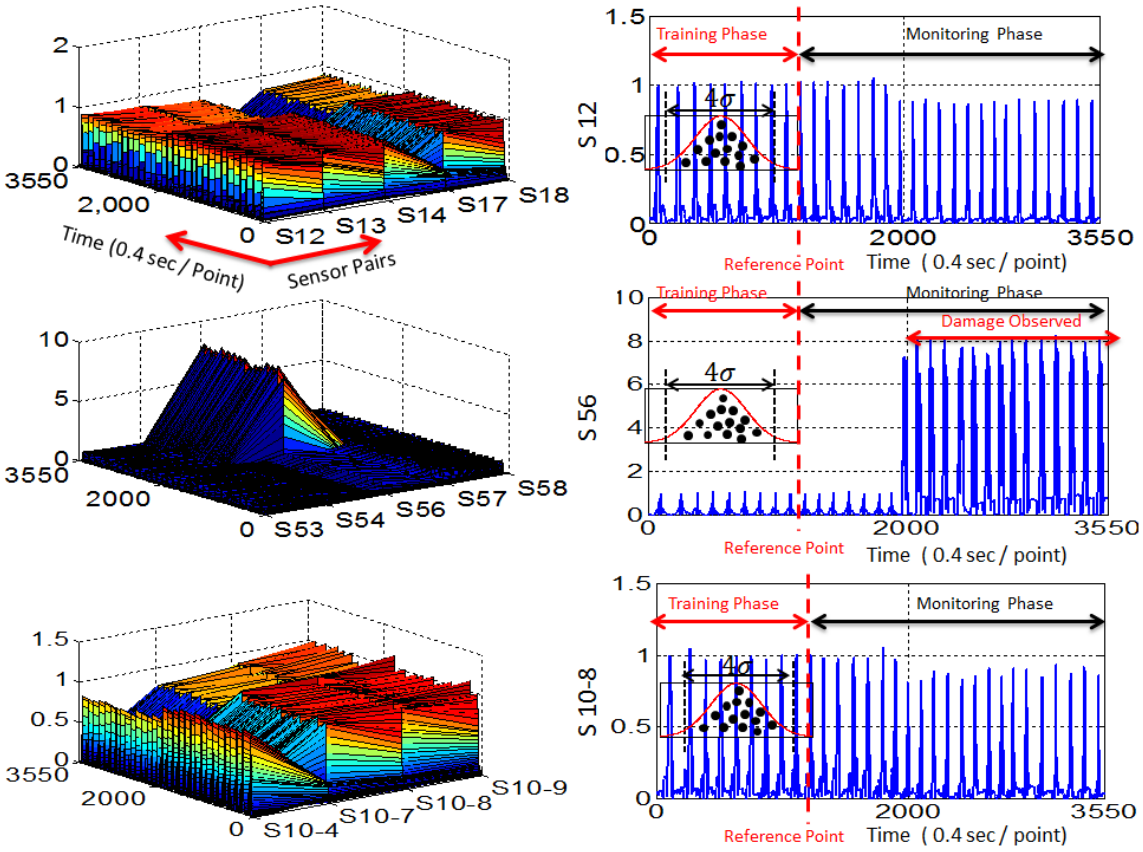

Figure 20: Robust Regression Analysis (RRA) corresponding to damage scenario 3

RRA conceals almost comparable outcomes in terms of both damage intensity and location of abnormal response. Similar to CCA, there is not any expressive detection sensed near sensors 1 and 10, by means of RRA. In other words, CCA and RRA are in perfect agreement with each other.

4.6. Local Assessment (RRA and CCA)

The last two damage scenarios are local stiffness reduction. Scenario 4 is designed to remove 4 bolts on the first span and close to middle bearing while scenario 5 is removing additional 4 bolts, symmetrically, from the second span, see Figure 14 for more details. Through the next two following sections, detectability of CCA and RRA will be evaluated based on their sensitivity to local stiffness reduction.

4.6.1. Fourth Damage Scenario (Removing Four Bolts from the First Span)

As it was discussed above, the fourth damage scenario is removing 4 bolts from the first span and close to middle bearing. The results related to RRA and CCA for this case are presented in Figure 21 and Figure 22 respectively. The results reveal that both methods are efficient in detecting abnormal behaviour due to the induced damage. The correlation of sensor 4 with the other sensors is affected due to removing 4 bolts from a location close to this sensor. This abnormal behaviour is clearly illustrated in Figure 21. In addition to sensor 4, a slightly change is detected over sensor 3 which is also shown in Figure 21 and Figure 22 present RRA results. Based on RRA results, Figure 22, this damage scenario only influences the correlation of sensor 4 and other sensors.

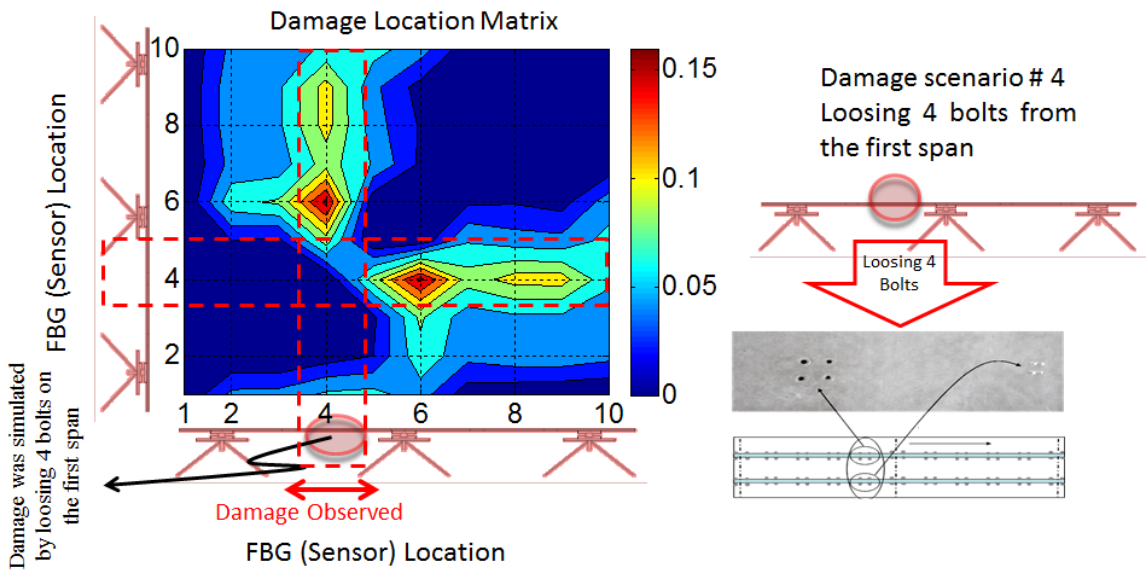

Figure 21: Damage location matrix corresponding to damage scenario 4

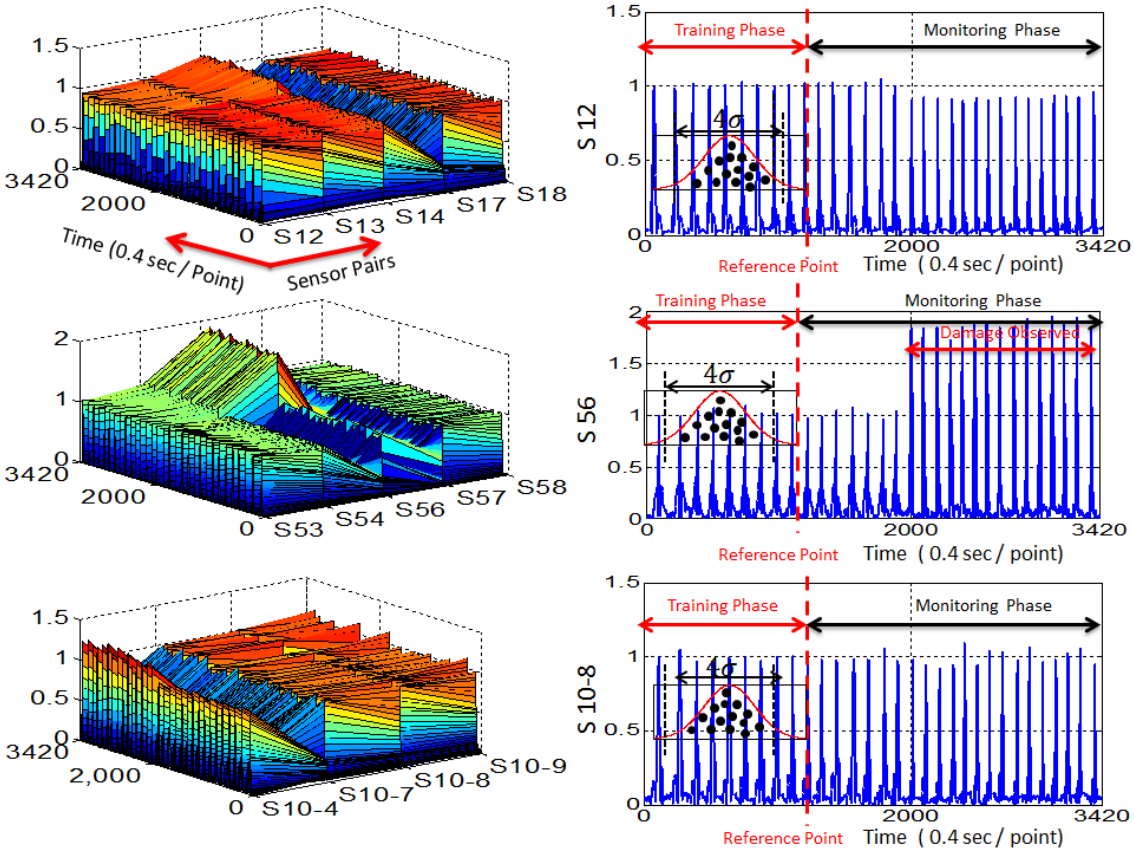

Figure 22: Robust Regression Analysis (RRA) corresponding to damage scenario 4

4.6.2. Fifth Damage Scenario (Removing Eight Bolts from the First and Second Span)

This damage scenario is designed to remove 8 bolts from both first and second span in a way it can effectively represent the lack of local connectivity which is very critical issue in bridge structure. CCA results are presented in Figure 23 while RRA results are shown through Figure 24. The first obvious point, which should be highlighted, is that removing another 4 bolts from the second span (in comparison to the previous scenario) will disperse the damage. In fact the distribution of damage due to lack of local connectivity is seems to be worse than the first two scenarios, which were fixing the boundary condition in terms of distribution issue. It is evidently perceived from Figure 23 that the correlations of sensors 4, 5 and 6 with other sensors are affected due to this induced damage. Therefore CCA algorithm was able to precisely detect the location and intensity of abnormal behaviour caused by lack of local connectivity in bridge. As a final point, RRA results, which are presented in Figure 24, are discussed here.

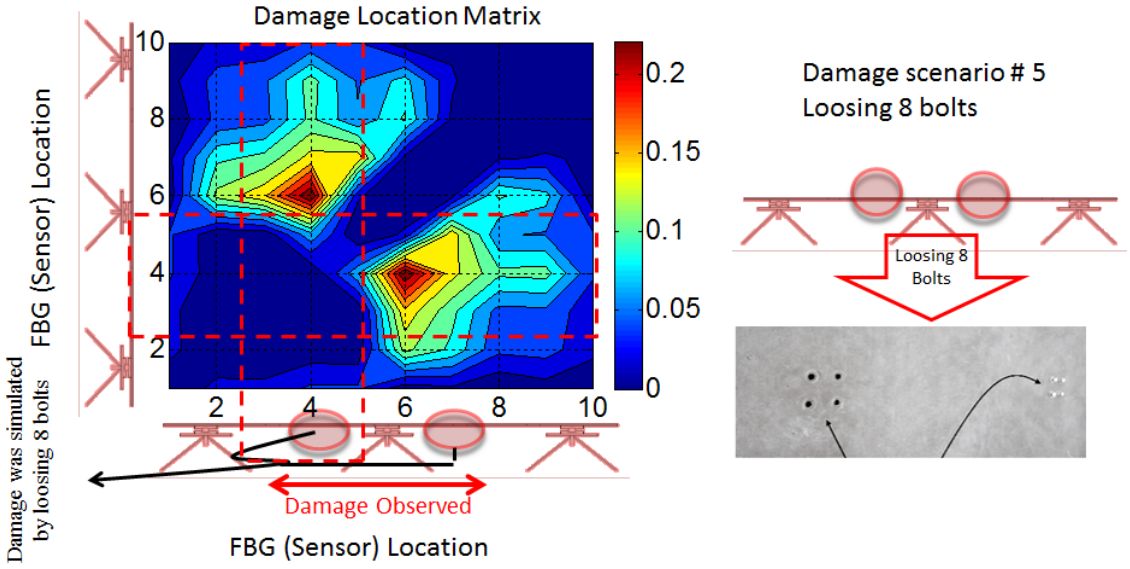

Figure 23: Damage location matrix corresponding to damage scenario 5

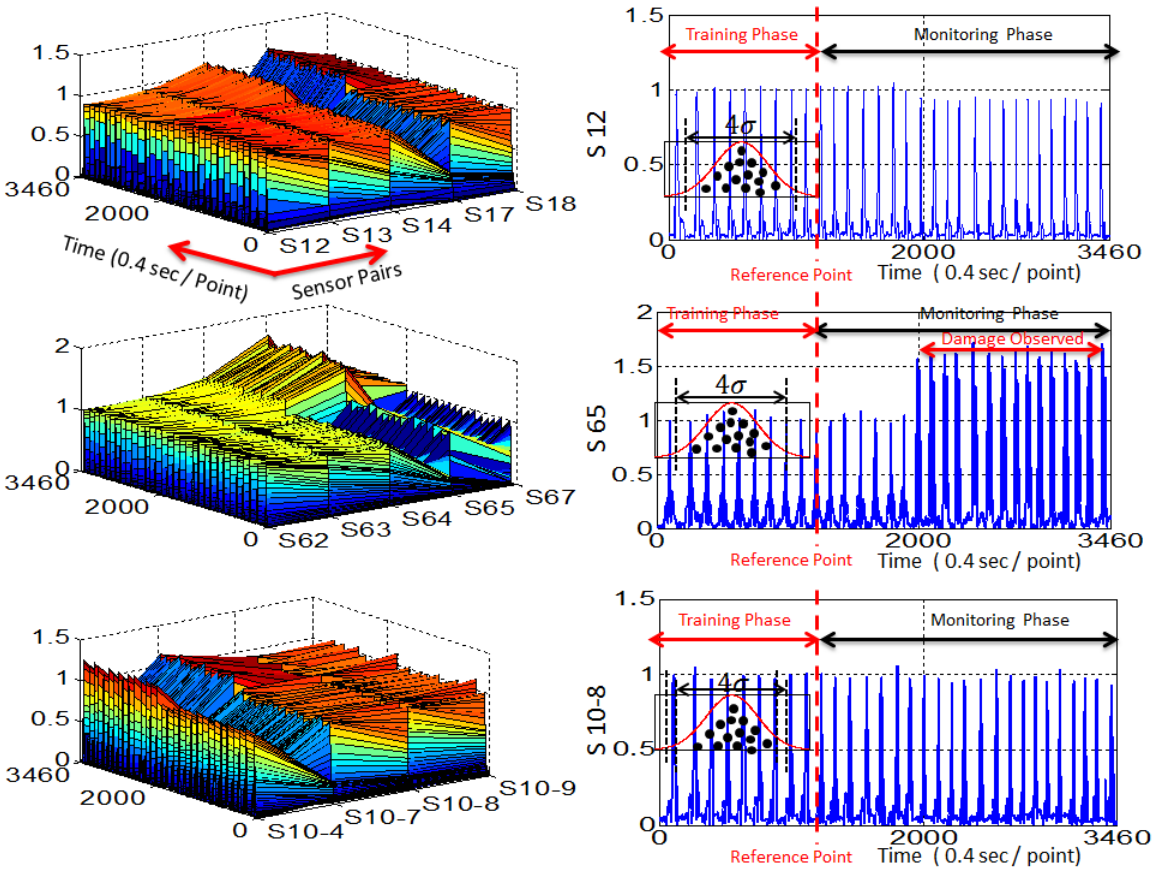

Figure 24: Robust Regression Analysis (RRA) corresponding to damage scenario 5

It is shown that correlation of sensor 1 and 10 with all other sensors are not affected due to this damage while correlation of sensor 6, which was located close to the damage location is altered. In other words, RRA results obtained for this condition exposed the detectability of this detection algorithm in dealing with lack of local connectivity.

4.7. Damage Assessment (MPCA and MCCA)

A total number of 30 data sets, 15 from baseline condition and 15 from damage condition, have been considered in this study. Each data set consisted of approximately 10000 to 13000 data points. This results in a main matrix with 360175 rows (data points or measurements) and

12 columns (number of FBG sensors or variables). Taking this information into account, the size of the moving window was chosen as 13000 x 12 while the moving rate (or window overlap) is selected as 2000 points. In order to develop a confidence interval, the first 50000 points have been considered as training (baseline) phase for both MPCA and MCCA algorithms. In fact, the first 193875 points (measurements) out of 360175 points are captured from a baseline structure while only the first 50000 points are involved in developing the confidence interval. Since this is multivariate data analysis, the results of selective sensors are presented instead of individual sensors.

Consequently, in order to conduct a fair comparative study as well as to fully understand the capability of the algorithms for both global and local damage detection, two sensors close to damage location and one senor away from damage were selected for illustration purposes.

Therefore, for the first three cases, the MPCA results corresponding to sensor 1 (close to first bearing), sensor 5 (close to middle bearing) and sensor 10 (close to third bearing) are presented while for case 4 (local stiffness reduction) sensors 4 and 6 (both close to damage locations) and sensor 10 (away from damage location) are selected. Correspondingly, for case 5 (severe local stiffness reduction), sensors 4 and 7, which are both located close to the location of removed bolts and sensor 10 (away from damage location) were selected as representative sensors for evaluating the efficiency of MPCA algorithm. Alternatively, for MCCA illustration, correlation of sensors 1, 5 and 10 with sensors 2, 3 and 4 will be presented respectively for the first three cases while correlation of sensors 4, 6 and 10 with sensor 1, 2 and 3 are illustrated for case 4. Consistently for case 5, correlation of sensor 7, 8 and 10 with sensor 1, 2 and 3 will be monitored for the sake of verifying the proficiency of MCCA algorithm. In the following

subsections the corresponding results for both MPCA and MCCA and different scenarios will be discussed.

4.8. Damage Assessment (MPCA and MCCA)

4.8.1. First Damage Scenario (Fixing the First Boundary Condition)

The main idea behind this damage case is to simulate one of the most common faults in bridge type structures, which is altering the boundary condition from roller condition to fixed condition. In fact, this type of change will result in redistribution of force in the structure and may cause unexpected bending moment at boundary location which can has detrimental effect on the performance of the structure. The corresponding results for MPCA and MCCA are presented separately in Figure 25 and Figure 26.

Each graph, as it was mentioned, is separated into two parts so called training and monitoring phase. As it is observed MPCA precisely detected the abnormal behavior due to this damage. Dramatic change in principal component value of sensor 1 is detected while only slight change is noticed over sensor 5 and almost no change at the location of sensor 10. The PCA value for sensor 1 is well separated before and after damage. In effect, the values of PCA for sensor 1, after damage occurred, are clearly out of the confidence interval developed in training phase.

In other words, shifting the boundary condition from roller into fixed condition caused unexpected extra moment force at the location of sensor 1 which subsequently resulted in dramatic shift in PCA value computed from this sensor. This alteration, force redistribution, is even slightly sensed over sensor 5 close to the middle bearing which is predictable based on

structural analysis since it is a continuous section. However, since there is a major shift in the mean PCA values and some points go beyond the confidence intervals, it can be concluded that damage is felt at sensor 5 as well. In contrast, there is not any abnormality detected for sensor 10 and as a result it can be mentioned with 99 percent confidence that the structure around this sensor has not experienced any force redistribution issue. In the case of MCCA, the correlation of sensor 1 with sensor 2, 3 and 4 showed obvious variations after damage occurred. However, slight change over sensor 5 and no significant alteration over sensor 10 are observed.

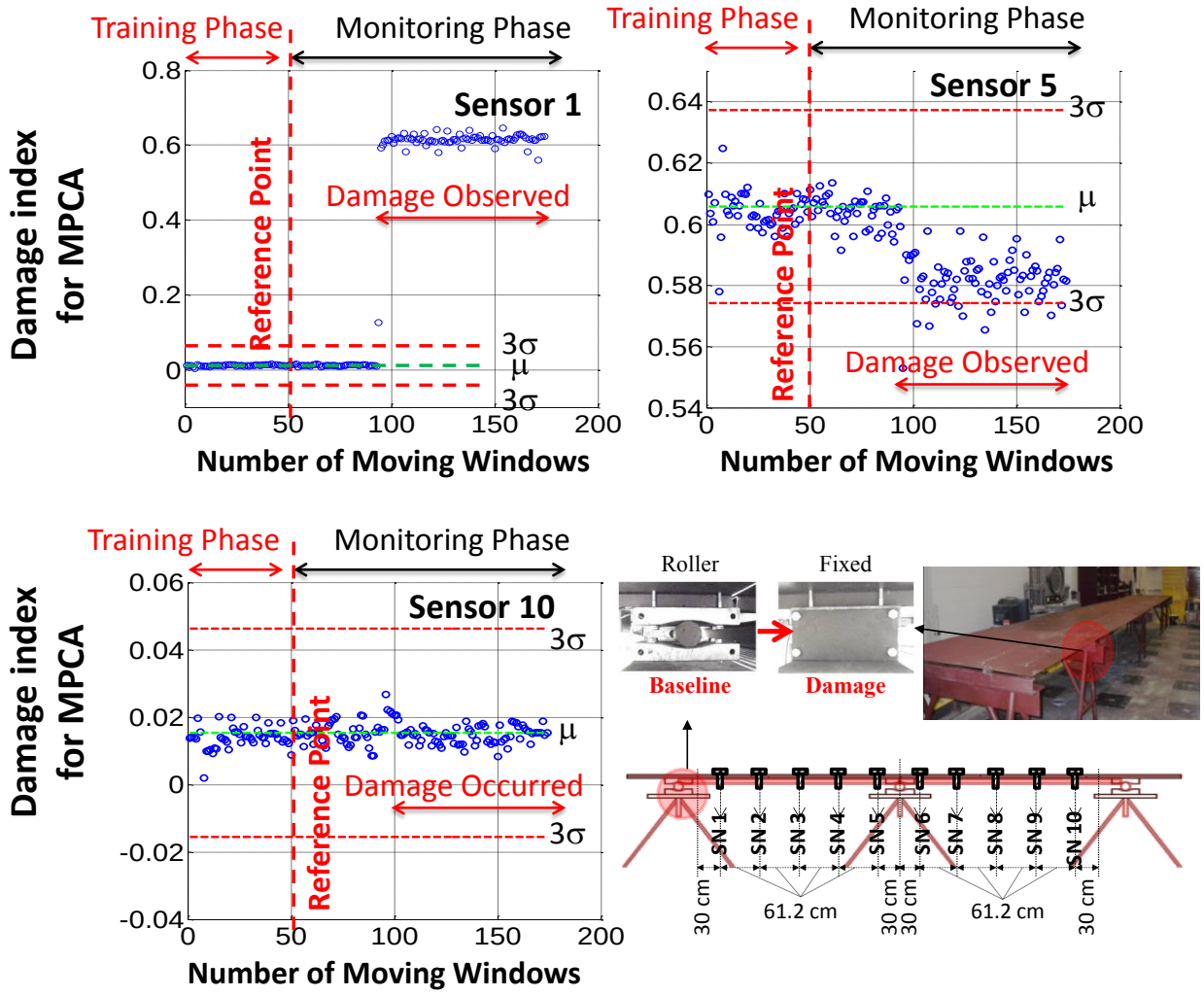

Figure 25: MPCA results for selected sensors (case1)

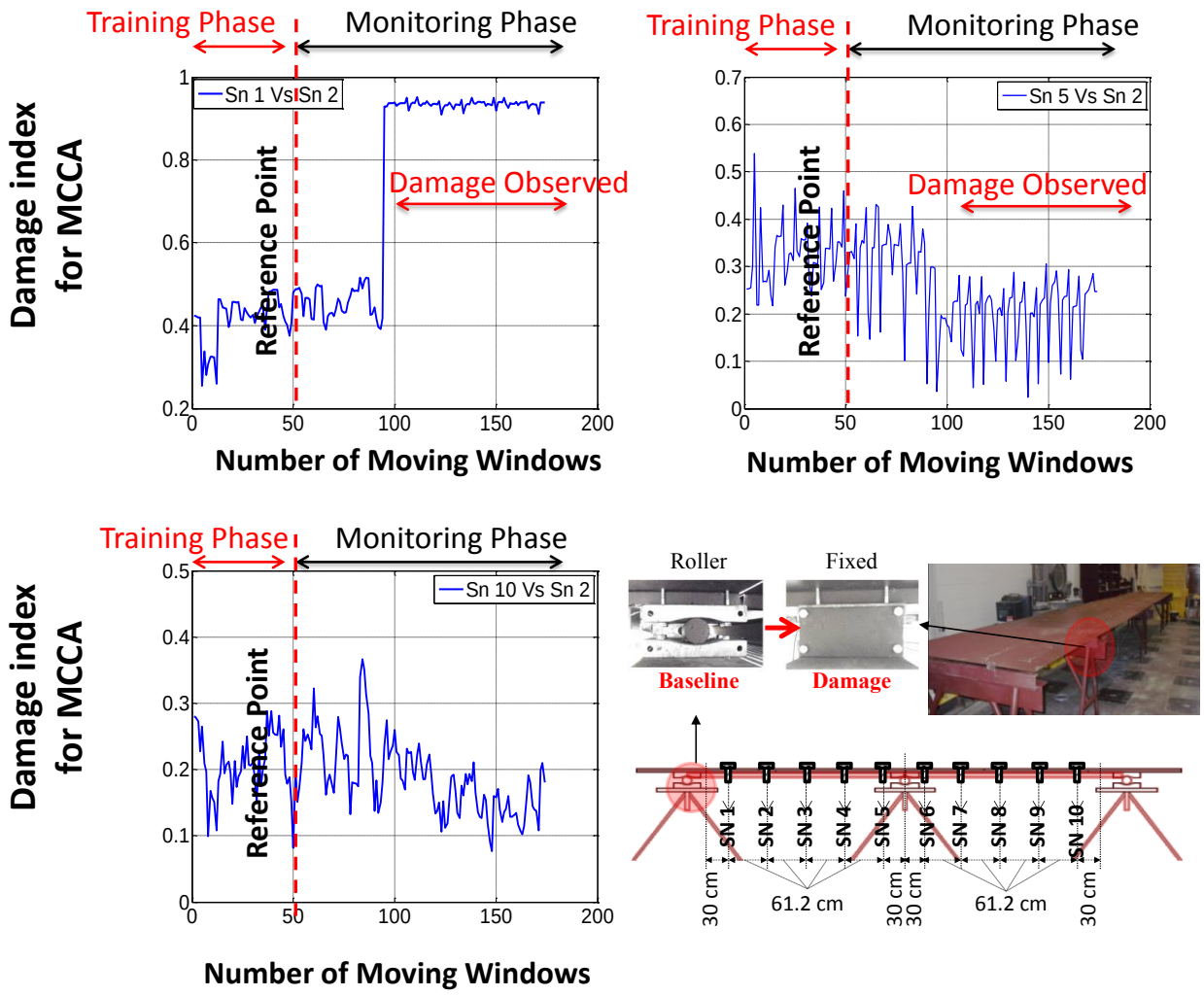

Figure 26: MCCA results for selected sensors (case1)

However, it should be also mentioned that, in terms of computational time needed for each algorithm, MCCA algorithm is superior. Also, significantly more complicated mathematical calculations are involved in MPCA. This can become critical issue when dealing with large amounts of real time data from a real life structure. Therefore, depending on the application and the priority, one of these algorithms can be selected and implemented.

4.8.2. Second Damage Scenario (Fixing the First Two Boundary Conditions)

The second damage scenario was designed and implemented to simulate the situation in which a number of bearings are experiencing the fixing issue. For that reason, the middle bearing was fixed in addition to the first one. The results for this case are summarized in Figure 27 and Figure 28. In the second case, sensor 1 again shows the most dramatic change similar to case 1. However, in this case an abrupt jump is observed in the location of sensor 5 (close to the middle bearing).

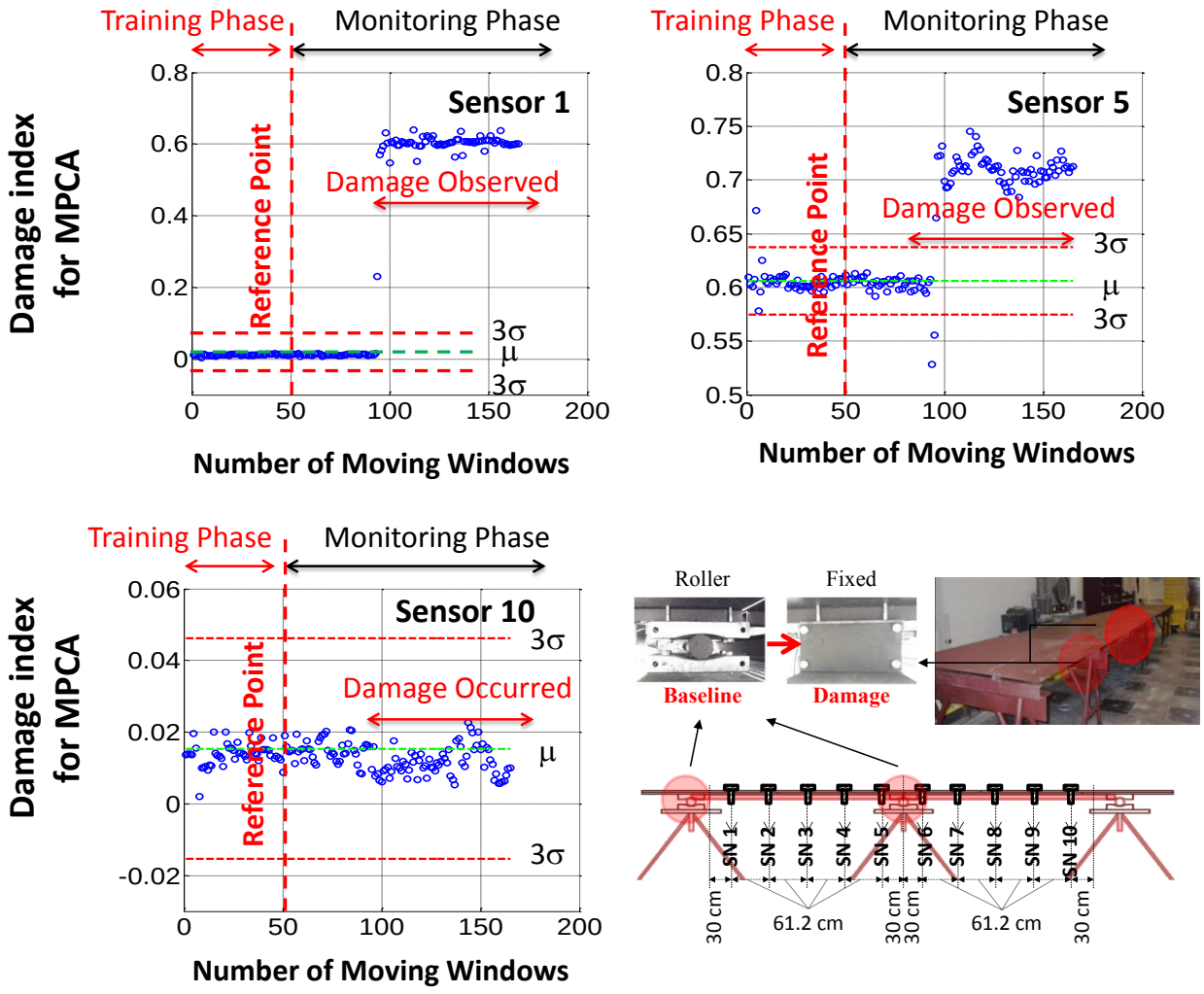

Figure 27: MPCA results for selected sensors (case2)

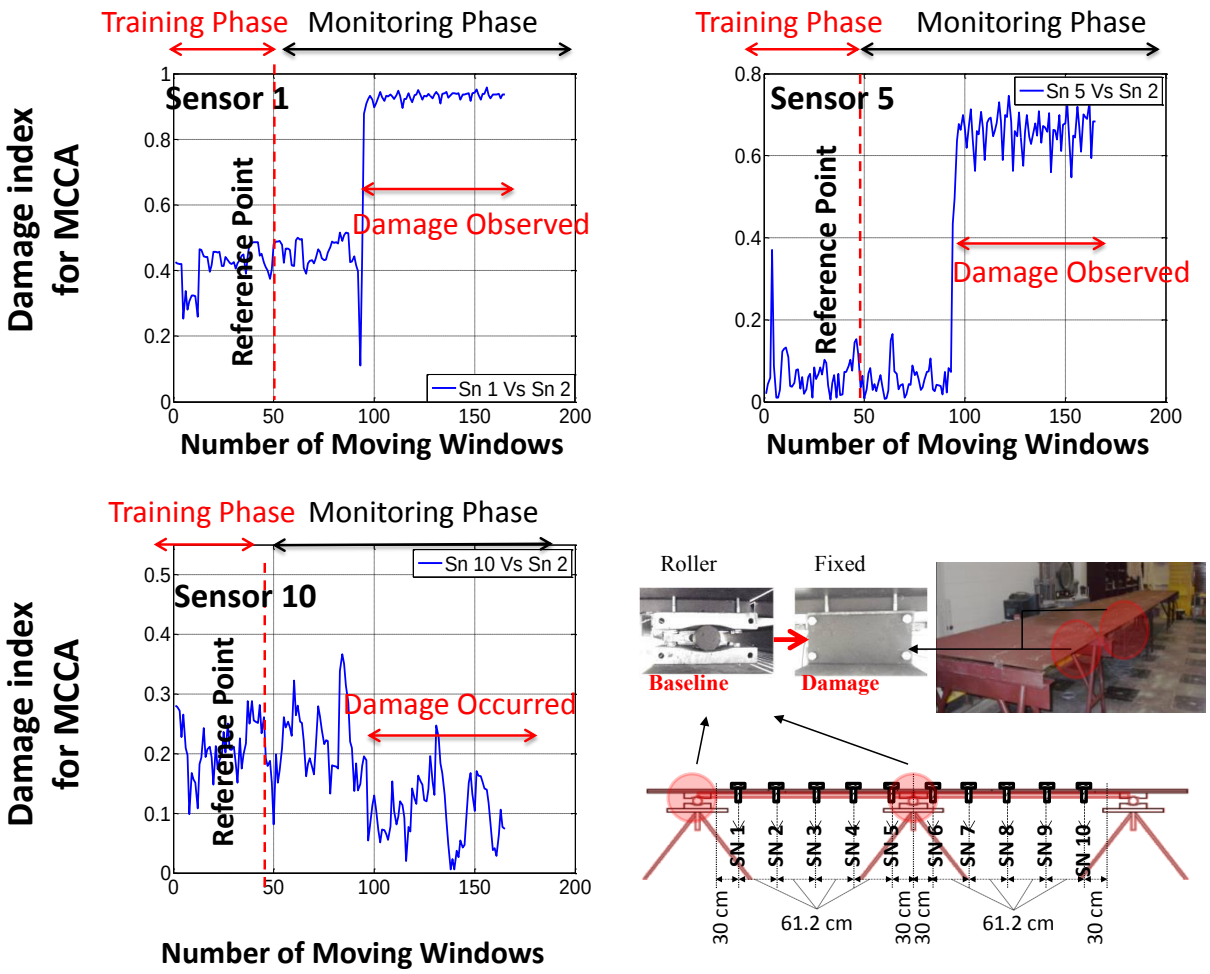

Figure 28: MCCA results for selected sensors (case2)

This damage is perhaps the most severe damage scenario, which is simulated in this study, and it is noticeable from the results. The PCA and coefficient values for both sensor 1 and 5 show obvious change after damage occurred. In fact, all the sensors located on the first span experienced the same situation.

4.8.3. Third Damage Scenario (Fixing the Middle Boundary Condition)

MPCA and MCCA outcomes for the third case are plotted in Figure 29 and Figure 30, respectively. Since only the middle boundary condition is altered, only sensor 5 experienced a significant

change. However, it is expected to have some minor unexpected force redistribution near the first and the last boundary. It is observed from MPCA and MCCA results that only sensor 5 expresses damage while almost no significant variation detected around sensor 1 and sensor 10.

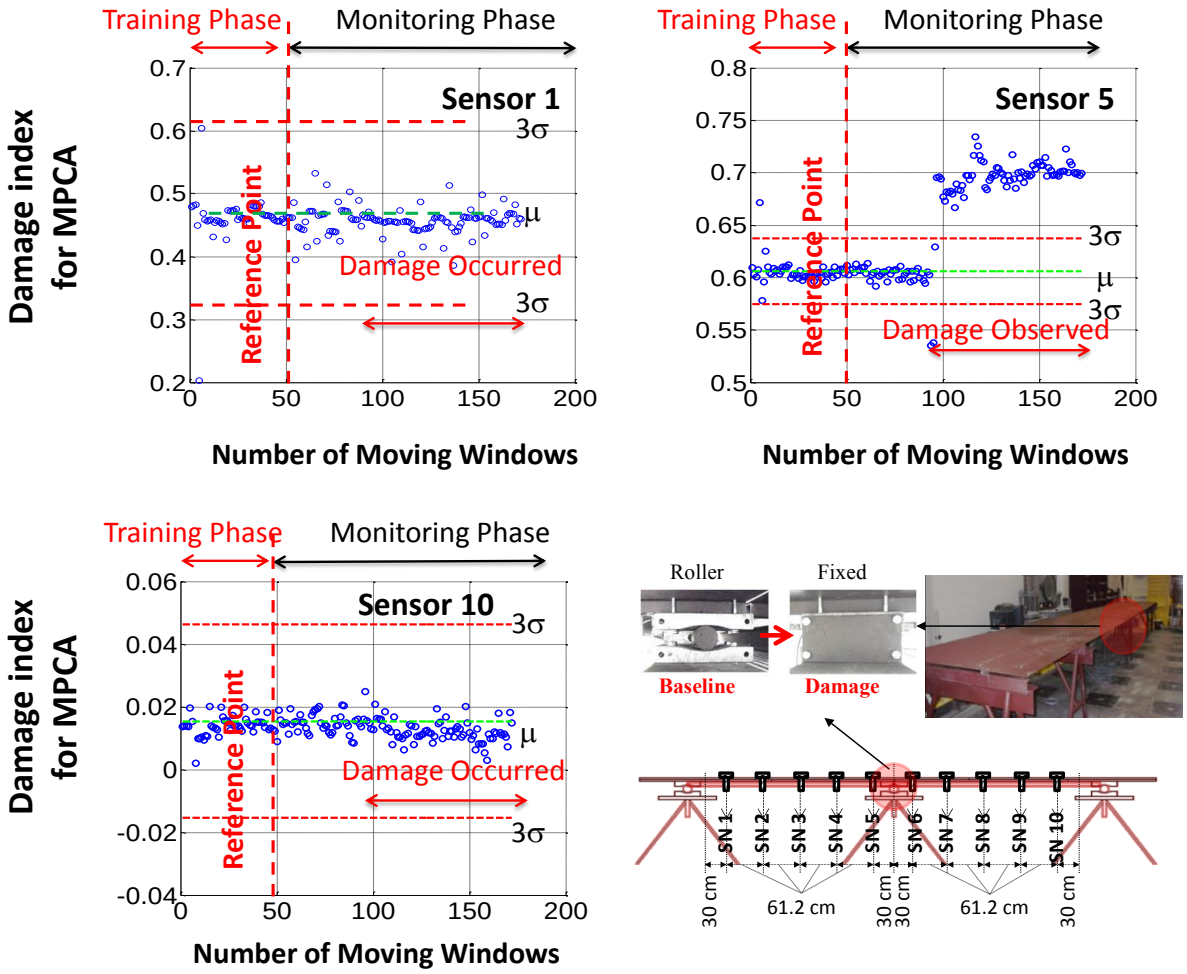

Figure 29: MPCA results for selected sensors (case3)

4.9. Local Assessment (MPCA and MCCA)

4.9.1. Fourth Damage Scenario (Removing Four Bolts from the First Span)

The fourth scenario is a local damage, which is common in bridge type structures. This damage scenario deals with lack of local connectivity, which was simulated on the 4-span bridge

by removing four bolts from the first span and close to middle bearing. The MPCA algorithm detects significant change at the position of sensor 4, which is at the location of the removed bolts.

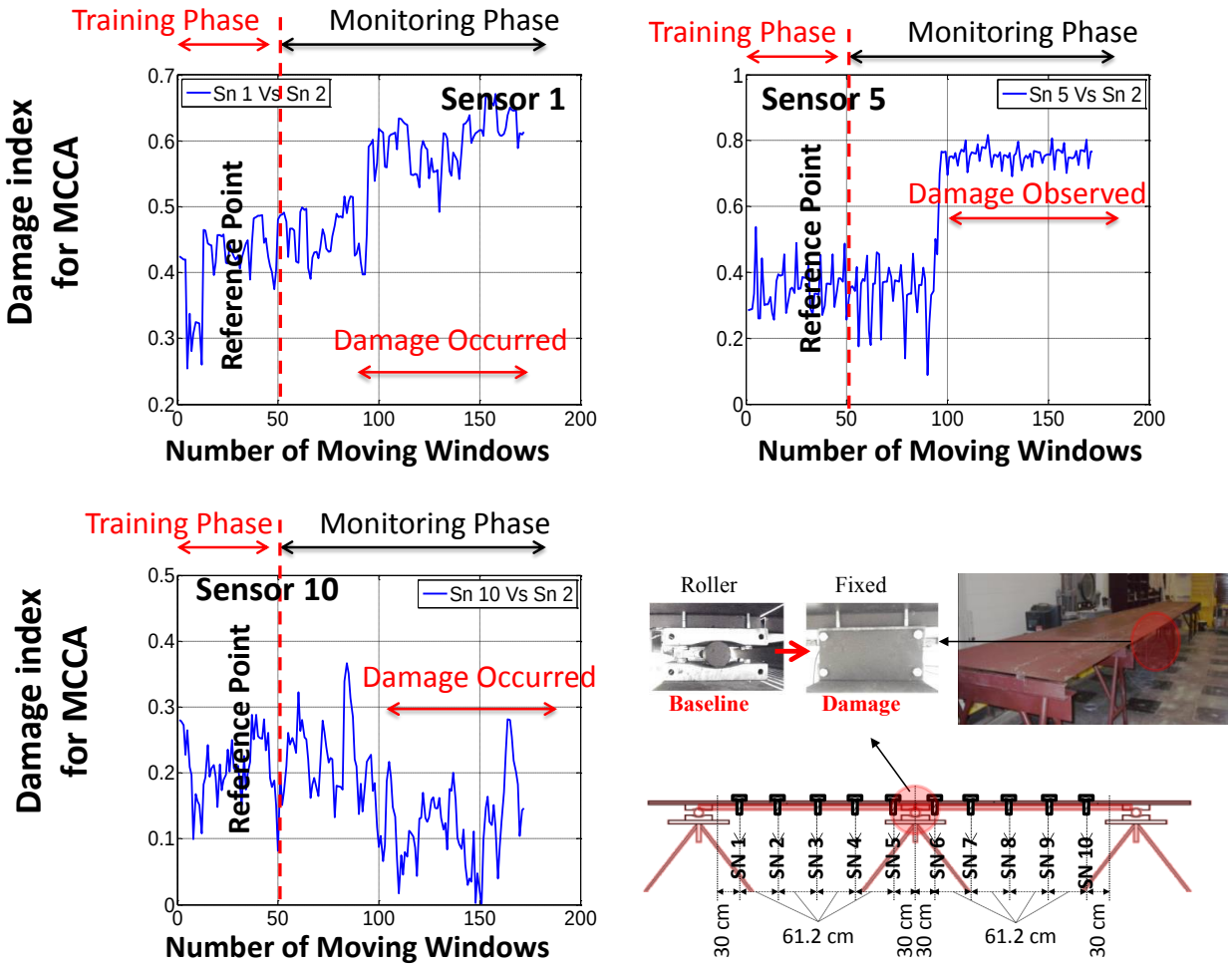

Figure 30: MCCA results for selected sensors (case3)

In addition, changes in principal component values are noticed to some extent around sensor 6 as well but not at the location of sensor 10. Similar results are obtained by MCCA algorithm. Performance of MPCA and MCCA for this case is very similar. The results for this case are shown in Figure 31 and Figure 32.

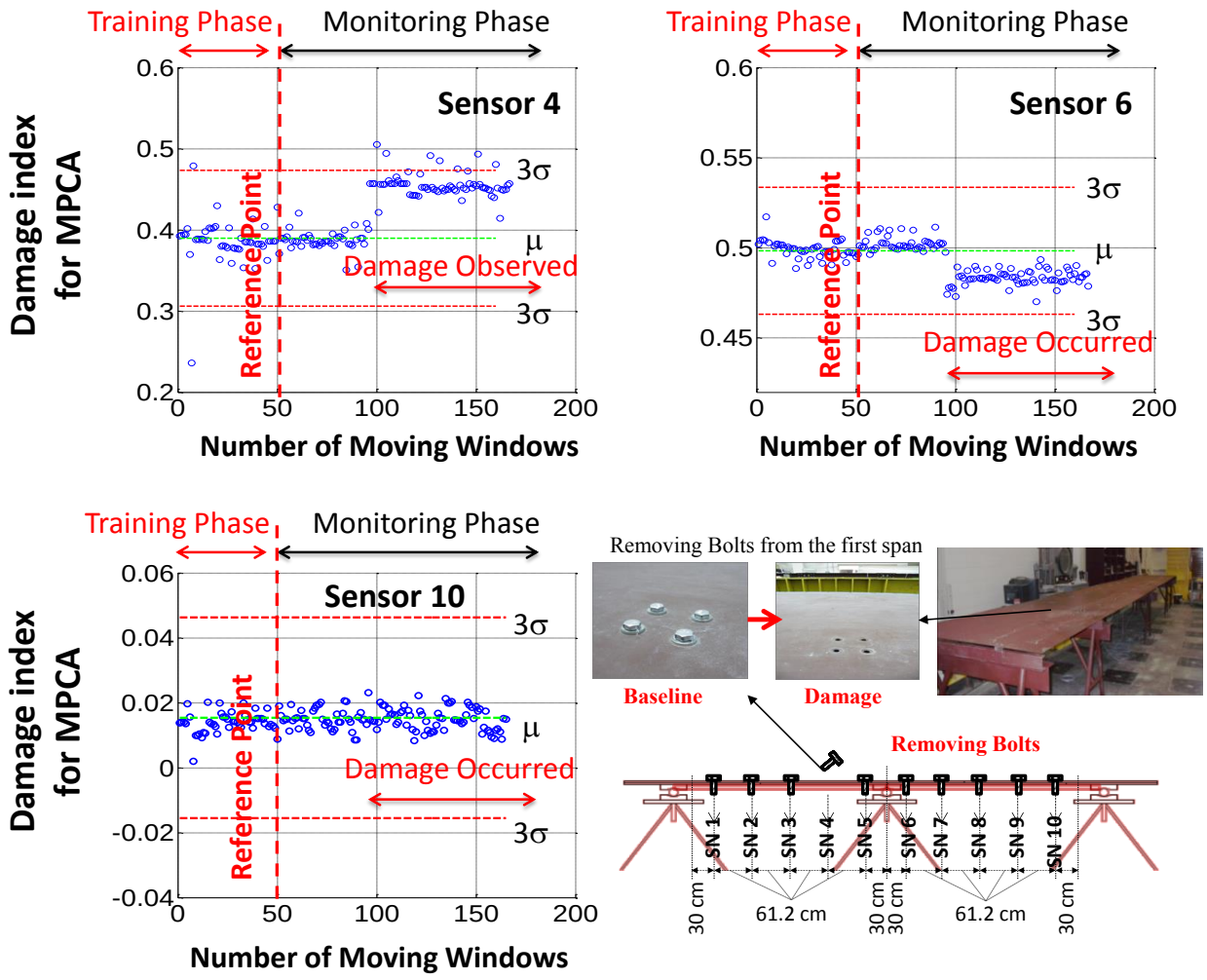

Figure 31: MPCA results for selected sensors (case4)

4.9.2. Fifth Damage Scenario (Removing Eight Bolts from the First and Second Span)

To end with, the last damage scenario simulates a distributed lack of local connectivity. For this reason, another four bolts are removed from the second span, which adds up to 8 removed bolts. Principal component values corresponding to both sensor 4 (close to the four bolts removed from first span) and sensor 7 (close to 4 bolts removed from second span) were affected due to this damage.

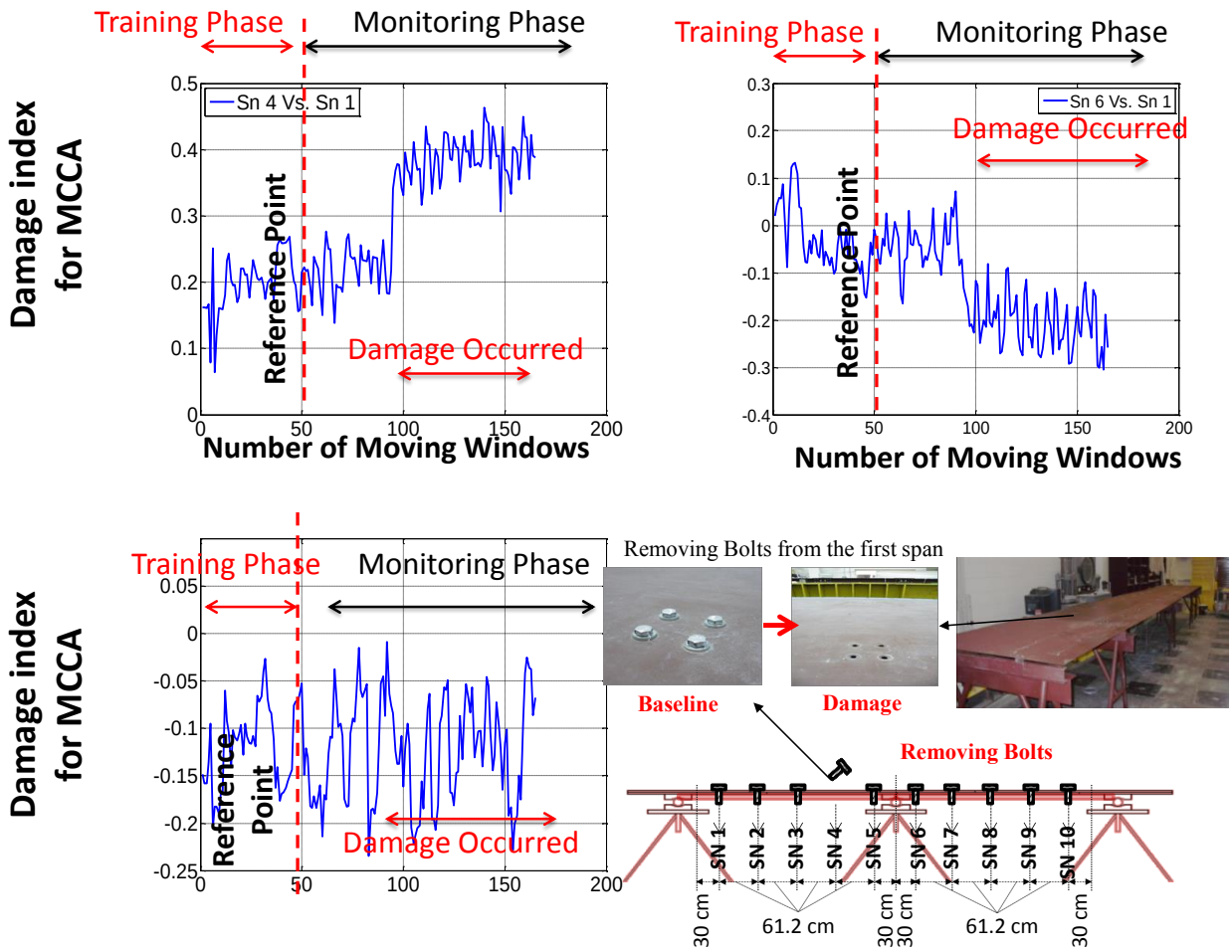

Figure 32: MCCA results for selected sensors (case4)

However, this value has not experienced any significant changes around sensor 10, which is located far from damage location. Similar observations can be made for MCCA method. The results are summarized in Figure 33 and Figure 34.

The only dissimilarities which can be noticed by comparing results from MPCA and MCCA for sensor 10, is that MCCA algorithm again shows better potential in detecting minor damage occurred away from the location of damage. Taking these two local induced damage scenarios into account and evaluating the MPCA and MCCA for detectability purpose, it is

revealed that these methods are efficient not only in terms of detection but also in the sense of measuring the intensity of abnormal behavior.

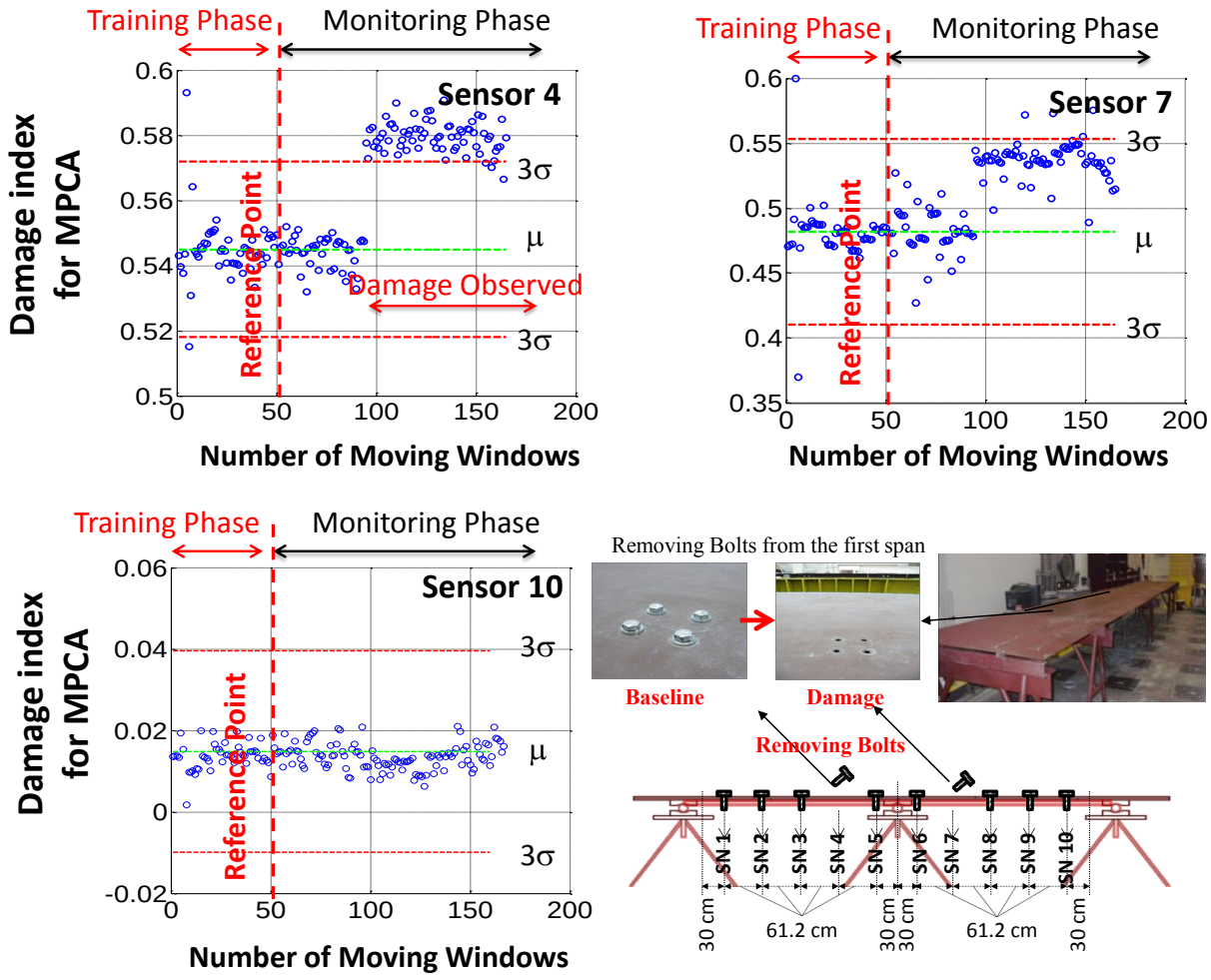

Figure 33: MPCA results for selected sensors (case5)

4.10. Concluding Remarks

The damage detection ability of four advanced multivariate statistics based algorithms is investigated for long term bridge monitoring application (long term response of structure was simulated) by taking advantage of FBG sensors. The CCA, RRA, MPCA and MCCA are four methods, which show promising results for real life and long term SHM. The effectiveness of

these algorithms was tested using a laboratory bridge structure instrumented with fiber optic sensors. The most common and critical damage scenarios have been selected and simulated on the structure including three global and two local damage scenarios.

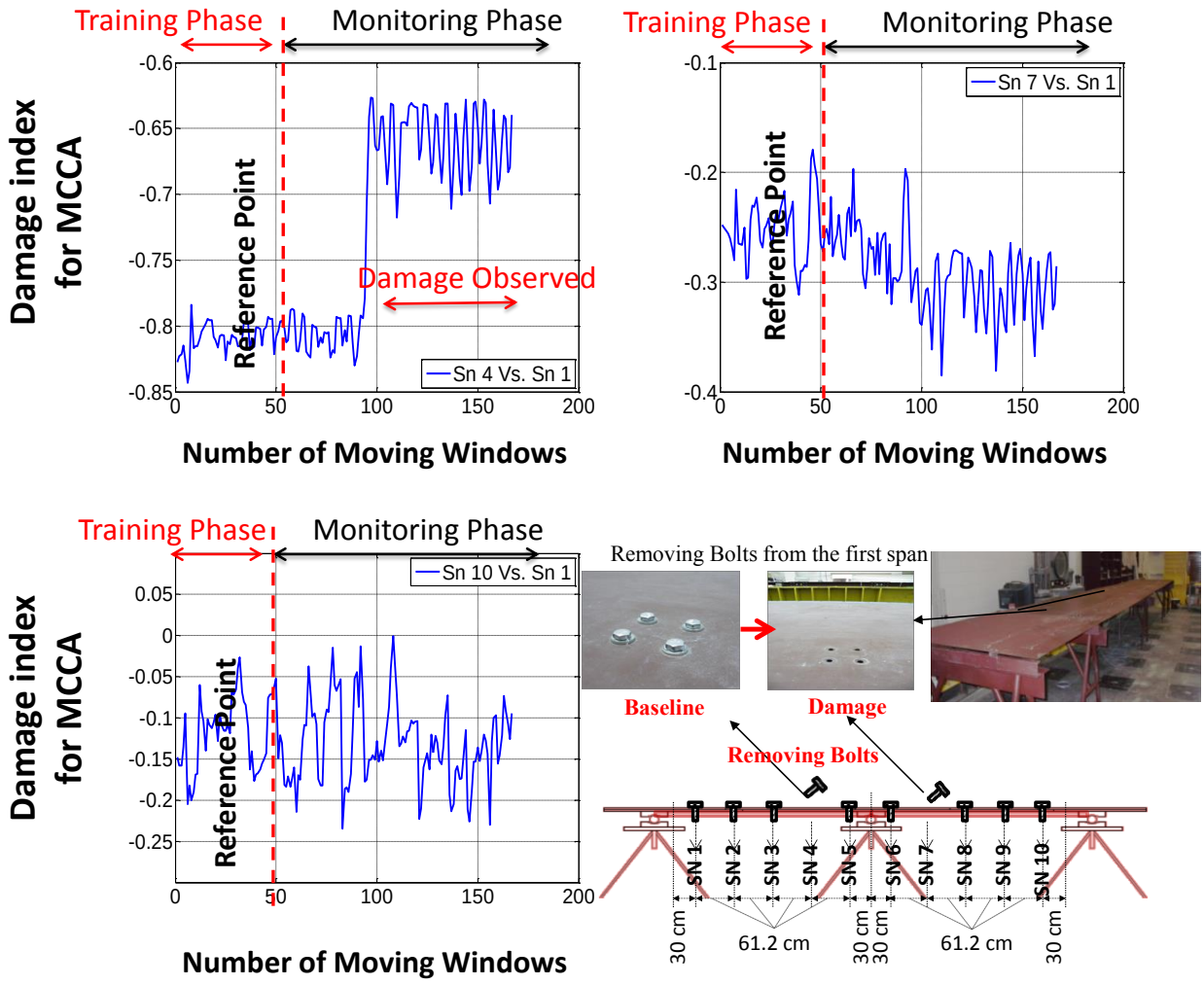

Figure 34: MCCA results for selected sensors (case5)

Afterwards, the proficiencies of the algorithms are tested for each case in damage detection, localization and intensity aspects. The results conceal that these methods are very promising for long term monitoring of structures.

However, throughout the next chapter a systematic comparison study is conducted based the new defined criteria. In addition, a new machine-learning damage detection algorithm is introduced to cover some of the main drawbacks associated with selected algorithms.

CHAPTER FIVE: AN INNOVATIVE MACHINE LEARNING ALGORITHM FOR LONG-TERM STRUCTURAL HEALTH MONITORING OF INFRASTRUCTURES: CONCEPT, LAB, AND REAL-LIFE STUDIES

5.1. Introduction

A systematic comparison study has been conducted on ten different data-driven based algorithms and it has been shown that only a few of these methods, including the Moving Principal Component Analysis (MPCA), Moving Cross Correlation Analysis (MCCA) and the Robust Regression Analysis (RRA) are applicable for long-term civil infrastructure monitoring [63-65]. Although these algorithms were proven to be more effective than other techniques, still there remain some main drawbacks associated with each method. For instance, the MPCA has a delay in detection whereas the RRA does not have a reliable detectability [63]. Therefore, neither of these techniques is quite reliable for the monitoring of critical infrastructure for which both detectability and timely detection are of the most concern.

Moreover, the other issue that has to be highlighted is that the above-mentioned comparative studies were conducted on numerically developed models of the civil structures, including a simple beam and a truss bridge. In fact, data were generated from numerically developed FE models with virtual sensors at different locations. However, in order to effectively evaluate the non-parametric algorithms for damage detection, long-term data from a real life structure is needed. This is an important issue because even if there are significant amounts of long-term data available from real life civil structures, to the best knowledge of the authors, there are only a few cases with the reported damage.

In response to these demands, three individual sections are designed for this chapter. The first section is dedicated to the presentation of an innovative machine-learning algorithm for damage detection. This real-time data interpretation method is designed and proposed to overcome some of the drawbacks associated with the existing methods. This method named as MPCA-CCA is developed by integrating the MPCA and CCA. The main intention is to reduce the delay in detection that comes with the MPCA and also improve detectability. Throughout the second phase (section) of this chapter, a systematic comparative study is conducted in which the MPCA, MCCA, RRA and MPCA-CCA are compared with respect to some critical criteria such as detectability, delay (time to detection), computational time, robustness to noise and window-size (required data sets for training phase) [93-94].

The data that is utilized for this section is collected from the experimental structure (4-Span Bridge) under different damage scenarios. Finally, the long-term SHM data from a unique real life structure is employed for evaluating the efficiency of the algorithms. For that reason, the Sunrise Boulevard Bridge is heavily instrumented with various types of sensors. More than 200 sensors were installed on both structural and mechanical components of the bridge. The baseline data has been collected continuously along with the data from three critical and common damage scenarios. It is shown that the MPCA-CCA outperforms MPCA other techniques in terms of detectability, timely detection and effect of noise.

5.2. An Innovative Machine-learning Algorithm (MPCA-CCA)

As it was pointed out, there is a main drawback associated with the MPCA algorithm. In fact, the associated delay in detection turns MPCA into an unreliable algorithm for monitoring of critical structures in which timely detection is of most concern. On the other hand, the RRA

algorithm has shown promising results in terms of time to detection (delay) but its detectability is considered a main weakness of this method. Consequently, neither of these techniques is desirable for real-time monitoring of civil infrastructure. Motivated by this issue, a combined machine-learning algorithm is designed and proposed in order to not only decrease the time to detection (delay in detection) but also increase the detectability of the existing methods, which accordingly makes it more competitive for real-life applications.

In order to achieve this objective, the damage indices that are derived based on the MPCA are further processed taking advantage of the Cross Correlation Analysis (CCA). The primary intention of adapting the CCA is to reduce the time to detection.

As a result, the algorithm is the integration of two statistical techniques including MPCA, and CCA. The steps that are involved in this algorithm are presented in Figure 35. The first three steps are the ones that were used for MPCA algorithms. For that reason, throughout the first step, the matrix of raw data is generated and consequently divided into two main portions named as training and monitoring phase. The data within the training phase is implemented for establishing the baseline condition.

In other words, the underlying distributions of the damage indices are learnt during the training phase and any significant variations from these distributions are reported as a change, which might be due to damage. Designing a fixed-size moving window which can move through the data is the next step in order and it is followed by conducting a PCA for the data inside each of the individual windows. The third step is to extract the damage indices for the MPCA, which was discussed in chapter 3. Having extracted the damage indices for the MPCA, the following step is to conduct a cross correlation analysis.

Basically, the idea behind designing the fourth step (Figure 35) is to track the correlation of different time series of eigenvector (the first principal component). The underlying assumption is that if damage occurs then it should affect the correlation coefficient of the eigenvectors.

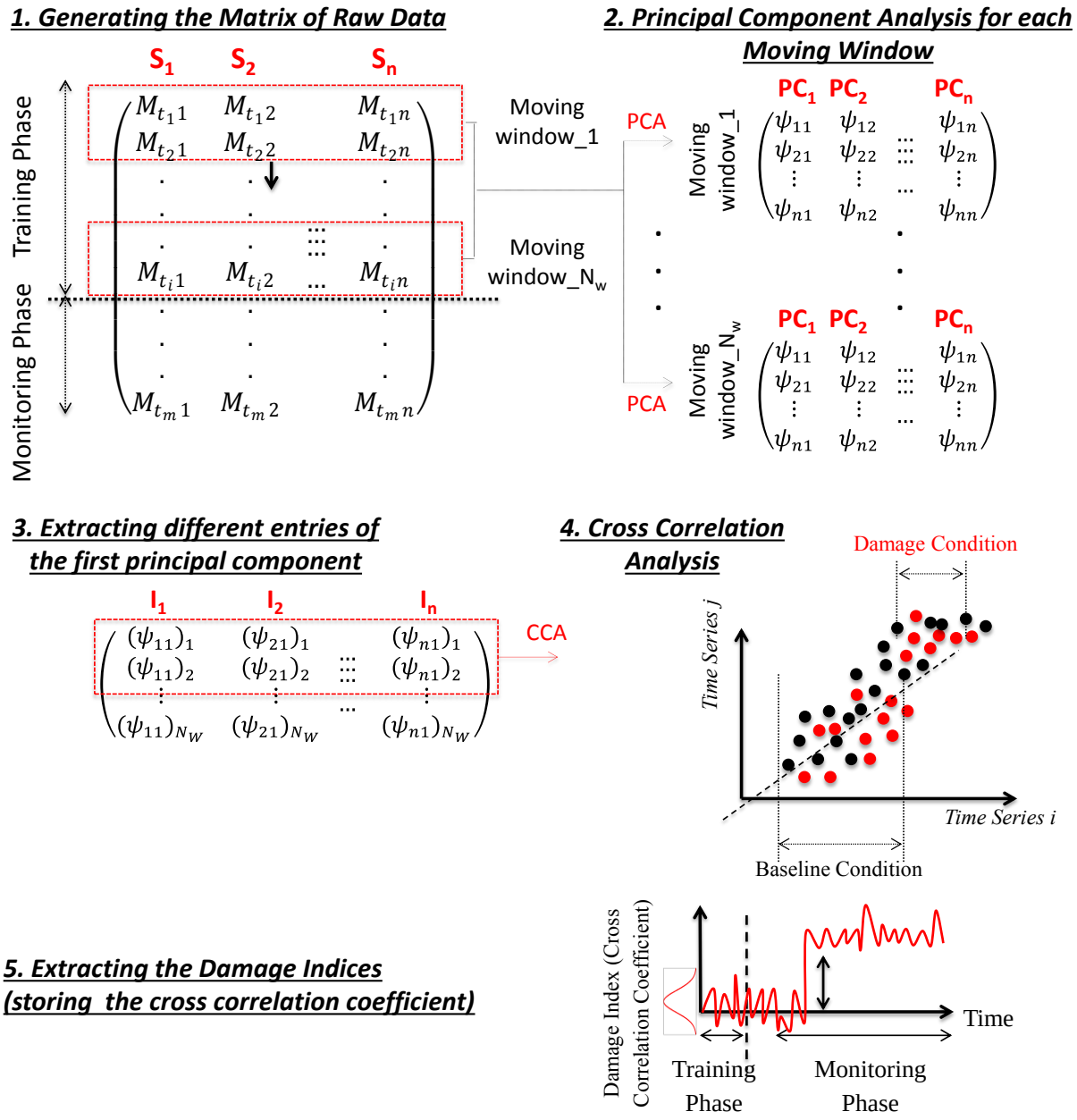

Figure 35: Steps that are involved in MPCA-CCA algorithms

Therefore, another fixed-size window is defined and moved through the matrix of time series. The CCA analysis is performed for each window and subsequently the correlation coefficients are determined. These coefficients are then monitored to detect any abnormal behavior in the system (step 5 in Figure 35).

Figure 36, presents the flowchart in which the above-mentioned procedure for MPCA-CCA algorithm is summarized. After learning the underlying distributions of the new damage indices (time history of correlation coefficient values) any variation from that is reported as abnormal behavior and accordingly utilized to take the corresponding maintenance action. The entire process for MPCA-CCA is coded in Matlab software. In the following sections, the efficiency of the proposed algorithm is challenged by conducting a systematic comparison study on the MCCA, MPCA, RRA and MPCA-CCA.

5.3. Part I: Lab Study on Four Span Bridge Using Fiber Bragg Grating Sensor (FBG)

5.3.1. Experimental Test (Experimental Structure and the Implemented Damage Scenarios)

In order to conduct a systematic comparative study, several experiments with a laboratory bridge model (UCF 4-span Bridge Model) were designed and tested. The in-housed developed FBG system is used as a measurement system. Three different damage scenarios (two global damages as well as one local) as shown in Figure 37 are considered for this systematic comparative study.

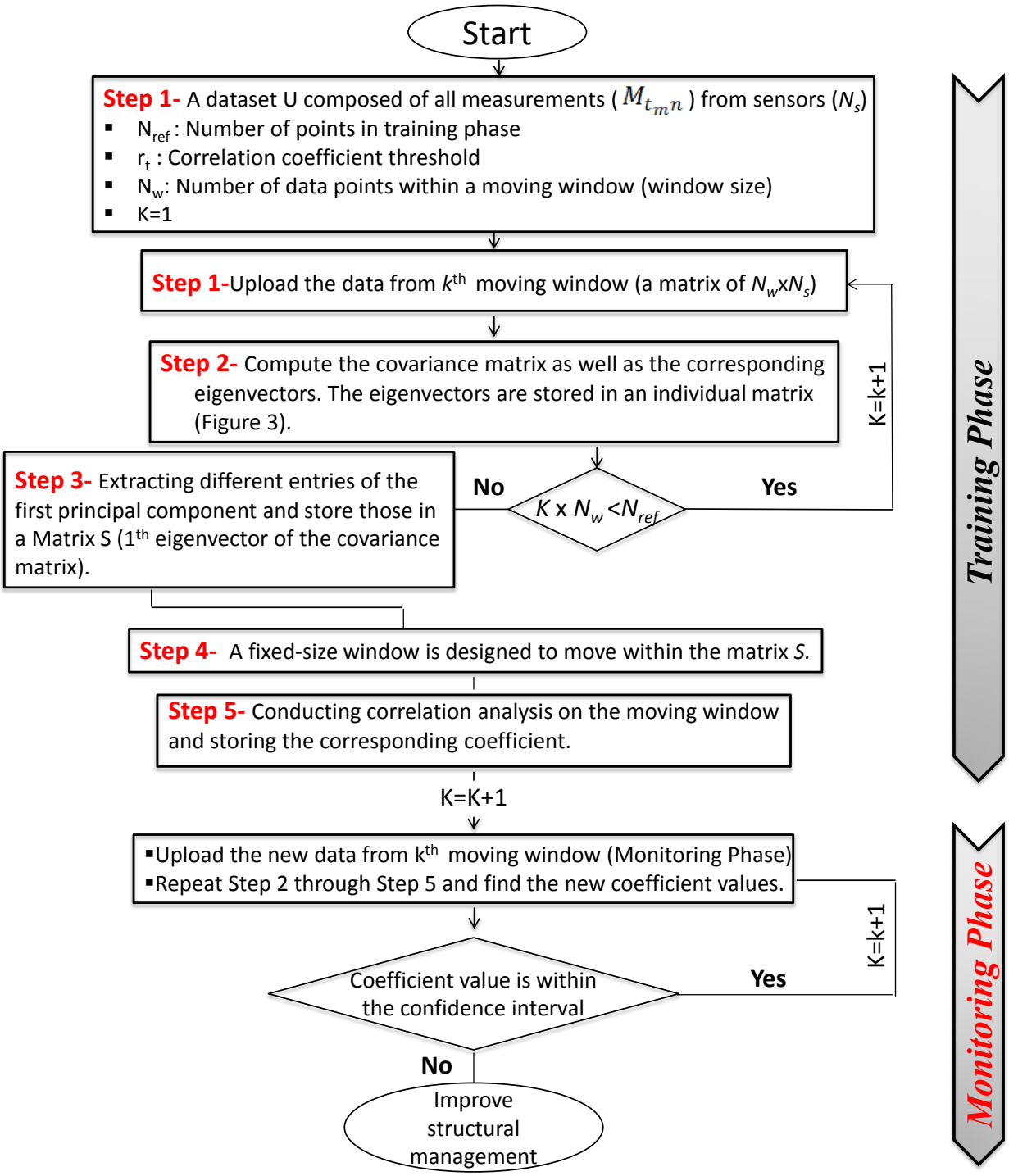

Figure 36: The sequential steps for conducting MPCA-CCA algorithm

The global damages were simulated by changing the boundary conditions while the local damage was simulated by removing 4 bolts from the first span of the bridge (see Figure 37).

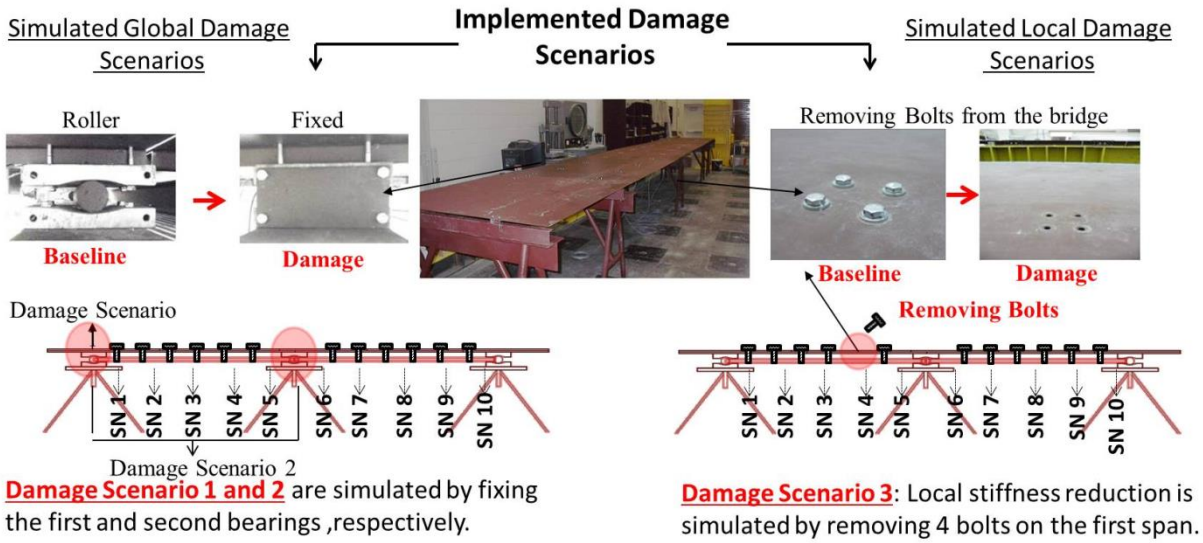

Figure 37: The implemented damage scenarios for systematic comparative study

5.4. Systematic Comparison of the Algorithms Using Experimental Data

In this section the results from the lab study are presented in a comparative fashion. Selective results obtained from different damage detection algorithms under individual damage scenarios are illustrated in Figure 38. In addition, the results are reviewed and systematically compared with respect to different criteria, including detectability, time to detection, effect of noise, computational time and size of the window. Therefore, considering these unique criteria, one would be able to select an appropriate algorithm for a desired application.

5.4.1. Detectability

Detectability is the primary feature of a reliable damage detection algorithm. As it is clear from the name, it refers to the ability of an algorithm to identify an abnormal behavior based on the signals streaming from a given structure.

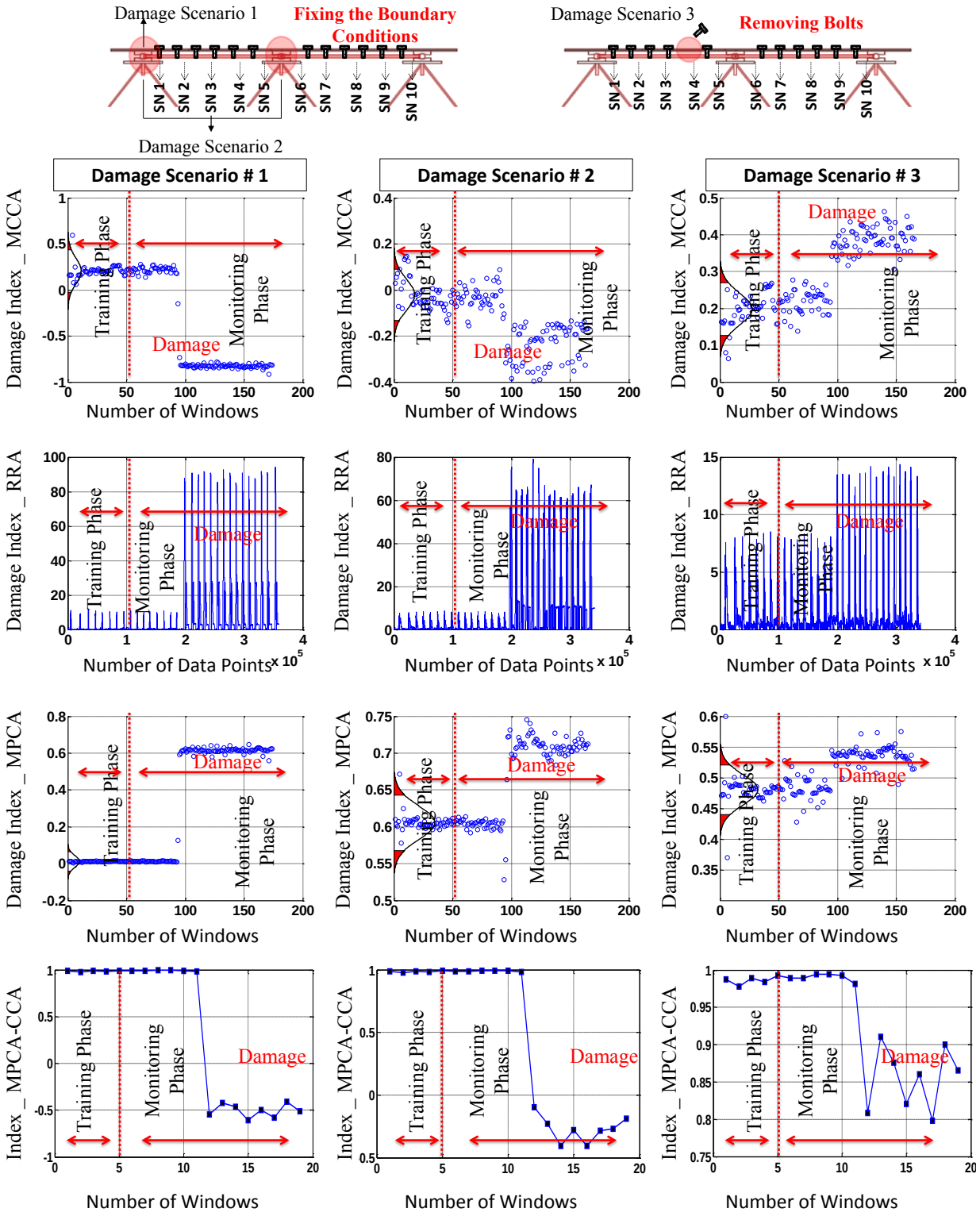

Figure 38: Selective results of different algorithms under different damage scenarios

Although it is a very critical aspect of a detection algorithm, and can significantly influence the selection of the algorithm, there is not any specific criterion to quantify detectability. In this study, as a first step to systematically compare the selected algorithms, a criterion is defined to quantify the detectability ability of a given algorithm.

When it comes to designing a network of sensors (number and location of sensors) for a given structure, there are always several scenarios or arrangements of sensors available. In other words, there is not any straightforward approach for designing a network of sensors, in particular with respect to civil structures. Therefore, a robust algorithm in terms of detectability is the one which is less sensitive to the arrangement of sensors. In fact, a reliable algorithm is one that can detect damage regardless of the arrangement of sensors (network design). In this study, the detectability is calculated utilizing the following equation:

$(N_C)_{\text{Damage}}$= The number of the sensor networks that generate the data with which the algorithm is able to detect the damage

$(N_C)_{\text{total}}$= The total number of sensor networks that can be designed for a given structure.

$$\text{Detectability} = \frac{(N_C)_{Damaged}}{(N_C)_{Total}} \times 100 \quad (15)$$

In fact, the detectability increases when the $(N_C)_{Damaged}$ increases which indicates that the algorithms is less sensitive to the arrangement of sensor. For instance, consider a case in which a designer has to design a network of sensor including two FBGs for monitoring the 4-Span Bridge. As it is demonstrated in Table 2, there are 10 candidate locations for installing two FBG sensors and as a consequence there are $\binom{10}{2} = 45$ different configurations or designs available for that purpose.

Table 2: Potential design scenarios for network of FBG sensor (4-Span Bridge)

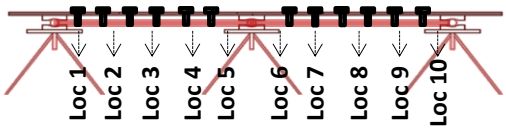

Design ID	Locations	Design ID	Locations	Design ID	Locations
1	(1-2)	16	(2-9)	31	(5-6)
2	(1-3)	17	(2-10)	32	(5-7)
3	(1-4)	18	(3-4)	33	(5-8)
4	(1-5)	19	(3-5)	34	(5-9)
5	(1-6)	20	(3-6)	35	(5-10)
6	(1-7)	21	(3-7)	36	(6-7)
7	(1-8)	22	(3-8)	37	(6-8)
8	(1-9)	23	(3-9)	38	(6-9)
9	(1-10)	24	(3-10)	39	(6-10)
10	(2-3)	25	(4-5)	40	(7-8)
11	(2-4)	26	(4-6)	41	(7-9)
12	(2-5)	27	(4-7)	42	(7-10)
13	(2-6)	28	(4-8)	43	(8-9)
14	(2-7)	29	(4-9)	44	(8-10)
15	(2-8)	30	(4-10)	45	(9-10)

The data is generated under different damage scenarios and collected using all the possible designs for sensor networks (45). Finally, employing Equation 15, the detectability indices are computed and the results are plotted in Figure 39. The results reveal the fact that, the MPCA-CCA algorithm has a better detectability in comparison with other techniques and with respect to all the considered damage scenarios.

On the contrary, the RRA has the worst performance in terms of detectability. It is also noticed that, the performance of MPCA is slightly better than that of the MCCA and also that, the detectability of the MCCA, MPCA and RRA has considerably decreased when it comes to local detectability. On the other hand, it is realized that the detectability of the MPCA-CCA is more robust with respect to the type of damages (local and global).

5.4.2. Time to Detection

Another parameter that is playing an important role in selecting the algorithm is time to detection or the corresponding delay. Time to detection is the period of time between the moment that the damage occurs and the moment that the damage is detected by the algorithm. Timely detection is very important for most of the structures, especially critical ones such as nuclear plants or aircrafts. In fact any delay in detecting damage in such a structure may result in detrimental consequences. Figure 39 presents the delay in detection associated with each damage detection technique.

The very first observation is that, unlike in detectability, with respect to time to detection, the RRA algorithm has by far the most reliable performance among any other tested method. It is also observed that after the RRA, the MPCA-CCA algorithm has the least associated delay in detecting abnormal behavior. Alternatively, the MPCA and MCCA have the most delay in detection of change/damage. On the other hand, the MPCA-CCA algorithm is the most reliable technique (among the tested methods) in terms of detectability while it has the least delayed in detection after RRA. The performance of the MPCA and MCCA are acceptable when it comes to detection, however, these techniques do not express consistent behavior regarding to time to detection criterion. Therefore, considering these two criterions, the MPCA-CCA algorithm has the superior performance in comparison with other discussed methods.

5.4.3. Effect of Noise

The effect of noise on the detectability of different techniques is illustrated in Figure 39. The most important point is that the detectability of the MPCA-CCA is not sensitive to the

presence of noise in data. In other words, the detectability indices of the MPCA-CCA are almost identical for data with and without noise, which is an advantage especially for real-life and civil infrastructure applications. Alternatively, the RRA is the technique that is most influenced by the presence of noise in the data.

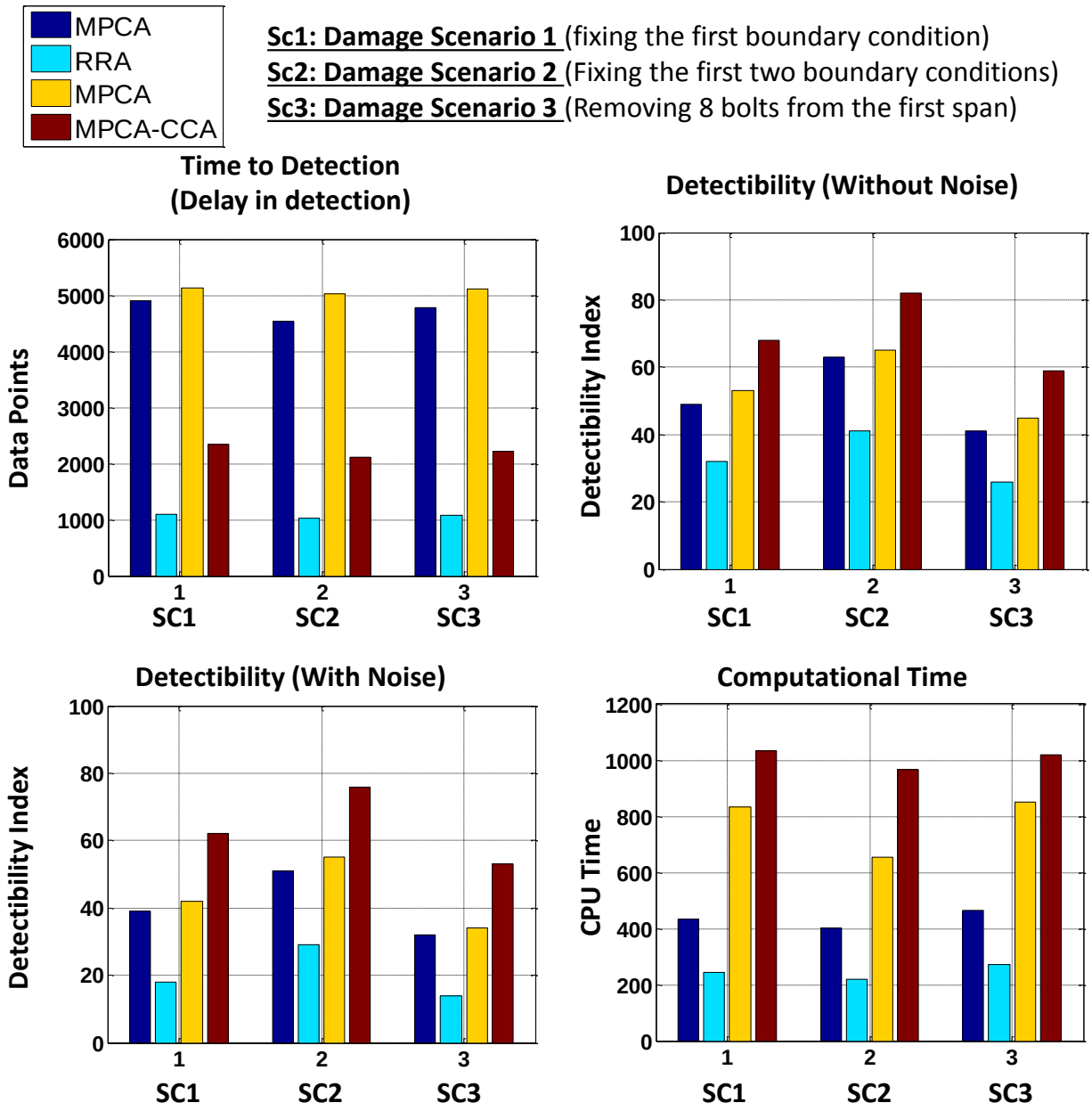

Figure 39: Systematic comparison study on the selective algorithms

In fact the detectability index (RRA) drops by 40% in the presence of noise. The performance of the MPCA and MCCA is also to some extent affected by the presence of noise.

5.4.4. Computational Time

The demanded time for a damage detection algorithm is referred to as computational time. This parameter becomes a critical issue in particular with respect to long term monitoring of a complex civil structure in which one is dealing with huge amounts of data. The RRA by far outperforms other techniques regarding computational time.

The MPCA-CCA obviously requires much more than the RRA since it is dealing with two statistics and machine learning techniques (CCA and MPCA). The MPCA also needs a significant amount of time to be performed. However, the MCCA needs much less time in comparison to the MPCA and MCCA-CCA. The results for computational time are presented in Figure 39.

5.4.5. Size of the Moving Window and Required Data for Training Phase

The size of the window is a key parameter for the MPCA and MCCA as well as for the MPCA-CCA algorithm. Commonly it is recommended that the window should be large enough so that the damage indices are not influenced by periodicity of the data. Alternatively it should be small enough to timely detect abnormal behavior. This is a very general prescription and in most of the cases there is not any straightforward procedure to identify the window-size. Therefore in this section a procedure is proposed as a method to define effective window-size for MPCA, MCCA and MPCA-CCA. It is worth noting that the window-size for the MPCA-CCA is

identical to the one used for the MPCA. Therefore in this section only the results related to the MPCA and MCCA are discussed.

Another important feature for an unsupervised damage detection algorithm is the amounts of data sets that are required for the training phase. The advantage is given to the algorithm that needs the least number of data sets to establish the baseline. The amount of data that is needed by an unsupervised algorithm for the training phase directly depends on the size of the window. As a consequence, a new approach is proposed in this study to identify the appropriate size of the window and accordingly the required training data-sets. The sequential steps for this approach are presented as follow:

Step 1: The largest periodicity in the data (P) is identified.

Step 2: A vector of window-size is generated as follows:

Window Size= [0.1P, 0.2P… 3P, 4P]

Step 3: The damage indices are derived for all the window-sizes (in the vector) and the stochastic process for the corresponding damage indices are plotted (see Figure 40). The optimized window-size is the smallest one that results in a stationary process as it is illustrated in Figure 40. The corresponding results for the MPCA and MCCA are visualized in Figure 40. The horizontal axis indicates the size of window whereas the vertical axis presents the mean of the corresponding damage indices. The results are presented for the first damage indices.

The left plot in Figure 40 contains 10 plots, which are the corresponding mean of damage indices calculated by the MPCA algorithm while the right one expresses the mean of damage indices for the MCCA. As it is noticed, the size of the window that is required for the MCCA

(8500 data points) is significantly less than the one needed for the MPCA (11500 data points). In other words, the MCCA requires less data for training in comparison to MPCA and accordingly to the MPCA-CCA. This is a major advantage for an unsupervised detection algorithm.

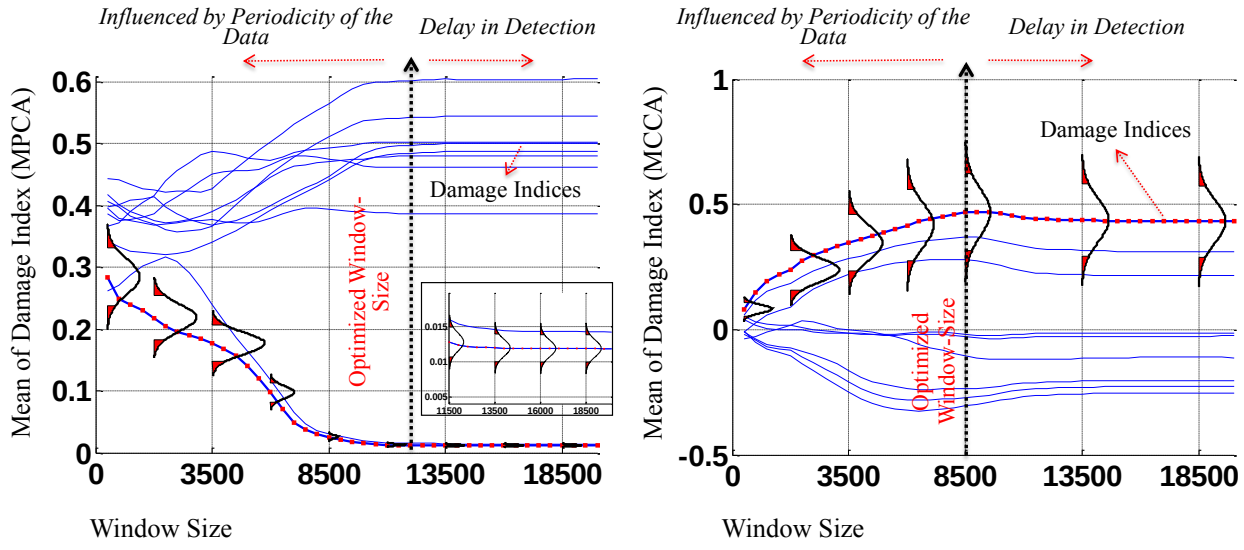

Figure 40: The procedure for selecting an optimized size for the moving window

As it is obvious from Figure 40, if the window size is selected less than 11500 data points for the MPCA, then the damage indices are influenced by periodicity of the data. This significantly reduces the detectability of the MPCA algorithm.

On the other hand, selecting any window-size larger than 11500 data points will cause delay in detection. Therefore, in the case that there is limited amount of data available from a baseline (healthy) structure, the priority is given to the MCCA as the best option for processing and interpreting of the data. Therefore, Table 3 is generated based on the above-mentioned criteria including detectability, effect of noise, computational time, time to detection (delay in detection) and the required size of window. This Figure can be utilized as a reference for selecting an appropriate algorithm for a particular application.

Considering all the selected criteria, the proposed algorithm (MPCA-CCA) can be chosen as a reliable damage detection algorithm. The performances of these algorithms are further investigated and challenged utilizing the data from a unique real-life structure.

Table 3: Systematic comparison of the selective non-parametric algorithms (darker colors indicates more advance performance)

Criteria / Method	Detectability with Noise		Detectability without Noise		Delay in Detection	Computational Time	Required Training Data
	Global	Local	Global	Local			
RRA							
MCCA							
MPCA							
MPCA-CCA							

5.5. Part II: Real-life Study Utilizing the Data from Sunrise Movable Bridge

The objective of this part is to explore the efficacy of the MPCA and MPCA-CCA algorithms (as two of the effective methods) for detecting abnormal behavior from the large-size SHM data sets which are collected over years. In fact, the algorithms are challenged in terms of not only detectability performance but also the ability to handle large-size SHM data sets, which is a big advantage for long-term monitoring of civil infrastructure.

Therefore a movable bridge, Sunrise Boulevard Bridge, has been instrumented with various types of sensors and has been monitored for the past five years, as it is shown Figure 41. The data has been collected continuously from the baseline and also some of the critical and common damage conditions.

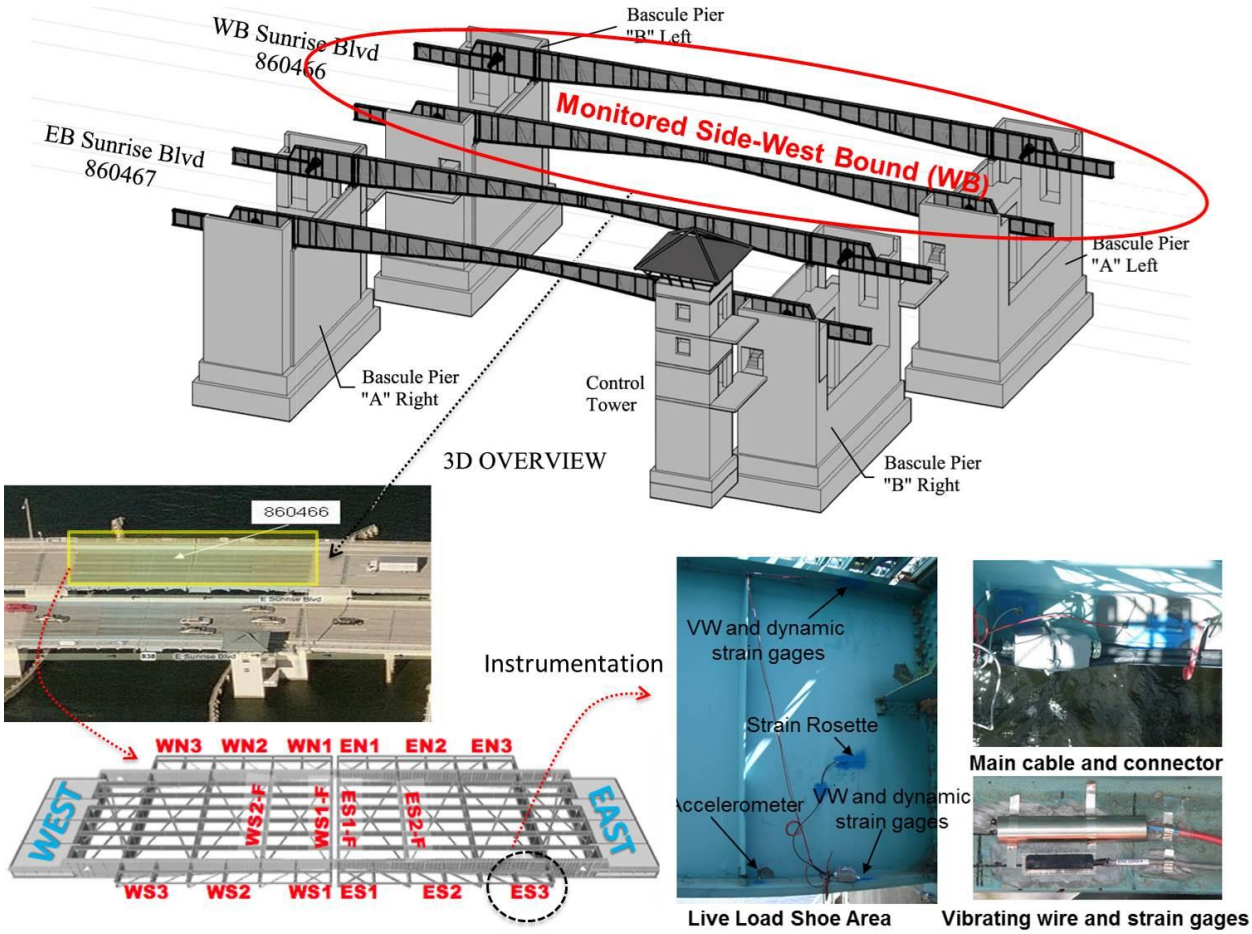

Figure 41: Sunrise Boulevard Bridge, Fort Lauderdale, Florida, United States

In fact, having access to data from damage conditions is one the unique aspects of this study since there are only a few cases where damage data from a real-life structure is available. The selected movable span of the bridge is the West-bound span of two parallel spans on SR-838, crossing a canal in Ft. Lauderdale, FL.

This span was constructed in 1989. It has double bascule leaves, with a total length of 35.7 m, and a width of 16.3 m, carrying three traffic lanes. The most critical electrical, mechanical and structural components are monitored by a comprehensively designed monitoring system consisting of an array of 160 sensors which add up to 200+ channels [92].

The structure is equipped with appropriate sensors at the most critical locations including, girders, floor beams, stringers, live load shoes (LLSs) and span locks (SPs). In this study, the strain data that is collected by dynamic SGs (Hitec weldable) at 12 individual locations along the bottom flange of the main girders is used (Figure 42).

The data is captured with 250 Hz sampling frequency. Figure 41 illustrates the locations of SGs and corresponding nomenclatures, WN refers to West North and ES refers to East South.

In a 24-h period, three prescheduled time slots (morning and early and late afternoons), corresponding to peak hours of operation are selected for data collection. Each data set is collected for 5 min continuously for each data set. Field tests were conducted to establish thresholds for conditions that are critical for the maintenance and operation of the bridge. These conditions will be referred to as "damage". In collaboration with FDOT engineers, some of the most common structural maintenance problems are identified and subsequently implemented on the movable bridge to simulate the damage condition. These damage scenarios are discussed as follow.

5.5.1. Implemented Damage Scenarios

Critical issues that create maintenance problems on the bridge are discussed and simulated on the Sunrise Boulevard Bridge based on the detailed investigation of the bridge inspection reports and interviews with the bridge engineers. The two main structural damage scenarios for this study are live load shoe (LLS) shim removal and span lock (SL) shim removal. A combined damage scenario was also applied to the structure. First, the West South LLS shims were removed (Case-1), then the West South SL shims were removed for the combined damage

scenario (Case-2), and finally the LLS shims were installed again to see only the SL effect on the structure (Case-3), as it illustrated in Figure 42.

The Live Load Shoes (LLS) are the support locations of the main girders when the bridge is in closed position (Figure 42). For the Sunrise Blvd. Bridge the LLS is located forward of the trunnions. Cracking and wear are rarely seen on the live load shoe, but mainly, operational problems, such as loss of contact, are of concern. If misaligned or improperly balanced, the bridge may not fully sit on the LLS. In that case, the dead load and traffic load are transferred to the gears and shafts, which cause damage to mechanical assemblies. Small gaps also lead the girders to pound on the live load shoes, which results in further misalignment, additional stresses, fatigue damage, and excessive wear.

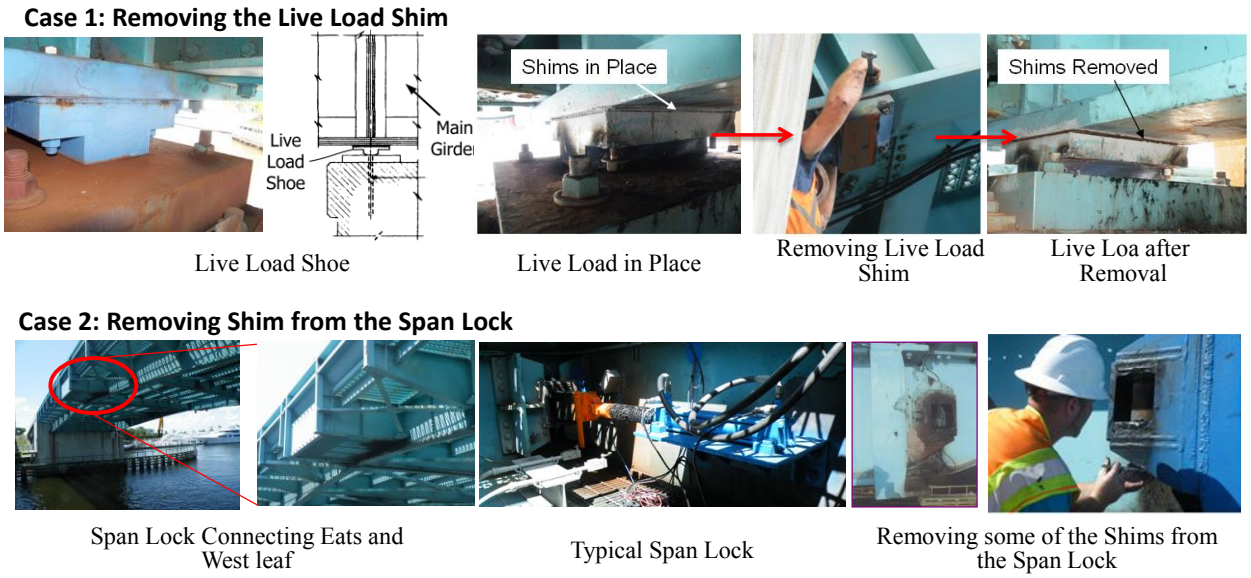

Figure 42: Simulating the maintenance issues as individual damage scenarios on the Sunrise Bridge

Case-1 is the creation of a gap (around 1/8" up to 3/16") between the West South LLS and resting support pads, which corresponds to non-fully seated LLS (Figure 42). This will cause

misalignment and problems for proper opening and closing of the leaves. Moreover, because of the inadequate support conditions, bouncing may occur in the girders, creating additional stresses due to impact as well as stress redistribution possibly subjecting the structure to different internal forces.

In double leaf bascule bridges, Span Locks (SL) are used to connect the tip ends of the two cantilever bascule leaves forcing both leaves to deflect equally (Figure 42). Consequently, this situation prevents a discontinuity in the deck during the operational traffic. In most of the span locks, there are two main components: the receiver and the rectangular lock bar.

5.5.2. Results from Real-Life Study

The corresponding results for the MPCA and MPCA-CCA are summarized in Figure 43 through 45. The results are quite interesting since the MPCA algorithm was found ineffective for real-life bridge monitoring. In the earlier study, it is shown that this algorithm (MPCA) is quite effective for detecting the abnormal behaviors which were simulated on the 4-Span Bridge in structural laboratory. However, when it comes to long-term monitoring of a movable bridge only the MPCA-CCA remains effective. It was already discussed in the first part of the study that the MPCA-CCA has several advantages in comparison to others in terms of detectability, time to detection and also immunity to noise.

The damage index, which was calculated by the MPCA algorithm and it is displayed in Figure 43 is bounded within the confidence interval. There is not, therefore, any abnormal behavior that can be observed during the time that damage was introduced (the highlighted part in Figure 43). Alternatively, the corresponding damage index for the MPCA-CCA is sensitive

enough to detect the induced damage, live load shoe shim removal. Figure 43 displays an abrupt jump in the results related to the MPCA-CCA right after inducing the damage.

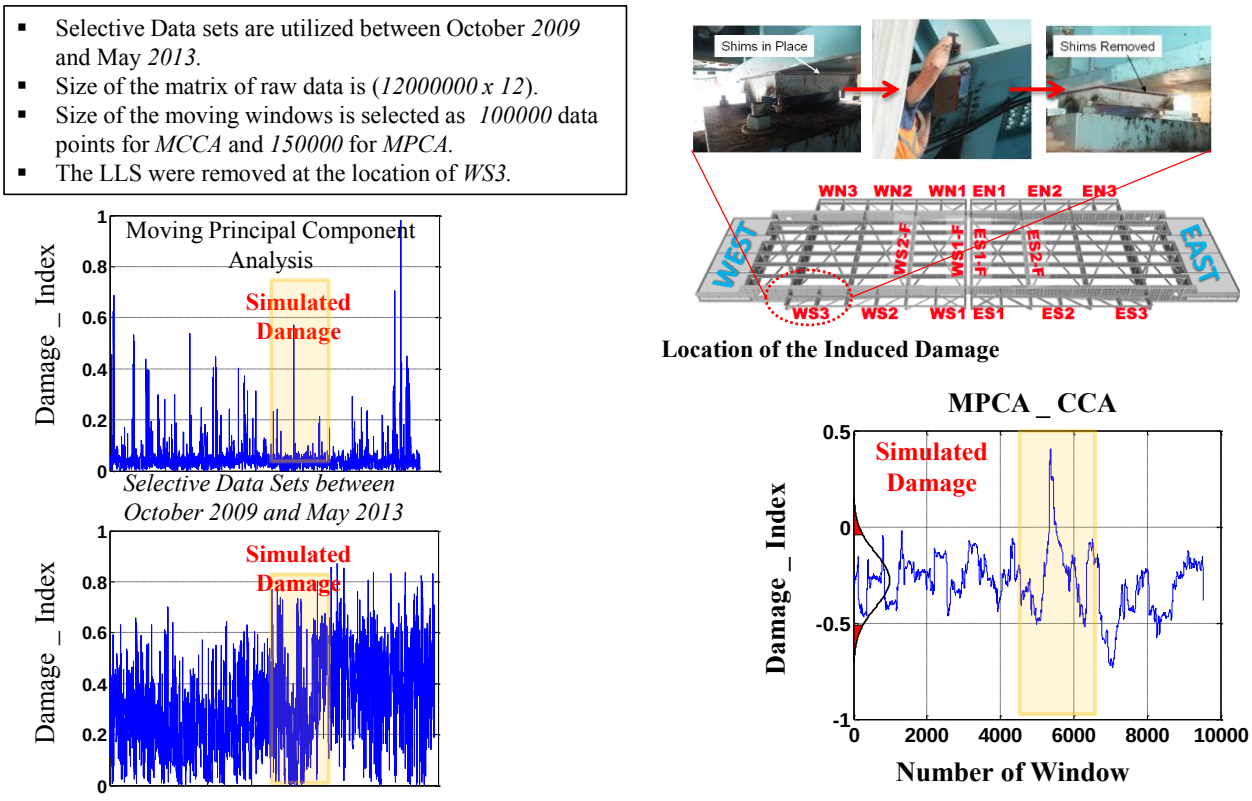

Figure 43: The corresponding results for case 1(removing some of the shim from the live load shoe close to the location of WES3 sensor)

Figure 44 illustrates the corresponding results for the second damage scenario which is the most severe induced damage scenario in this study. It is obvious that the MPCA has failed to capture the malfunction while the MPCA-CCA could detect it clearly. In fact, integrating the MPCA with the CCA increases the detectability of the MPCA algorithm to a level that it allows it to be considered a reliable algorithm for real-life applications. Moreover, after fixing the structure and replacing the live load, the damage index from MPCA-CCA is shifted back to the level it was before inducing the damage.

This is an important conclusion since it is revealed the fact that the damage index from MPCA-CCA can be directly linked to the performance condition of the structure. As a result, although the MPCA has shown promising results with respect to lab study, it is not a reliable one for long-term bridge monitoring.

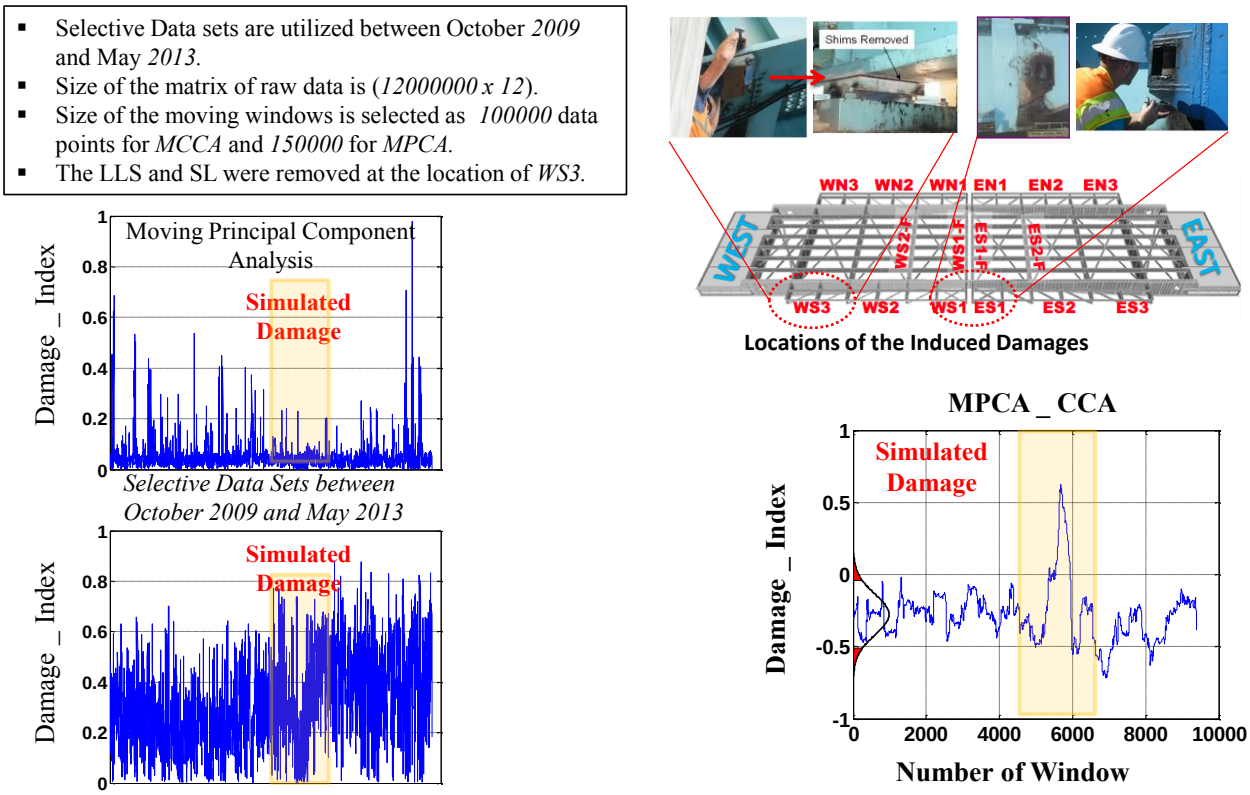

Figure 44: The corresponding results for case 2 (removing some of the shim from the span lock and live load shoe close to the location of WES3 and WS1 sensors)

Finally, Figure 45 presents the results for the third damage scenarios. As it obvious from the results, similar to the previous cases, only MPCA-CCA could detect the induced damage. This further emphasises the reliability of the proposed damage detection algorithm (MPCA-CCA).

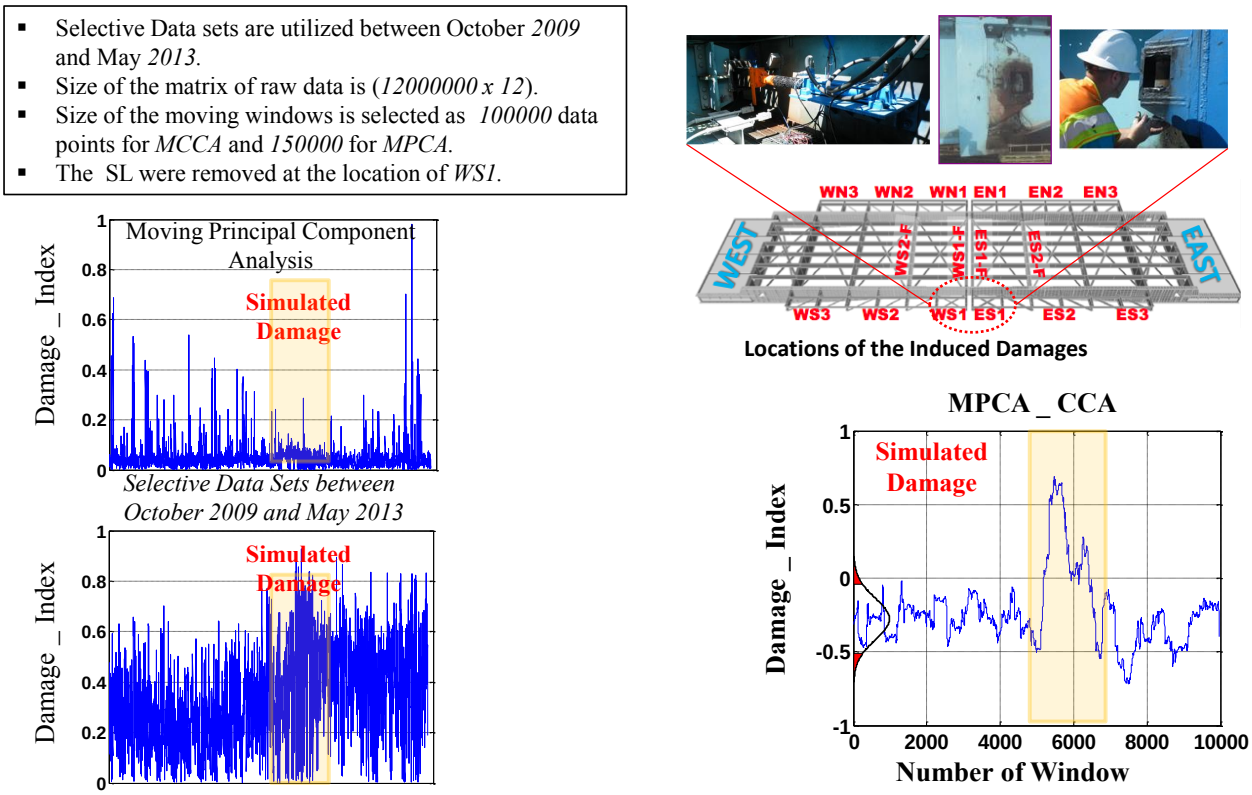

Figure 45: The corresponding results for case 3 (removing some of the shim from the span lock and close to the location of WS1 sensor)

5.6. Concluding Remarks

This chapter has been dedicated to investigate the efficiency of some of the selective damage detection algorithms in conjunction with a new designed algorithm for long-term monitoring of civil infrastructures. A systematic study is conducted between the proposed algorithm and other selective ones introducing critical criteria including local and global detectability, computational time, delay in detection and the amount of required training data sets. A new approach is introduced for identifying the detectability and also the amount of required training data sets.

An experimental study is conducted using an in-house developed FBG system and the 4-Span Bridge. Some of the critical damage scenarios associated with bridge structures are identified and simulated on the 4-Span Bridge and the data is accordingly collected using FBG sensors. It is shown that the proposed algorithm outperforms the existing methods in terms of detectability and time to detection (delay in detection).

It is also observed that the RRA algorithm has a better performance with respect to computational time as well as time to detection. The MCCA is preferred when it comes to amount of the required training data sets. Finally, the MPCA has an acceptable performance regarding detectability while it is not reliable when it comes to time to detection. In addition to the lab study, the proposed algorithm is further challenged and explored utilizing the data from a unique real-life structure, the Sunrise Movable Bridge.

The data is unique in the sense that it includes the data from both baseline and damage conditions. In fact, some of the critical damage conditions are induced on the Sunrise Movable Bridge and the data is collected under traffic load. This data is then fed into the MPCA-CCA algorithm to test the detectability of the proposed method. It is concluded that the MPCA-CCA algorithm could detect the introduced damage while the MPCA has failed to identify any abnormal behaviors. Therefore, the MPCA-CCA can be implemented for continuous real-life monitoring of civil infrastructures.

CHAPTER SIX: A MACHINE LEARNING APPROACH TOWARD ON-LINE OPERATIONAL MONITORING OF THE CRITICAL MECHANICAL COMPONENTS OF A MOVABLE BRIDGE

6.1. Introduction

In this chapter an investigative study for automated data processing method is developed using non-parametric data analysis methods for real-time condition maintenance monitoring of critical mechanical components of a movable bridge. A maintenance condition index is defined for identifying and tracking the critical maintenance issues. The efficiency of the maintenance condition index is then investigated and demonstrated against some of the corresponding maintenance problems that have been visually and independently identified for the bridge.

6.2. Condition Assessment of the Critical Mechanical Components of the Sunrise Movable Bridge

For static structures, monitoring of structural components is usually the only concern for maintenance, safety and operation; however, for movable bridges, the monitoring of mechanical and electrical components is equally important. Bridge opening and closing operations induce additional stress on the structural and mechanical components of a movable bridge due to mechanical and dynamic forces.

Therefore, a properly designed monitoring system for a movable bridge should be considered all structural, mechanical and electrical components of a movable bridge. This chapter is concentrated on the mechanical part of the project where the objective is to monitor the maintenance conditions of mechanical components (see Figure 46).

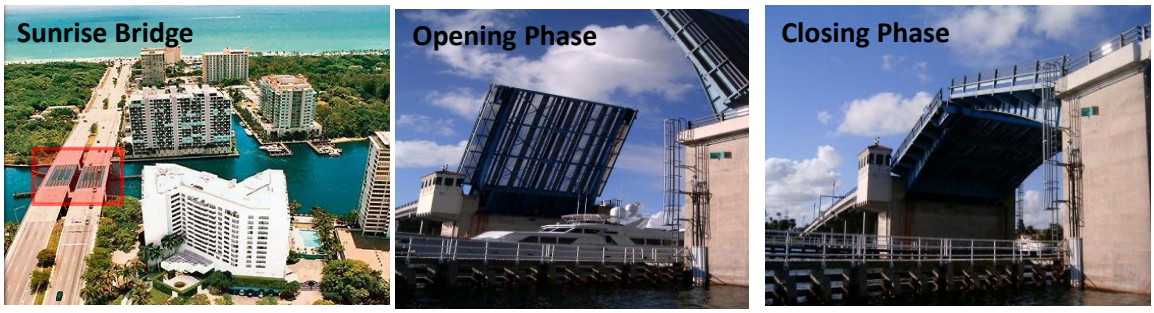

Figure 46: Sunrise Bridge in Ft. Lauderdale, Florida

The most important components are the gearbox, motor, rack and pinion, shaft, open gear and trunnion. Locations of some of these components are schematically illustrated in Figure 47. In this study, the corresponding data sets from gearbox, motor and rack and pinion are utilized.

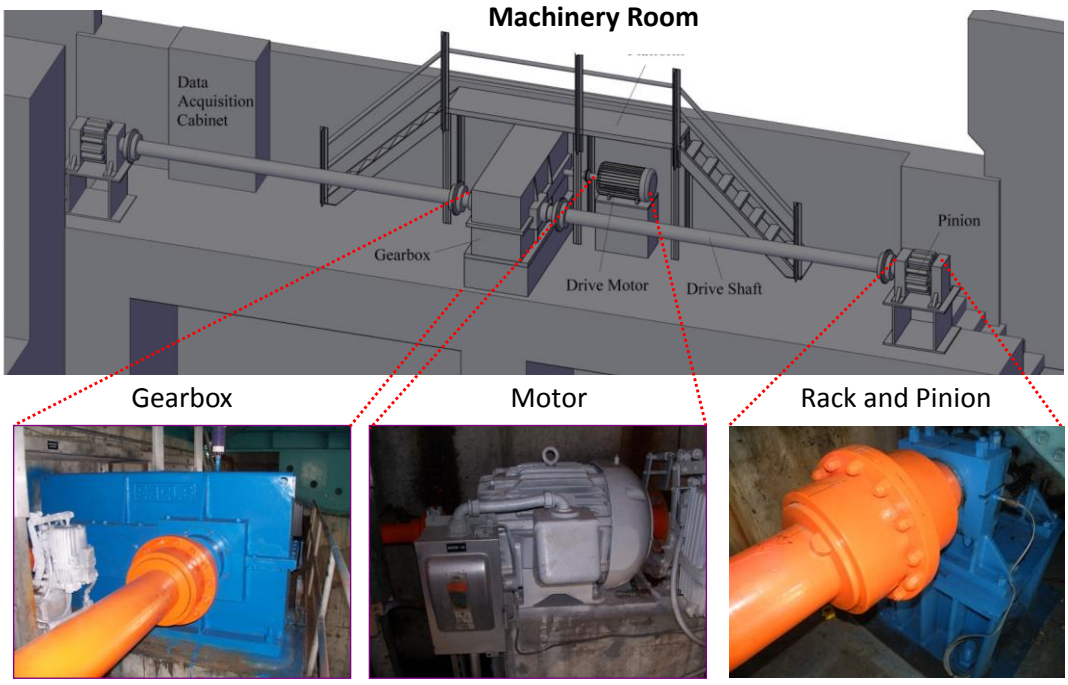

Figure 47: Machinery Room for the mechanical components of the Sunrise Bridge

Herein, a brief discussion on each of these components including their functionality and the implemented sensors are presented.

6.2.1. Critical Mechanical Components

6.2.1.1. Gearbox

The gearboxes contain the assembly that transmits the torque generated by the motor to the shafts (Figure 48). When the gearboxes experience deterioration or lack of lubrication, some change in the vibration and sound characteristics during the bridge operation should be noted. Abnormal vibration is an indicator of wear in the gears. Oil viscosity is also an important parameter for proper functioning of the gearbox. Considering these issues, the monitoring system included four accelerometers to measure the vibration of the gearbox during bridge opening and closing events.

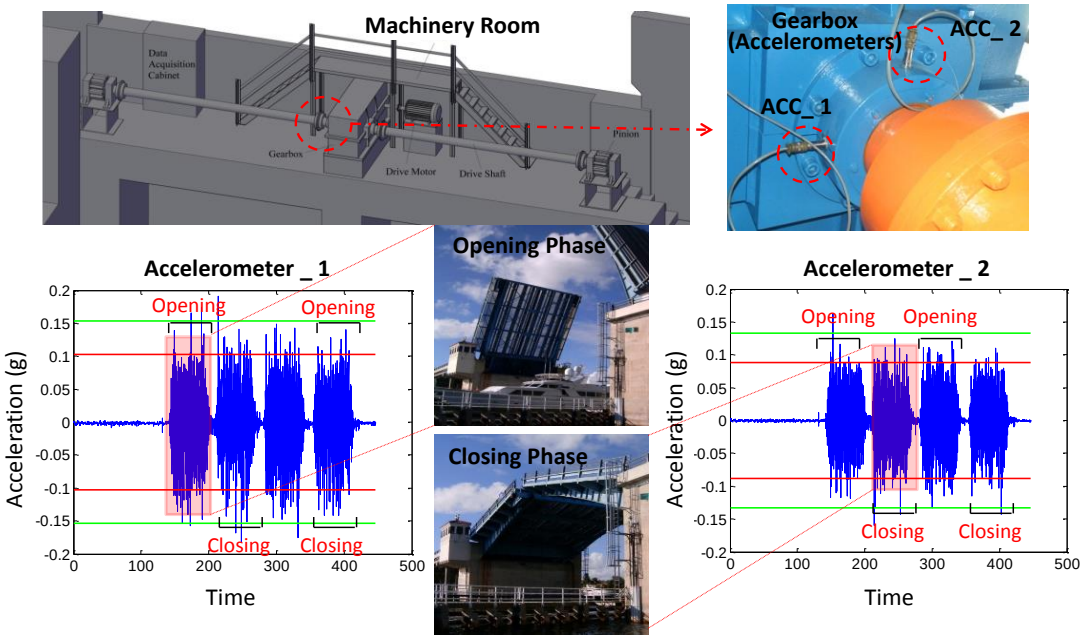

Figure 48: Sample measurement from the gearbox during opening and closing phases

Furthermore, microphones were also installed in the vicinity of the gearbox to determine its acoustic signature for opening and closing events. In this study, as mentioned earlier, the data collected with accelerometer during opening phase is used (Figure 48).

6.2.1.2. Electrical Motor

The electrical motors generate the torque required for the opening and closing of the bridge. Some of the indicators for improper functioning of the electrical motors are high amperage, high temperature, high vibration level and high revolution speed.

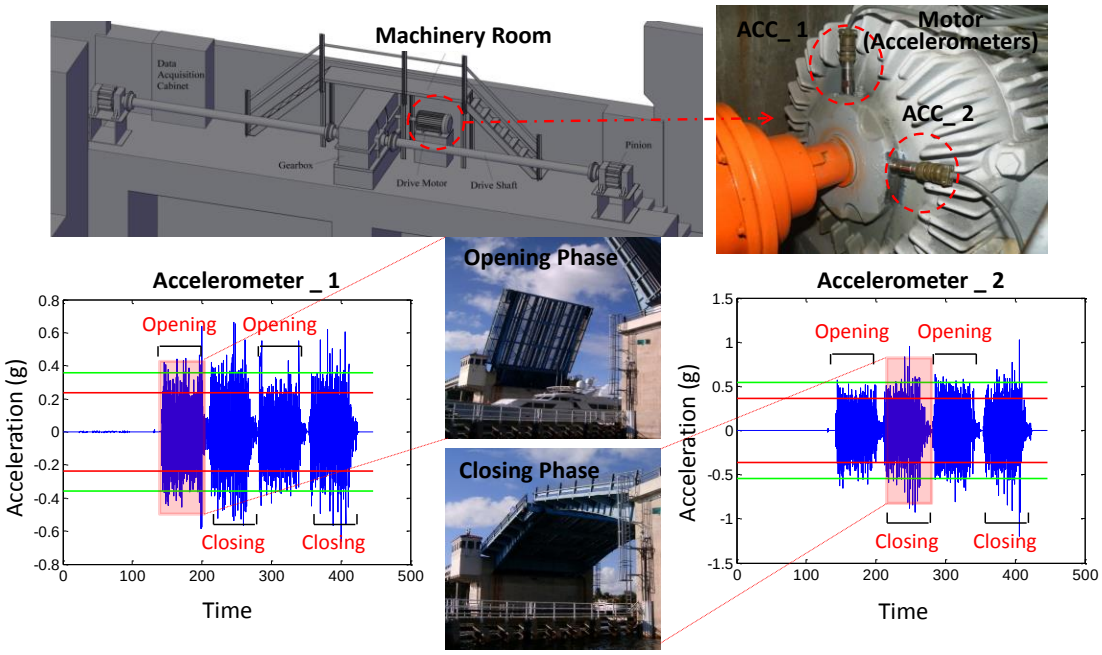

Figure 49: Sample measurement from the motor during opening and closing phases

Therefore, it was decided that the monitoring system would include ampmeters to measure the amperage levels for each one of the electric motor phases, two accelerometers to measure the vibration on the motor during the bridge openings and closings, and infrared temperature sensors to monitor the temperature of the electrical motor (Figure 49). Similar to the gearbox, the vibration data collected using the accelerometers is investigated to disclose the maintenance condition of the electrical motor.

6.2.1.3. Rack and Pinion

The open gears are the main gears, which are part of the leaf main girder and receive the torque from the rack and pinion assembly. Corrosion due to lack of lubrication, excessive strain, out-of-plane rotation and misalignment are common problems for open gears. Another concern is loading sequence problems, which mean that the drive shafts begin rotation in delayed sequence. This has an adverse effect on the condition of the open gears, usually by causing impact loading.

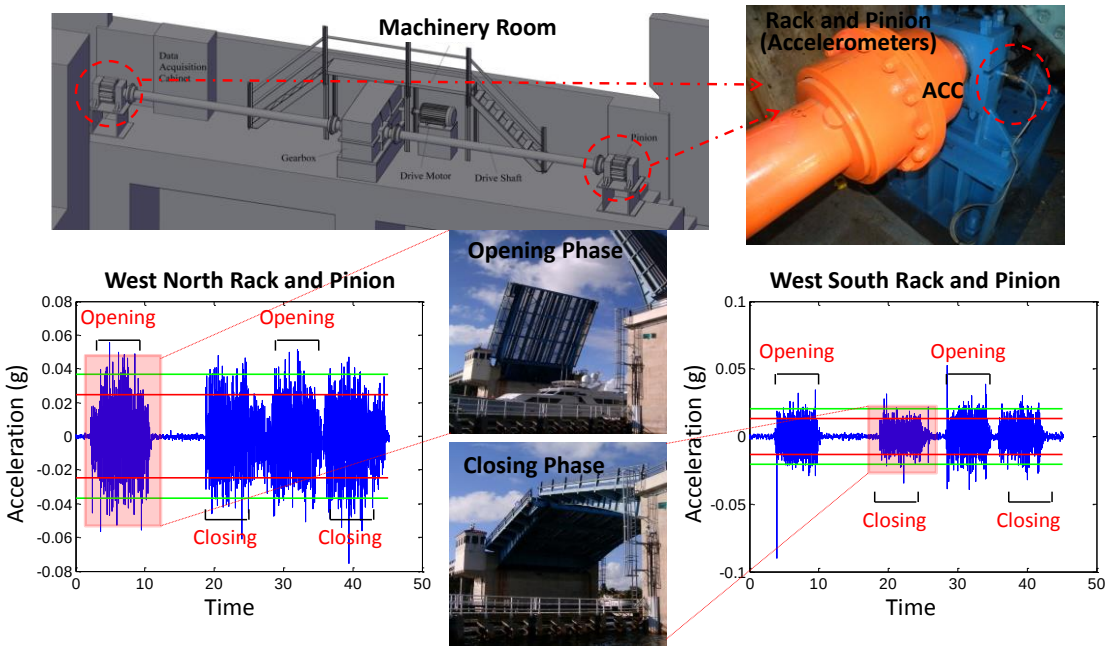

Figure 50: Sample measurement from the Rack and Pinion during opening and closing phases

Routine maintenance is required on the gear teeth. If the gear teeth are not kept lubricated at all times, wear and corrosion due to grinding of the rack and the pinion will occur. To monitor the condition and maintenance needs of the open gears and rack and pinions, accelerometers were installed at the base of the rack and pinion to monitor its vibrations (see Figure 50).

6.2.2. Field Tests with Artificially Induced Damages and Long Term Monitoring

One of the primary objectives of this study is to collect data that serves toward establishing criteria for system –wide monitoring of a bridge population. In order to meet the objective, field tests were conducted to establish thresholds for conditions that are critical for the maintenance and operation of the bridge. These conditions are referred to as "damage". In collaboration with FDOT engineers, some of the most common mechanical maintenance problems are identified and subsequently implemented on the movable bridge to simulate such damage conditions. These common damages are discussed individually through the following sections.

6.2.2.1. Gearbox Oil Removal

The gearbox, also called the transmission, uses gears to provide speed and torque conversion from a rotating power source to another device. The gearbox is equipped to provide the necessary amount of oil to the various gear meshes and bearings, thereby resulting in smooth and trouble free operation. The gearbox should be regularly checked for any leaks to see if the gearbox has adequate oil. In this project, the oil in the gearbox was partially removed to provide data corresponding to such an undesirable condition. Figure 51 shows the removal of the oil from the gearbox. Only 25% of the oil was removed, and the effect of the oil reduction was monitored by six accelerometers attached to the gearbox during a few openings of the bridge spans.

6.2.2.2. Rack and Pinion Bolts Removal

The rack and pinion system is located between the shaft and the open gear; therefore, it can be considered a transmission zone for opening and closing operation forces. As a result, it

should be free from defects to ensure safe operation of the bridge. Here, the removal of bolts was the simulated damage scenario, and the effect of the absence of these bolts was monitored by two horizontal accelerometers at north and south part of the rack and pinion. Figure 51 shows the Rack and Pinion with the removed bolts.

Extracting the Oil from the Gearbox Removing the Bolts (Rack and Pinion)

Figure 51: Simulation of common critical maintenance issues on mechanical components

The efficacy of the MPCA for anomaly detection of machinery components of movable bridges is explored in this section. In order to thoroughly evaluate the detectability of the MPCA algorithm, the data from both baseline (normal operation) and damaged (operation under significant maintenance issues) condition is required. The data from the baseline condition was collected during normal operation of mechanical components while the bridge was in opening phase. Regarding to the data from damaged condition, however, a comprehensive field test was designed and implemented. For that reason, the common damage scenarios associated with critical mechanical components are identified and simulated (on the relevant components) using the feedback from the Florida Department of Transportation (FDOT) engineers as well as the maintenance personnel. For the gearbox, it has been decided to extract some of the oil while the representative maintenance issue for the rack and pinion was simulated by removing some of the

bolts from the north site. Having collected the required real-life data (under both baseline and damaged condition) next in order is to generate the matrices of raw data from each individual component (gearbox and rack and pinion).

The data that was collected from each source (accelerometer) are inserted into individual column. As a consequence, the number of the columns for each matrix depends on the number of the sensors that was installed on the corresponding component. For instance, the matrix for the gearbox component includes four columns since there are four accelerometers installed. The MPCA algorithm is performed separately on each matrix to extract the covariance matrix and the relevant eigenvectors and damage indices.

It should be also mentioned that, the field test was conducted on October 21, 2009 where the oil was extracted from the gearbox and the bolts were removed from the rack and pinion. Upon inducing the damage scenarios on gearbox and rack and pinion, the sample data sets were collected during the opening phase. Furthermore, the sample data sets for the baseline condition were selected from the data sets before and after October 21, 2009 when the bridge was functioning in a normal condition. The results are summarized in individual section as follow.

6.3. Detection of Maintenance Issue in Gearbox (Extraction of Gearbox Oil)

As explained earlier, one of the most common sources of damage to the gearbox is lack of oil. In light of this fact, 25% of oil was extracted from the gearbox at the Sunrise Boulevard Bridge in order to study the efficacy of the MPCA algorithm for anomaly detection. The damage indices calculated by the MPCA algorithm are presented in Figure 52. As it is obvious from the Figure, the damage indices are quite sensitive to the simulated damage. The underlying

distributions of individual damage indices, as shown in Figure 52, are learnt during the normal operation (baseline condition). Consequently, any significant variation from these baseline conditions is reported as damage or critical maintenance issue.

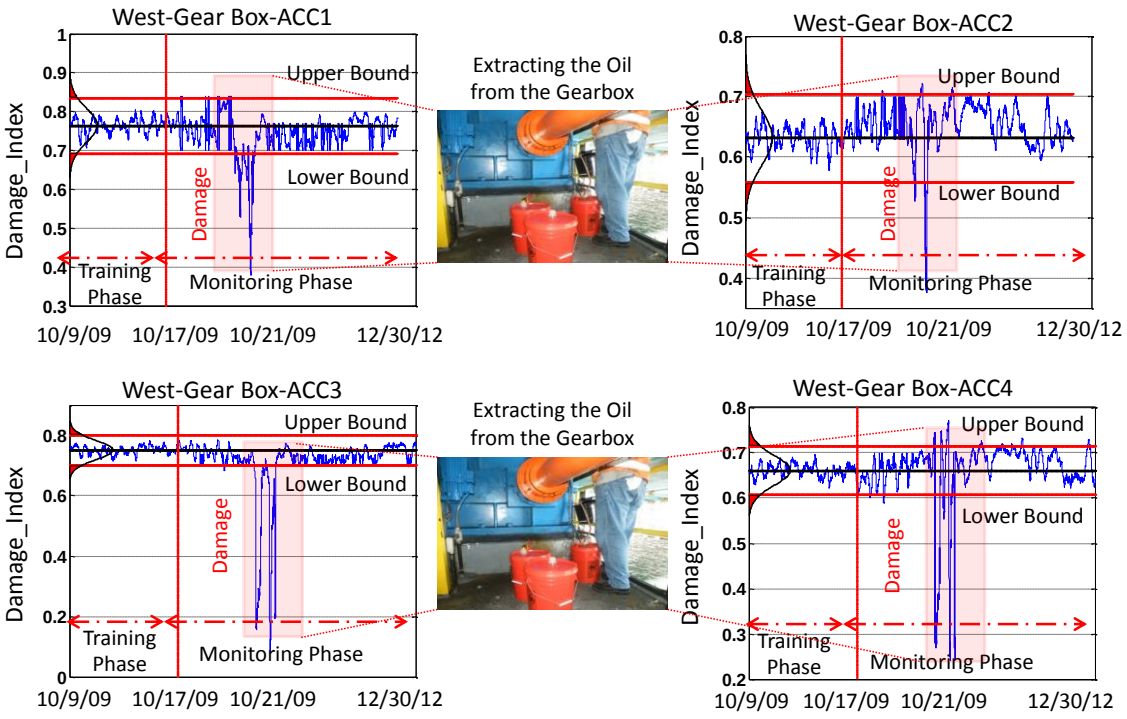

Figure 52: The MPCA results for gearbox fault detection

As it is observed from Figure 52, the calculated damage indices are confined within the established confidence interval prior to introducing the damage (extracting oil). However, once 25% of the oil is extracted from the gearbox, the computed damage indices experience an abrupt jump which is observed in all indices in Figure 52.

This reveals the importance of regularly checking the gearbox leakage and the oil level. In fact, any leakage in gearbox (that causes reduction in the oil level) induces additional vibration to the gearbox which might be resulted in major gearbox issue.

Once the extracted oil is replaced, the damage indices shift back to normal range. Lack of necessary amount of oil to gear meshes and bearings affect the smooth and trouble free operation of gearbox. Any malfunction in gearbox will directly influence the functionality of the motor and open gear will subsequently affect the entire bridge operation.

Having calculated these damage indices in real-time, provides the opportunity for the bridge owner to timely detect and identify any possible abnormal behavior in gearbox. Being timely informed can save both time and money for the bridge owner. Considering the results that are observed in this section, the MPCA can be regarded as a reliable technique for gearbox condition monitoring.

6.4. Detection of Maintenance Issue in Rack and Pinion (Removing bolts)

Two bolts were removed from the north rack and pinion in order to simulate one of the most common maintenance issues (damages) associate with this critical component. The results for both damage indices are illustrated in Figure 53. It is realized that the first damage index for the rack and pinion exhibits an abrupt jump due to the damage, while there is not any significant variation in the second damage index.

Therefore, the MPCA can also be considered as an effective and reliable technique for identifying the corresponding maintenance issues of rack and pinion. However, the authors realized that implementation of MPCA for long term monitoring of gearbox and rack and pinion still has a main practical issue which will be discussed in the next section.

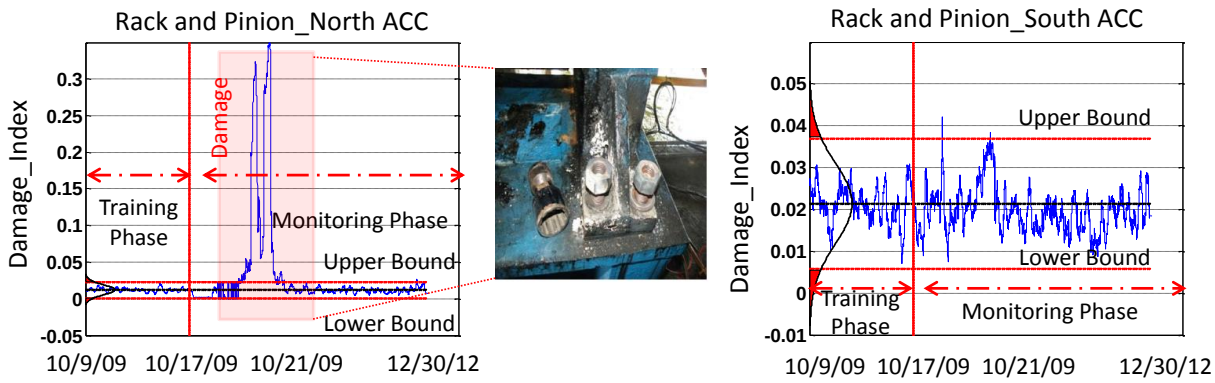

Figure 53: The MPCA results for Rack and Pinion fault detection

6.5. A Data Interpretation Framework for Long-term Maintenance Monitoring of Mechanical Components

The application of MPCA algorithm for detecting the corresponding maintenance issues of gearbox and rack and pinion were discussed through the previous section. Although the damage indices have shown promising results in terms of being sensitive to abnormal behavior (maintenance issues), the application of MPCA for long term condition monitoring is still challenging.

The size of a single data set that is collected from an opening phase (bridge opening) is 16000 data points. Considering that there are approximately ten openings during a day, the size of the data matrix will be equal to 48 $\times 10^5$ for one month data and eventually 576×10^5 over a year. For instance, the data that are utilized for this study is collected between November 10, 2009 and May 3, 2013 which includes 5647 openings. This means the size of the matrix will be 90352000 data points. Preforming the MPCA on such a matrix requires significant amount of time and also in some cases results in computational issues.

Therefore, in order to make the MPCA more efficient for long-term processing of the mechanical data, a modified version of this algorithm is proposed in this study. The performance of the proposed algorithm is verified taking advantage of long-term SHM data along with the corresponding maintenance actions.

In fact, after processing the SHM data with the algorithm and extracting the condition index for motor and gearbox, the next step is to study the condition index along with the maintenance actions which are separately reported by FDOT personnel. These maintenance actions are extracted from the maintenance logs which are submitted to FDOT by the maintenance personnel for the last 4 years.

Through this, all the corresponding maintenance issues that have been occurred to the gearbox and motor (during the last 4 years) are identified and classified. Alternatively, the condition indices for the same component are derived utilizing the SHM vibration data which has been collected since 2009.

The efficiency of the SHM system and the proposed method is then explored by performing a correlation study between the derived condition index and the extracted maintenance actions. In order to reduce the size of the matrix and at the same time keep the sensitivity of the condition index, four statistical features are selected and extracted from each data set which represents the vibration level of the corresponding components. The statistical features that are selected to extract from a data set are as follow:

Note: $X_i = \{x_1, x_2 \dots x_n\}$ is a data set collected during i^{th} opening

1. Average of the ten largest values of each data set.

$$Feature\ 1 = \frac{1}{10}\sum_{n=1}^{10} x_{d_n} \quad (16)$$

Where $X_d = \{x_{d1}, x_{d2} \ldots x_{dn}\}$ is the result of sorting X_i in descending order.

2. Average of ten minimum values of each data set.

$$Feature\ 2 = \frac{1}{10}\sum_{n=1}^{10} x_{a_n} \quad (17)$$

Where $X_a = \{x_{a1}, x_{a2} \ldots x_{an}\}$ is the result of sorting X_i in ascending order.

3. Standard deviation of each data set.

$$Feature\ 3 = \sqrt{\frac{1}{n}\sum_{j=1}^{n}(x_j - \bar{X})} \quad (18)$$

4. Root mean square of each data set.

$$Feature\ 4 = \sqrt{\frac{1}{n}({x_1}^2 + {x_2}^2 + \cdots + {x_n}^2)} \quad (19)$$

The framework (Figure 54) is divided into two individual sections so called training and monitoring phase. The sequential steps for the proposed framework are summarized in Figures 54 and 55. Throughout the training phase, the algorithm learns the underlying distribution of damage indices under baseline condition. In fact, the main intention of the training phase is to establish the confidence intervals for individual components during the healthy condition.

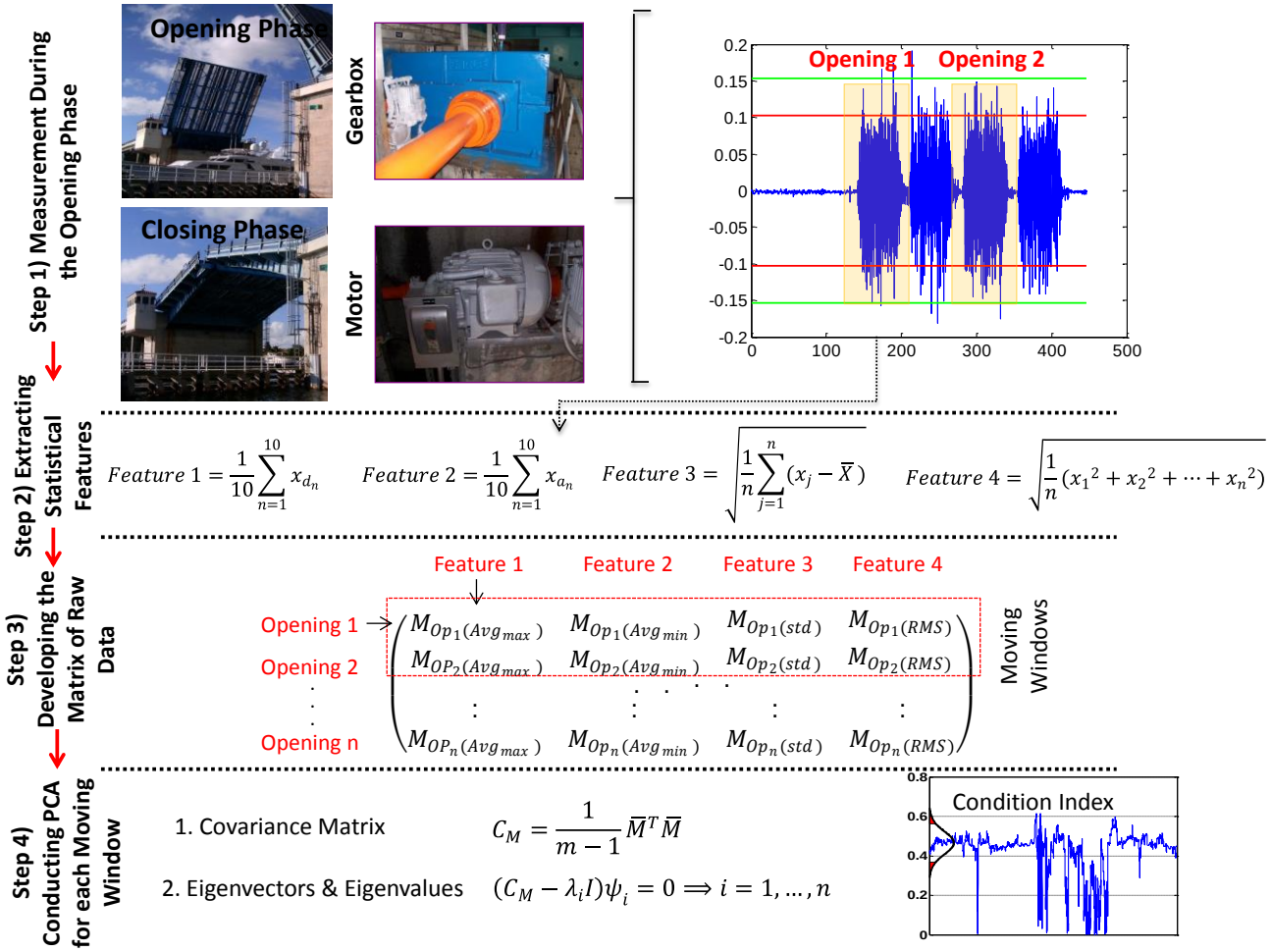

Figure 54: The Steps involved in the proposed framework

Once the underlying distributions are learnt, the subsequent phase is the monitoring section where any variations from the threshold are considered as change/damage. Therefore, each of the statistical features is inserted into an individual column and by that the matrix of data is generated.

Through the following section the performance of this framework is tested using the SHM data as well as the extracted maintenance actions.

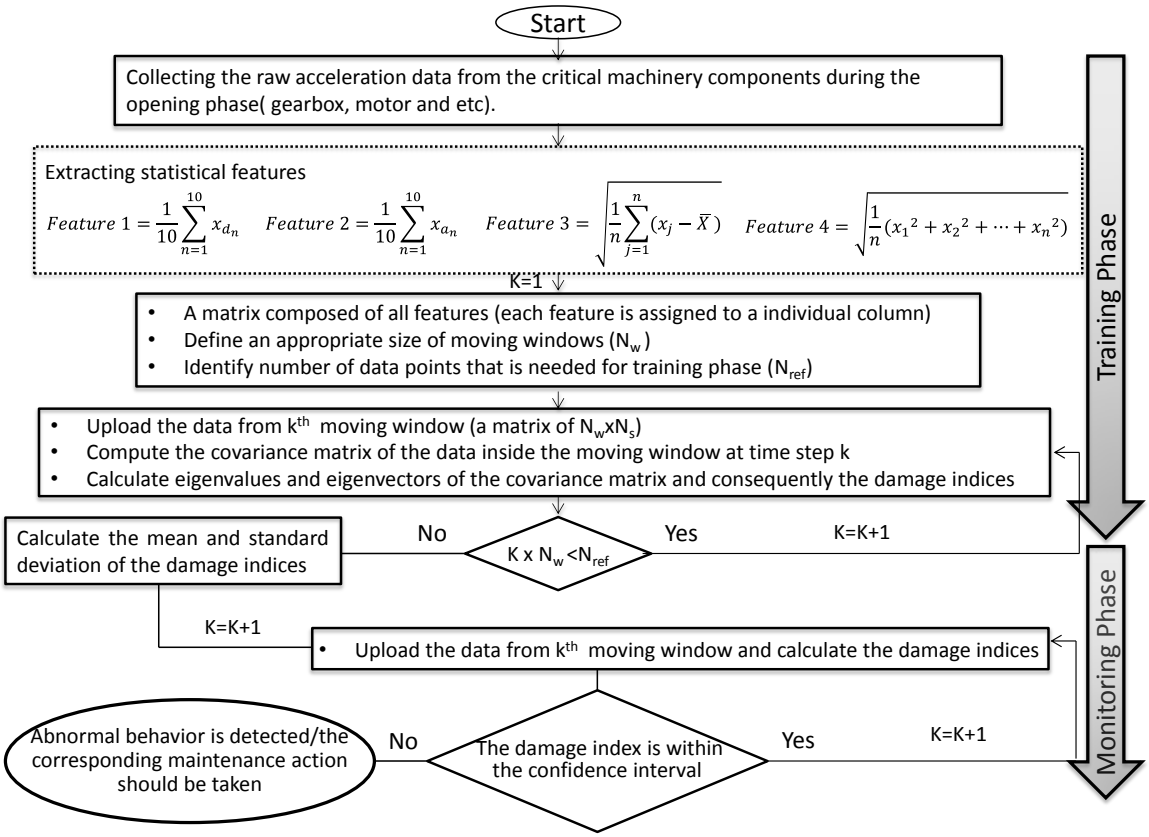

Figure 55: The sequential steps for the proposed framework

6.5.1. Analysis of the FDOT Maintenance Reports

In order to compare and link the monitoring data and the maintenance records, it is important to develop a numerical scheme for the maintenance actions. An extensive study is conducted by evaluating the maintenance and inspection reports from 09/2009 to 5/2013 that were obtained from the engineers and the maintenance personnel of the Sunrise Bridge.

All the maintenance reports were analyzed to have a good understanding about maintenance schedule and procedure at the Sunrise Bridge. Subsequently, all the critical maintenance actions were identified and classified. Throughout the following sections, the

derived condition indices for gearbox and motor are investigated along with the corresponding maintenance action.

6.5.2. Correlation of the Damage Indices and the Gearbox Maintenance Actions

Time history of the condition index is calculated according to the procedure explained in Figures 54 and 55. The results for the gearbox are shown in Figure 56 in which the time histories of statistical features are plotted along with the time histories of condition indices for each individual gearbox accelerometer.

The idea is to investigate the correlation of condition index values and the maintenance actions extracted from the maintenance reports. It is realized that the variations observed in the index values are consistent with the critical maintenance actions that has been experienced by the gearbox component over the past 4 years. This indicates the fact that the condition indices which are derived through the proposed framework can be deployed as a reliable indicator for assessing the maintenance condition of the gearbox. Therefore, the variation in the values of the condition index is linked to a critical maintenance issues related to the gearbox which in turns used by bridge owner to take a timely appropriate maintenance action.

In this study the SHM data sets that were collected between November 5, 2009 and January 5, 2010 is considered as training data sets (training phase). Hence, as the first step, the confidence interval is established for the training phase. In other words, the underlying distributions of the extracted condition indices are learnt for the training data sets (see Figure 56).

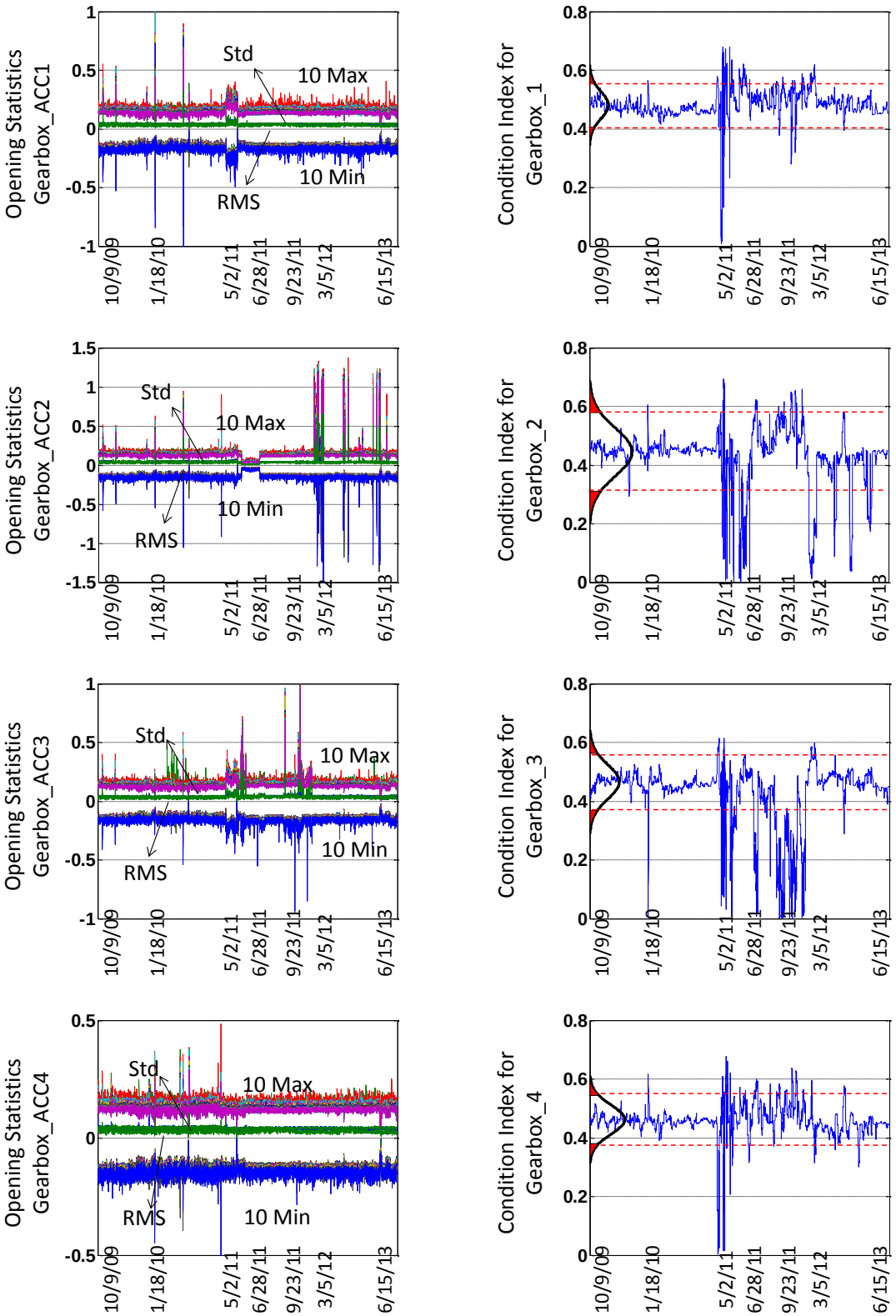

Figure 56: The corresponding condition (damage) indices for gearbox component

The corresponding confidence intervals are plotted for each damage (condition) index in Figure 56. As observed from Figure 56, all the calculated damage indices demonstrate abnormal behavior between May 2, 2011 and March 5, 2012.

Since the condition indices are conveying almost the same information and for the sake of brevity, the concentration is dedicated to the third index in Figure 56. As a result, the third condition index is displayed individually in Figure 57 along with the time histories of statistical features as well as the extracted critical maintenance actions.

Despite the fact that the condition index values are confined within the confidence interval during the training period, the values have exceeded the threshold on January 13, 2010 for the first time. The abnormal behavior continued for five days until January 18, 2010, when the condition values reverted to the normal condition (within the established confidence interval). The root cause of this behavior further investigated through the maintenance reports (logs), where it is realized that on January 18, 2010 the gear reducer break was replaced by FDOT maintenance personnel.

As it is shown in Figure 57, the relevant maintenance actions for gearbox are listed in order of occurrence. An important issue that has to be pointed out is that the bridge maintenance personnel were not able to detect this issue until January 18, 2010, which was almost 5 days after the abnormal behavior in gearbox initiated. Alternatively, The SHM system was able to identify and detect this malfunction immediately after it occurred, which is big advantage. In fact, this malfunction could have been eventually led into a major operational issue for the movable bridge. This can highlight the importance of having SHM system for timely detection of critical issues, which can avoid the operational issues besides saving money and time.

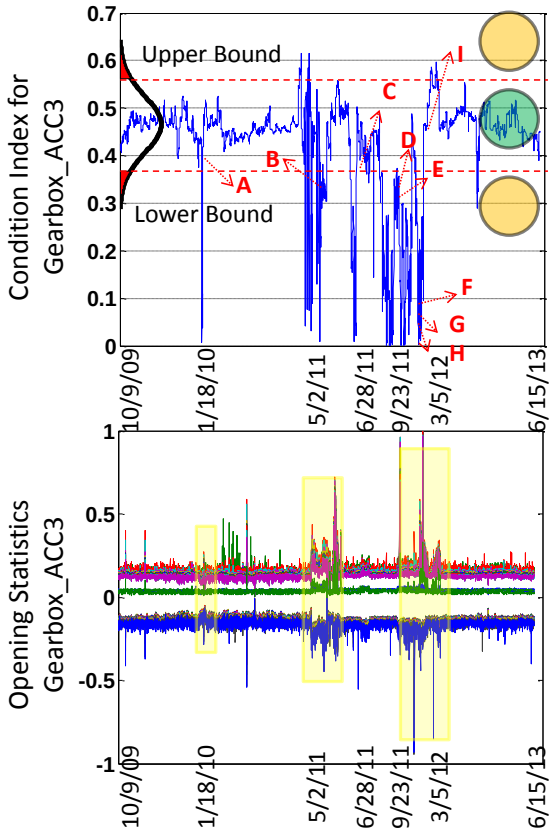

Point ID	Date	Maintenance Action
A	1/18/2010	Replace Gear Reducer Break as Needed
B	5/2/2011	Replace West Span Gear Box Input Shaft Seal
C	6/28/2011	Replace output shaft seal on West Gearbox
D	9/21/2011	Check F.A. Span Motor for Motor Replacement
E	9/23/2011	Check F.A. Span Motor for Motor Replacement
F	9/26/2011	Removed Brake on F.A. Span Motor
G	9/27/2011	F.A. Span Motor Bearing trouble shoot
H	9/28/2011	The Motor was Repaired
I	3/5/2012	Replace Gearboxes Breaks

Figure 57: The third gearbox condition index along with the time history of the statistical features and the corresponding critical maintenance actions

After the gear reducer brake was replaced, the gearbox operated in a normal range until April 12, 2011, where the fluctuation is again observed in the condition index. Inspection of the maintenance reports reveals the fact that on May 2, 2011 the input shaft seal for the gearbox had been replaced.

Indeed, the input shaft seal has experienced a major problem, which started on April 12, 2011 and identified by FDOT maintenance personnel with almost two weeks delay on May 2, 2011. Similar to the first issue, this could have been resulted in a major problem for the bridge. On the other hands, however, the functionality issue of the gearbox was detected without any delay by taking advantages of the proposed condition index. This is another evidence for the

efficiency of the SHM system along with the proposed data interpretation framework for tracking the condition of machinery components.

Having replaced the input shaft seal for the gearbox, the index shifted back to baseline (normal) condition as it can be observed from Figure 57. Only after 6 weeks of normal operation, the condition index went again beyond the developed confidence interval started on June 17, 2011. Having the maintenance reports analyzed for the Sunrise Blvd. Bridge, it is understood that the output shaft seal was replaced for the west gearbox on June 28, 2011. Similar to previous cases, this abnormal behavior was also identified by SHM system ten days ahead of FDOT maintenance personnel.

Replacing the output shaft seal for the gearbox, the index changed back to the normal condition again. The gearbox did not experience any significant maintenance issues until September 21, 2011 where the electrical motor had an operational problem and caused a dramatic alteration in the value of the condition index. In fact, this time the problem was not due to the gearbox, but instead the motor which is connected directly to it had an operational issue. There are several notes in the report from September 21, 2011until September 27, 2011 related to the motor's abnormal behavior.

There were some serious problem associated with the motor including bearing and brake issues. As it is clearly noticed from Figure 13, these functionality issues in the motor led into operational problem in the gearbox during the same period. Based on the information from the maintenance logs, the motor was repaired on September 28, 2011. Finally on March 5, 2012 the gearbox brakes were replaced by new ones allowing the condition index to change back to the normal range.

After this point the gearbox operated in normal condition for more than one year (until June 15, 2013) and the index continued bounded within the confidence interval, meaning that there were not any critical issues related to the gearbox.

6.5.3. Correlation of the Damage Indices and the Motor Maintenance Actions

The second critical component of the movable bridge, which is studied here along with the relevant maintenance actions, is the electrical motor. This component is directly linked to the gearbox which in turn causes the close interaction. In order words, a malfunction issue in either of motor or gearbox can influence the performance of the other component.

The corresponding damage indices calculated for motor are displayed in Figure 58. It is realized that both condition indices demonstrate some abnormal behavior between May 2, 2011 and March 5, 2012 which is exactly in the same period that gearbox expressed some malfunction issues. This good consistency between the condition indices of motor and gearbox and their meaningful correlation with maintenance actions reveal the fact that the proposed condition assessment framework is a reliable one for long term performance monitoring of machinery components.

The second damage index is selected to study along with the extracted information from the maintenance reports. The second condition index as well as the statistical features and a list of relevant maintenance actions (for motor) are presented in Figure 58. The variations in condition index have been interpreted through the maintenance actions extracted from the maintenance reports. After investigating the maintenance reports, the variations of the condition

index were found to be very meaningful. The variation started around May 2, 2011 in which the gearbox started facing some operational issues.

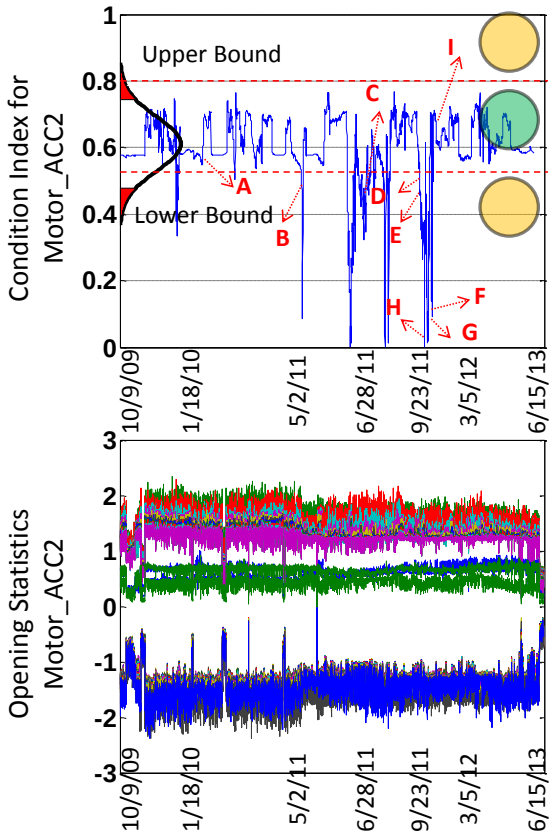

Point ID	Date	Maintenance Action
A	1/18/2010	Replace Gear Reducer Break as Needed
B	5/2/2011	Replace West Span Gear Box Input Shaft Seal
C	6/28/2011	Replace output shaft seal on West Gearbox
D	9/21/2011	Check F.A. Span Motor for Motor Replacement
E	9/23/2011	Check F.A. Span Motor for Motor Replacement
F	9/26/2011	Removed Brake on F.A. Span Motor
G	9/27/2011	F.A. Span Motor Bearing trouble shoot
H	9/28/2011	The Motor was Repaired
I	3/5/2012	Replace Gearboxes Breaks

Figure 58: The motor condition index along with the time history of the statistical features and the corresponding critical maintenance actions

This variation continued until September 28, 2011 when the motor was replaced due to major malfunction issues. Similar to gearbox case, all the abnormal behaviors were timely detected by SHM system. This can prove the efficiency of both SHM system and the proposed condition assessment framework. Therefore, considering both gearbox and motor, the established condition index can be used for condition assessment and in general fault detection of machinery components.

6.6. Concluding Remarks

The machinery components are critical elements for the functionality of the movable bridges. As a consequence, the continuous condition assessment of these components is necessary. In this study the efficiency of implementing SHM system for tracking the condition of the components including gearbox, motor and rack and pinion has been explored. For the purpose, the Sunrise Blvd. Bridge has been selected and heavily instrumented with various types of sensors. Accordingly the data has been collected over the past 4 years from all the mechanical and structural components of the bridge.

In addition to data sensing, the Moving Principal Component Analysis is employed for detecting any possible malfunction in the machinery components. In order to evaluate the application of MPCA for fault detection, some of the common and critical damage scenarios have selected taking advantages of the feedback from the FDOT engineers and maintenance personnel.

Therefore, the MPCA has been verified utilizing the data from both baseline (normal) and damage conditions. It has been shown that the MPCA is a reliable algorithm for detecting the abnormal behavior of the mechanical components. However, it is realized that the application of MPCA algorithm for large-size SHM data sets is very time consuming with respect to the size of the matrices. In light of the above-mentioned issue, the MPCA algorithm has been modified for long-term applications.

The proposed data interpretation methodology has been evaluated along with the maintenance actions that were extracted from the maintenance reports (logs). The reports have been prepared and documented by the FDOT maintenance personnel for more than 4 years. The

maintenance reports have been investigated and the critical maintenance action have been extracted and classified for the corresponding mechanical components. The condition indices were interpreted through the critical maintenance actions in order to test the reliability of the indices. The condition indices were found very meaningful in terms of being consistent with the extracted maintenance actions for gearbox and electrical motor.

CHAPTER SEVEN: A HYBRID FRAMEWORK FOR LONG-TERM PERFORMANCE ASEESSMENT OF INFRASTRUCTURES

7.1. Introduction

The objective of this chapter is dedicated to propose and design a hybrid data interpretation framework for SHM data so that the extracted information can be employed in performance assessment. As such, the objective of the present study is to develop a hybrid data interpretation framework for automated performance monitoring of infrastructures that combines the benefits of both parametric and non-parametric approaches and mitigates their shortcomings. The proposed approach can then be employed not only to detect the damage but also to assess the identified abnormal behavior.

Furthermore, another objective that is pursued in this study is to determine the number of sensors and their corresponding locations required to effectively monitor a potential infrastructure. In particular, the sensor network is optimized so that the collected information can be ultimately used in continuous performance assessment. The presented framework is categorized as a supervised classification approach wherein an algorithm is initially trained utilizing the data generated through Monte-Carlo simulation techniques and processed using Moving Principal Component Analysis (MPCA) to extract relevant features.

Then, statistical learning methods are used to learn the underlying distributions of the features during a training phase and a decision rule is developed in a hypothesis testing framework. Once the training phase is completed, the live SHM data are analyzed and classified using MPCA and hypothesis testing, respectively, to identify the performance status of the structure.

The framework is evaluated through both analytical and experimental studies. An experimental structure (UCF-4Span Bridge) is employed along with an In-house developed Fiber Bragg grating (FBG) system for simulating the common damages and collecting the corresponding SHM data, respectively. The framework has shown promising results in terms of both designing the sensor network and also the continuous evaluation of the structural performance.

The premise is that the continuously provided information can be exploited into the Performance–Based Engineering (PBE) framework to improve the knowledge and understanding of the structural performance levels.

7.2. An Integrated (Hybrid) Framework for Automated Performance Monitoring

The objective of this research is to develop a hybrid framework for continuous performance assessment of infrastructures through which the damages are not only detected but also effectively classified. The framework is termed hybrid since it is designed based on the integration of non-parametric (data-driven or model free) and parametric (model-based) approaches. The first step toward developing such an integrated framework is to study the structure in terms of the common damage scenarios.

A comprehensive study is conducted to identify the most common and critical damage scenarios that a given structure is likely to undergo in the course of its lifetime. This can be accomplished through several different sources including engineering judgment, feedback from experts, long-term performance of that specific type of structure, etc. Once this initial task (step 1) is carried out the following steps are followed to developing the hybrid framework.

7.3. The Procedure for Developing the Hybrid Framework

7.3.1. Simulate the Performance of the Structure under the Selected Damage Scenarios and the Corresponding Uncertainties using a Monte-Carlo Simulation Technique

The second major step is to conduct a Monte-Carlo simulation in order to simulate and predict the performance/responses of a given structure due to the occurrence of different damage scenarios. In addition, using Monte-Carlo simulation provides the opportunity to incorporate the uncertainty associated with the governing parameters (parameters which are affecting the desired responses of the structure) in the mathematical model of the structure and eventually in the predicted responses.

Initially, a calibrated (parent) Finite Element Model (FEM) of the structure is generated for the baseline (healthy) condition through the FEM updating. Upon finding the calibrated FEM for the baseline condition, the selected damage scenarios are individually simulated in order to develop the calibrated (parent) FEMs for each individual scenario. Therefore, there would be a representative calibrated FEM for each structural condition (including baseline and damage conditions), as visualized in Figure 59.

Lastly, based on the calibrated (parent) FEMs and the associated uncertainty of the governing parameters, a Monte-Carlo simulation is performed to produce offspring FEMs. The details of Figure 59 are discussed through the following subsections.

7.3.1.1. <u>Generating Offspring FEMs based on the Calibrated (Parent) FEMs</u>

In general, a wide range of computational algorithms that were developed based on the idea of repeated random sampling to reach numerical results are referred to as Monte-Carlo

methods or simulations. Some of the main applications of Monte-Carlo simulations include optimization, numerical integration and sampling from a probability distribution. In this study, the Monte-Carlo technique is employed for generation of samples from the uncertainty distribution associated to the sensitive parameters (Figure 59).

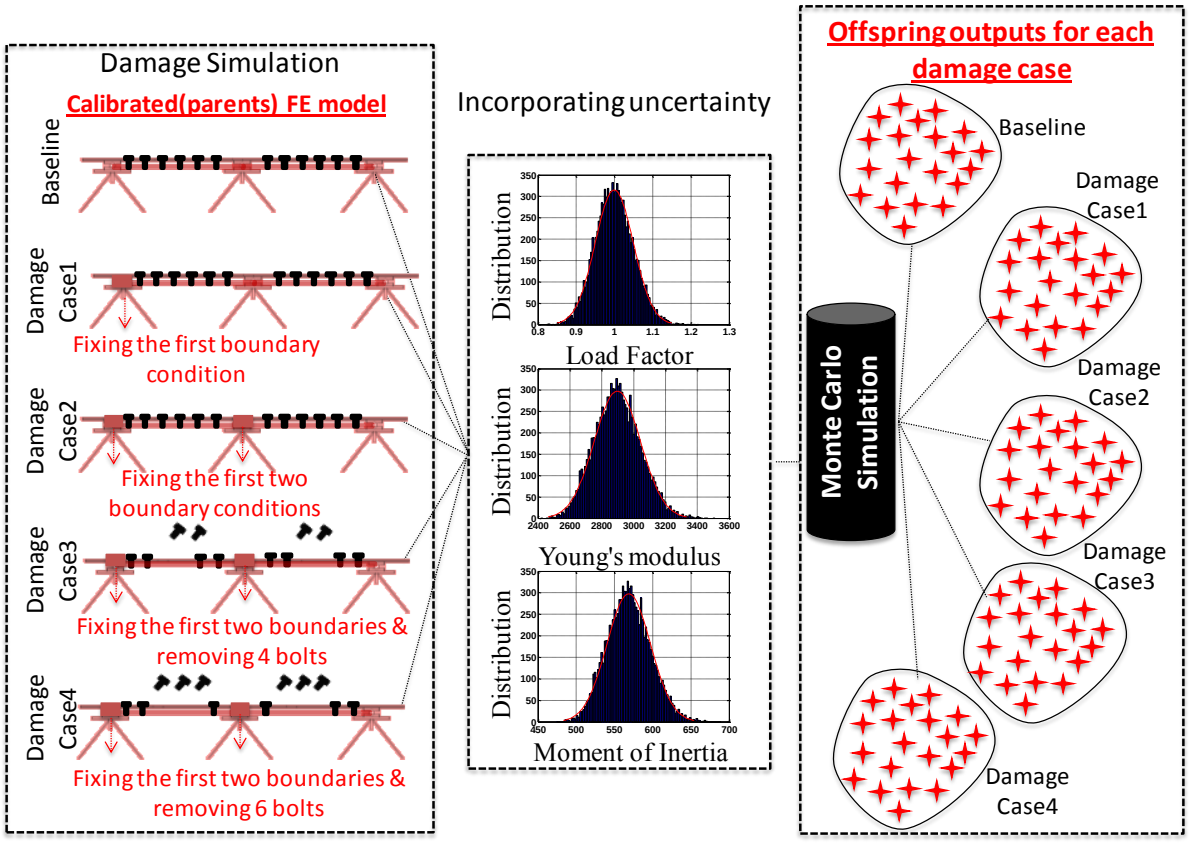

Figure 59: Monte-Carlo simulation for generating offspring FEMs

In other words, in order to construct an appropriate predictive model, thousands of offspring FEMs are generated from the probability distributions related to sensitive parameters utilizing the Monte-Carlo simulation. Having established the predictive model for each damage scenario, one can forecast the performance of the structure under a particular damage condition.

The number of offspring FEMs that is required for each calibrated (parent) model is derived from the following Equation:

$$Percent\ Error = 200 \times \sqrt{\frac{(1 - P_f)}{n \times P_f}} \quad (20)$$

Where P_f is the estimated probability of failure while *n* indicates the number of required simulations. In this study, a total of 10,000 offspring FEMs are generated from each parent FEM, which in turn results in a 0.01 probability of failure probability and 20% error. The generated offspring FEMs are analyzed under a simulated traffic load in order to compute the range of responses corresponding to each damage condition.

7.3.1.2. Uncertainty Associated with the Sensitive Parameters

Uncertainty plays an important role in engineering, particularly in reliability analysis. Based on the literature, the uncertainty has two main sources (although it may have several other sources) . The first one is so-called Aleatory Uncertainty and is associated with randomness; the second source is called Epistemic Uncertainty and is due to lack of information because of the data or the mathematical model. The effect of the second source can be reduced by improving knowledge in terms of measurements and modeling. In this study, the uncertainties associated with material properties, section properties and traffic load factor are considered in order to generate offspring FEMs (Figure 59).

7.3.2. Extracting the Performance Sensitive Features

Having developed and analyzed the offspring FEMs under the simulated traffic load, the responses are stored in individual matrices called matrices of raw data. Having 10,000 offspring

FEMs for each damage condition will eventually result in generating 10,000 matrices of raw data, as illustrated in Figure 60. These matrices are then processed using advanced statistical analysis methods in order to derive the damage sensitive indices as discussed in the following section.

7.3.2.1. Moving Principal Component Analysis (MPCA)

Monitoring of complex infrastructure over a long time will result in multi modal massive amounts of data. As a consequence, effective statistical methods are applied to extract the information from the collected massive data. Principal Component Analysis (PCA) is one of the most effective dimensionality reduction techniques that can significantly reduce the dimension of the data while retaining the informative part of the measurements.

For this study, the MPCA algorithm is employed (based on the great potential that it has shown for SHM applications) for processing the data and extracting the performance features, which are subsequently used to classify the damages. The application of MPCA in this study is outlined in the following steps and illustrated in Figure 60. The subsequent steps provide details about developing the matrices of raw data and calculating the damage indices as illustrated in Figure 60.

i. Generate the matrices of raw data by assigning the time history of the measurements from each variable (sensor) to individual columns, as illustrated in Figure 2. It should be also noted that each matrix contains data from a baseline as well as a corresponding damage scenario, i.e., the data consists of history before and after a given damage scenario.

ii. The notations that are used in Figure 60 are:

iii. M_{D_i} : Matrix of raw data corresponding to damage D_i.

iv. $u_{S,D_i}(t)$: Measurement of sensor S under condition D_i at time t.

v. $s \in \{1,2 \dots N_s\}$: Refers to the sensor index where Ns is the total number of sensors.

vi. $D \in \{B, D_1, \dots D_4\}$: Performance condition of the structure (B refers to the baseline condition while D_i represents damage scenario *i*).

vii. $U_{D_i}(t_k)$ is the matrix with rows $u_{D_i}(t),\ t = t_k, \dots, t_{k+N_W}$

viii. N_s: Total number of sensors installed on the structure.

ix. N_m: The total number of the measurements/ observations from a sensor under a baseline and a given damage condition.

x. N_W: The size of the fixed-window whose exact role will be explained later.

xi. $k \in \{1,2, \dots, N_m - N_w\}$: Time Step.

xii. Since the matrices of raw data may include different physical variables which are collected with different types of sensors (strain gauge, accelerometer, microphone and etc.), the variables have to be scaled before implementation. In this study the data was scaled in such way that all the variables have zero mean and unit variance.

xiii. Selecting the size of the moving window (Nw) is a key parameter for performing MPCA. There is a fundamental tradeoff associated with the choice of the size of the window since it should be selected large enough so that it is not influenced by periodicity in data, but also small enough in order to timely detect any abnormal behavior.

xiv. Computing the covariance matrix Ck and subsequently the corresponding eigenvectors and eigenvalues for kth time steps (data within the kth moving window) using the following equations (Figure 60).

$$C_k = \sum_{j=k}^{k+N_w} u_{D_i}(t_j)^T u_{D_i}(t_j) = U_{D_i}{}^T(t_k).U_{D_i}(t_k) \qquad (21)$$

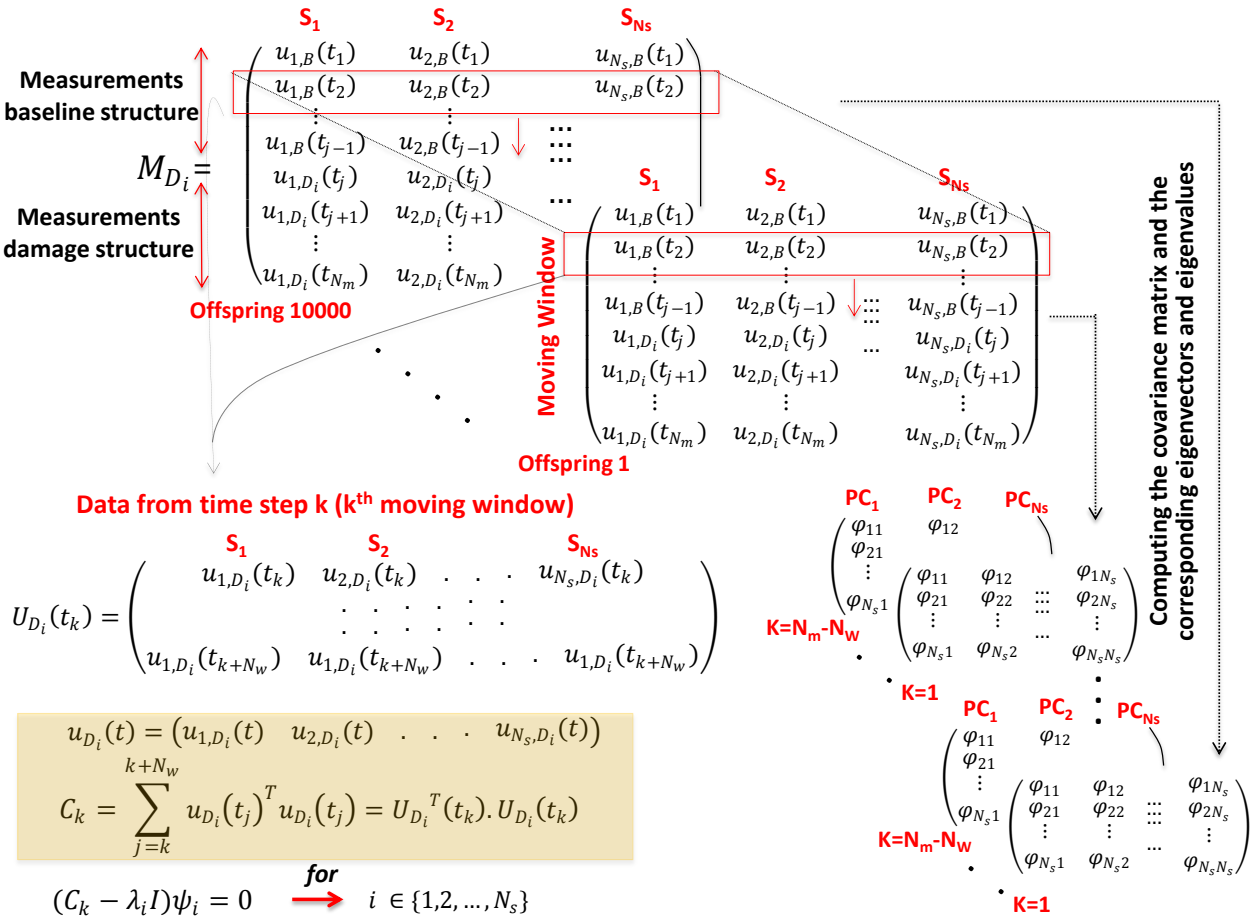

Figure 60: Matrices of raw data and the procedure for conducting MPCA

xii. Extracting the eigenvectors (ψ_i) and eigenvalues (λ_i) of the covariance matrix as shown in Figure 2 and Equation 22.

$$(C_k - \lambda_i I)\psi_i = 0 \qquad (22)$$

7.3.2.2. Damage Indices

The first objective of SHM is to timely detect and identify abnormal behavior so that catastrophic failure can be avoided. In order to achieve such an objective, we have to select sensitive damage indices that reflect the corresponding malfunctions.

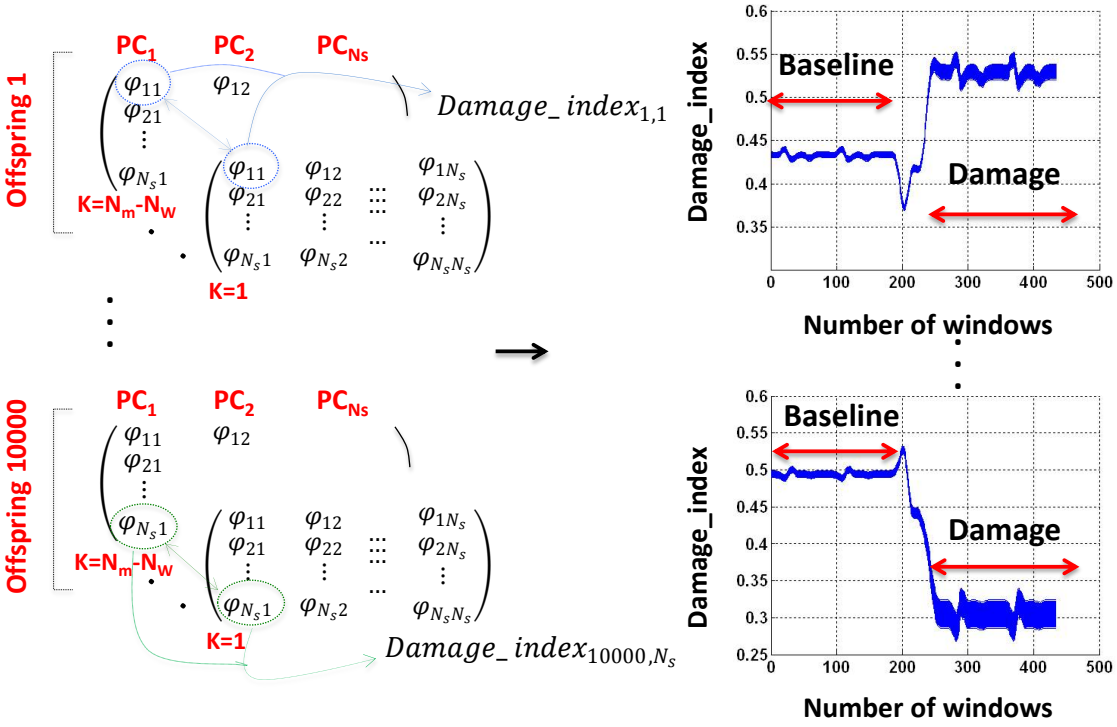

Figure 61: The procedure for deriving the damage indices

The damage indices that are adopted for this study are based on the first principal component of the data, which in most cases contains the most informative portion (largest variance) of the data, Different entries of the first principal component, as visualized in Figure

61, are restored individually and introduced as the damage indices. These damage indices are derived based on Equation 23.

$$Damage\_index_{e,s}(k) = (\psi_{s1})_{k,e} \quad (23)$$

Where $e \in \{1,2 \dots 10000\}$ refers to the number of the simulation (offspring) while $k \in \{1,2 \dots N_m - N_w\}$ indicates the time step.

7.3.2.3. Performance Sensitive Features

The second major objective of SHM, after detecting damage, is to be able to evaluate and assess the damage. Thus, a feature that is sensitive to the performance of the structure is demanded. Therefore, after deriving the damage indices, the subsequent step is to extract performance-sensitive features that can intuitively reflect the performance level of the structure. Knowing the performance condition of the structure can be of significant value for infrastructure owners as they can take an appropriate action according to different states of structural performance.

Herein, the performance-sensitive features are considered as the separation of the extracted damage indices due to experiencing different damage conditions. These features are derived through the following Equation.

$$x_s(e) = \frac{\sum_{k=1}^{\frac{N_m-N_w}{2}} Damage\_index_{e,s}(k)}{\frac{N_m-N_w}{2}} - \frac{\sum_{k=\frac{N_m-N_w}{2}}^{N_m-N_w} Damage\_index_{e,s}(k)}{\frac{N_m-N_w}{2}} \quad (24)$$

The intuition is that different types and levels of damages induce different levels of separation in the damage indices, and as a result this can be a potential feature to classify the damage.

7.3.3. Learning the Distributions of the Performance-Sensitive Features

Once the corresponding performance-sensitive features are extracted for each individual damage level (scenarios) using Equation 24, the following step is to learn the underlying distributions. In fact, by learning the underlying distributions for individual scenarios, the framework can be used to predict and classify the new incoming features into the relevant categories and accordingly identify the current performance status of the structure. While there are various statistical learning techniques available, hypothesis testing is used in this study to classify the features.

For completeness, we briefly describe the main problem of binary hypothesis testing. The goal is to decide between two hypotheses, H_0 (termed the null hypothesis), and H_1 (the alternative hypothesis). Given an observation X, the goal is to decide which of the two hypotheses has occurred, as shown in Equation 25.

$$\begin{cases} H_0 : X \sim N(m_0, K_0) \\ H_1 : X \sim N(m_1, K_1) \end{cases} \quad (25)$$

Where m_0 and K_0 are the mean and covariance matrix under the null hypothesis H_0, respectively, and m_1 and k_1 denote the mean and covariance under H_1. In other words, under hypothesis H_i, $i \in \{0,1\}$, the observation X has a Gaussian distribution with mean m_i and

covariance matrix K_i. The optimal decision rule is to compare a sufficient statistic to a threshold as shown in (Equation 26).

$$S(X) \gtrless_{H_0}^{H_1} \tau \quad (26)$$

If the sufficient statistic S(X) exceeds the threshold τ, we decide in favor of H_1, otherwise we choose H_0. For the Gaussian binary hypothesis testing problem in (Equation 25), the sufficient statistic is given by:

$$S(Y) = \frac{1}{2} Y^T \left({K_0}^{-1} - {K_1}^{-1} \right) Y + Y^T ({K_1}^{-1} m_1 - {K_0}^{-1} m_0) \quad (27)$$

The threshold τ is given by:

$$\tau = \frac{1}{2} \left[{m_1}^T {K_1}^{-1} m_1 - {m_0}^T {K_0}^{-1} m_0 + \ln \left(\frac{|K_1|}{|K_2|} \right) \right] \quad (28)$$

Where |K| denotes the determinant of the matrix K. Thus, Equation 26 is a decision criterion with which one can decide whether the observation belongs to hypothesis H_0 or H_1. Furthermore, the Receiver Operating Characteristic (ROC) curves are used to evaluate the performance of the decision rule. The ROC curves present the fraction of true positive out of positives (TPR= true positive rate) against the fraction of false positive out of negatives (FPR= false positive rate) at various threshold settings (Equation 26 through Equation 28).

In this study, the X (observation) is the extracted feature obtained from Equation 24 while m_0 and K_0 are the corresponding mean and covariance matrix. The objective is to first extract the

feature from the live SHM data (using MPCA) and with the hypothesis testing decide between H_0 (the structure is in baseline condition and maintenance action is not required), and H_1 (the structure is experiencing damage type *i* and consequently the corresponding maintenance action has to be taken).

7.4. The Proposed Hybrid Algorithm

Based on the aforementioned procedures, the proposed hybrid algorithm is summarized in Figure 62. As mentioned earlier, the goal of the designed algorithm is to first detect the damage and then to classify the damage.

In addition, using the proposed algorithm, one is able to also identify the optimal sensor configuration for the structure. In fact, the hybrid framework enables the designer to identify the minimum number of sensors to be installed on the structure so that the damage can be quickly detected and efficiently classified.

7.4.1. Identifying the Optimized Network of Sensor

As shown in Figure 62, the second phase of the hybrid algorithm is dedicated to design the network of sensors. Basically, the second phase is a try and error process whereby the locations and the number of required sensors are identified. It should be also noted that since the MPCA algorithm is fundamentally a multivariate technique, the minimum number of required sensors is two. Furthermore, it has to be pointed out that prior to design the network of sensors, the candidate locations (N_{loc}) have to be determined. In fact, the critical locations of the structures (based on the type of the structure) have to be identified and chosen as candidate

locations for installing the sensors. Given N_S sensors and N_{loc} locations, the total number of candidate configurations is given by

$$N_C = \binom{N_{loc}}{N_S} = \frac{(N_{loc})!}{(N_{loc} - N_S)!\,(N_S)!} \quad (29)$$

Therefore, for the first try the number of sensor (N_s) is equal to 2. For instance if the number of candidate locations (critical locations of the structure) is 10 then the possible number of configurations would be equal to 45. These networks are compared against each other based on the ROC curve. A better ROC curve means a better tradeoff between the probability of detection and the probability of false alarm.

In fact, if a given configuration results in a perfect ROC curve then we stop the search and select this configuration. However, if the performance can be further improved, then we increase N_s and the search process continues. This procedure is illustrated through the second phase of the algorithm in Figure 62. Having identified the optimized network, the matrices of raw data are generated and the underlying distributions of features are learnt (due to different damages) through the Monte-Carlo simulation which was described earlier.

Finally, in phase III we process the live SHM data and extract the features needed to classify the damage using hypothesis testing and the underlying distributions. This phase is conducted in real-time and the owner can be updated regarding the real-time performance of the infrastructure. Furthermore, in the case of damage, the relevant maintenance action is taken with the minimum possible delay.

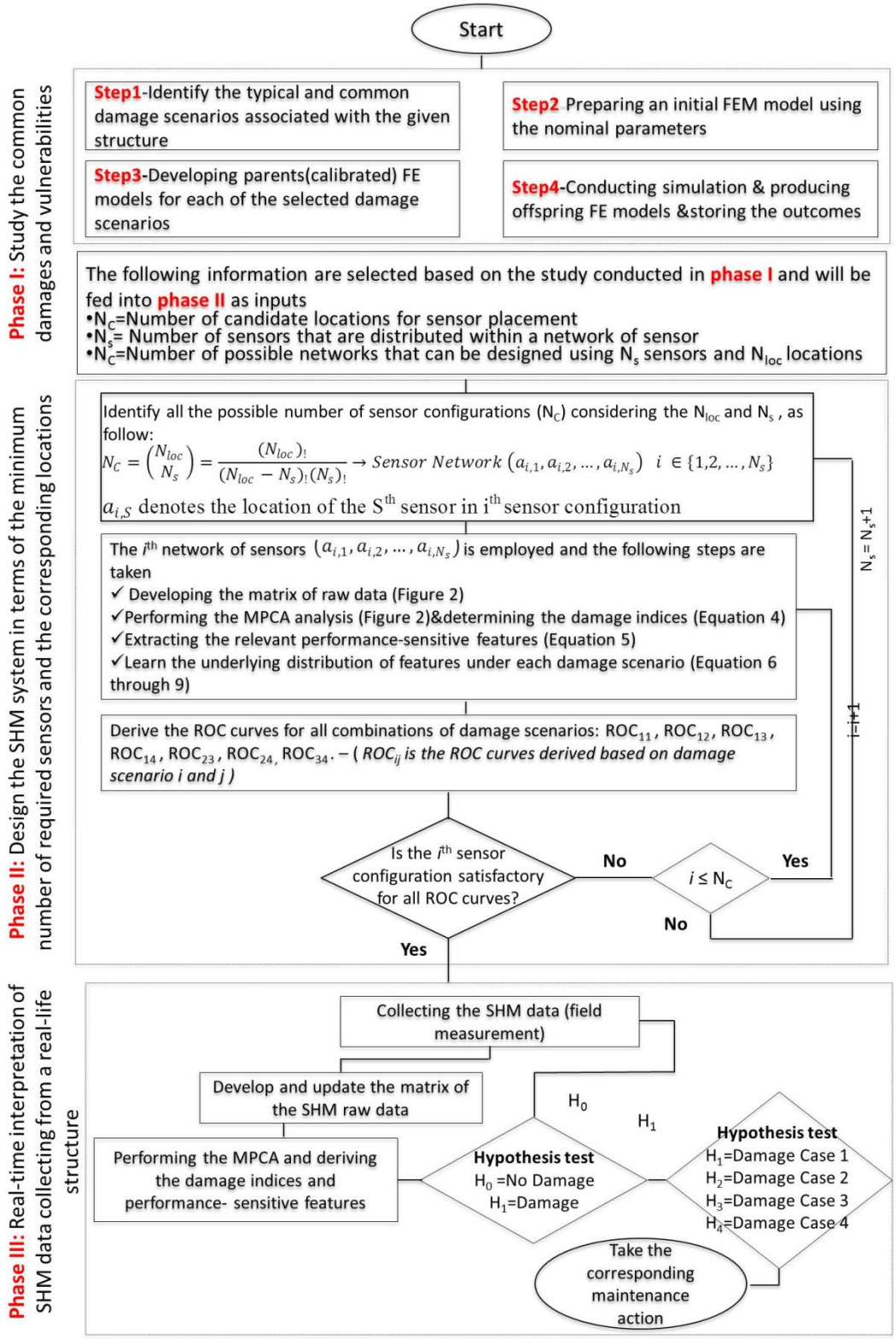

Figure 62: The proposed hybrid framework for continuous performance monitoring of civil infrastructure

7.5. Evaluation of the Proposed Approach through Comparison of the Experimental and Analytical Studies

7.5.1. Implemented Damage Scenarios

There are four damage scenarios that are considered for this study. Two cases (cases 1 and 2) are devoted to global type of damage by shifting from pinned to fixed or roller conditions or vice versa. Missing bolts and section stiffness reductions are also cases observed in existing bridges. The last two damage cases (Case 3 and case 4) are designed to simulate a mixed issue, namely the loss of connectivity between the girder and the deck as well as boundary deficiencies. The damage scenarios implemented in this study are demonstrated in Figure 63.

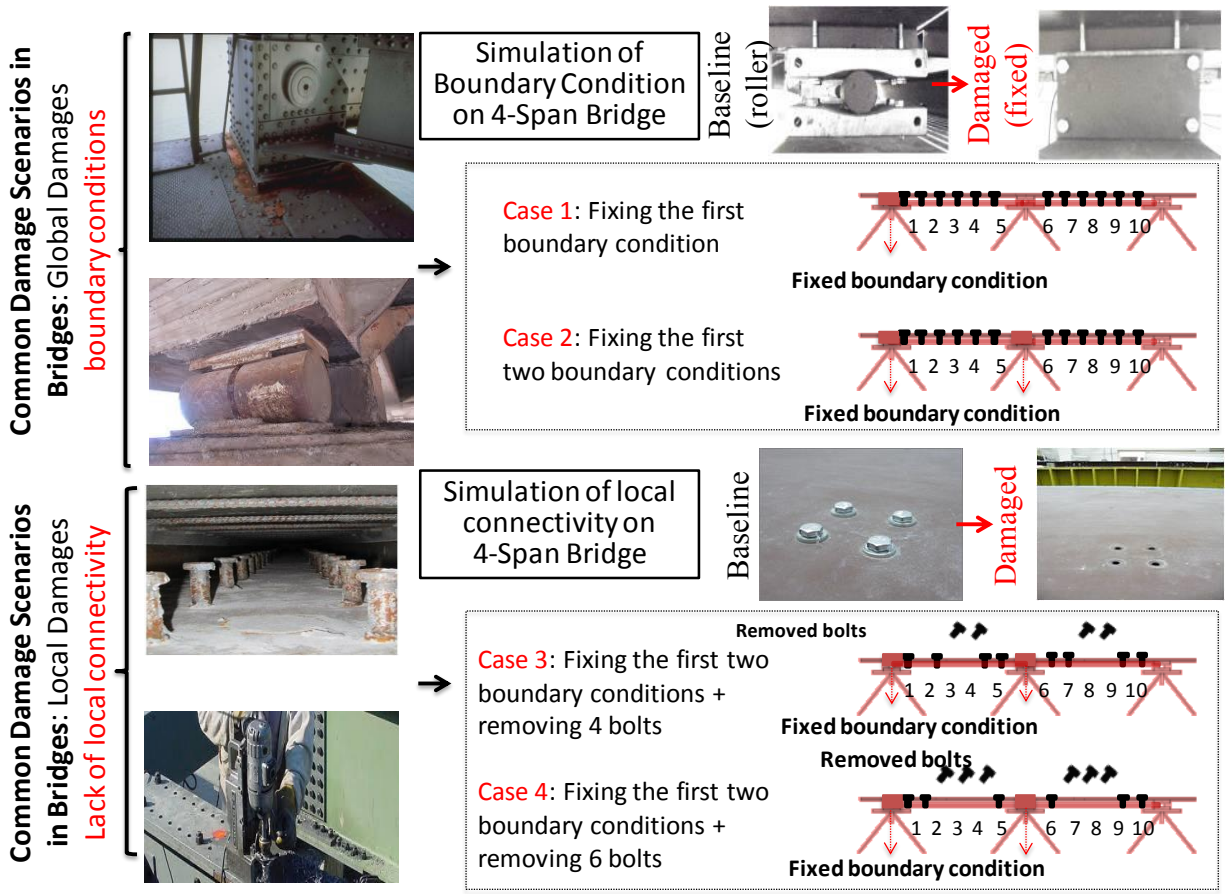

Figure 63: Implemented damage scenarios for 4-Span Bridge

7.5.2. Demonstration of the proposed hybrid framework

In this section, first the optimization of the network (Phase II of Figure 62) using the hybrid algorithm is demonstrated. Afterward, the efficiency of the algorithm in terms of assessing the performance of the structure is verified utilizing the SHM data collected from the 4-Span Bridge. Hence, the algorithm is implemented to design an optimized network of sensors for the 4-Span Bridge whereby the damages can be detected and effectively classified.

Thus, the first step (Phase I) as described in Figure 62 is to identify the critical damage scenarios associated with a given structure. The 4-Span Bridge is representative of a mid-span bridge and the corresponding critical damages were demonstrated in Figure 63. Before starting the try and error process of phase II to design the optimized network configuration, the candidate locations or critical regions of the structure (N_{loc}) are identified based on the positions and types of the implemented damage scenarios.

These candidate locations are the potential locations for installing the sensors. It should be also highlighted that optimizing the network in terms of locations and number of sensors will have a significant impact on the budget of the SHM project, in particular when it comes to large size civil infrastructures. With respect to the 4-Span Bridge, ten individual sections were initially selected as candidate positions to mount the FBG sensors shown in Table 2 (chapter 5).

Having selected the candidate locations, the objective is now to decide the minimum number of sensors that should be distributed over those locations so that the predefined objectives are met. The initial value for N_s (phase II of Figure 4) is 2 and as a consequence the number of possible network configurations is 45.

In order to pinpoint the optimized network (out of the 45 possible arrangements), one should identify which of the arrangements provides the most informative data to detect and classify the different abnormal behaviors. The designer requires a criterion whereby all the networks can be compared against each other and subsequently adopt the optimized configuration.

The benchmark which is utilized for this study is the ROC curve. An ROC curve is an efficient tool to visualize and assess the performance of a decision rule as it shows the tradeoff between the probability of detection and the probability of false alarm. If the ROC curves corresponding to different pairs of damage scenarios can be significantly improved, we increase the number of sensors and the process is repeated.

Herein, in order to visualize the consequences associated with miscalculation of sensor network design, three different types of designs are reviewed. The designs are categorized in three levels including unacceptable, poor or unsatisfactory and finally optimized. The first design that is being discussed here is an unacceptable design for the sensor network. This design, which is depicted in Figure 64, includes two sensors at locations 1 and 4. Additionally, the ROC curves corresponding to testing damage case 2 against 3 for all 45 networks are presented. As shown, the ROC curve for this design is fairly close to the 45 degree line indicating that this arrangement (locations 1 and 4) is unacceptable as it leads to an unfavorable tradeoff between the probability of detection and the probability of false alarm.

As it is also realized from Figure 64, the underlying distributions of the extracted performance-sensitive features for cases 2, 3 and 4 are almost indistinguishable, which leads to unfavorable tradeoff curves. However, the corresponding distribution of case 1 is still well

separated from other distributions. This is due to the fact that the level of induced damage in case 1 is much lower than the damage induced in cases 2, 3 and 4.

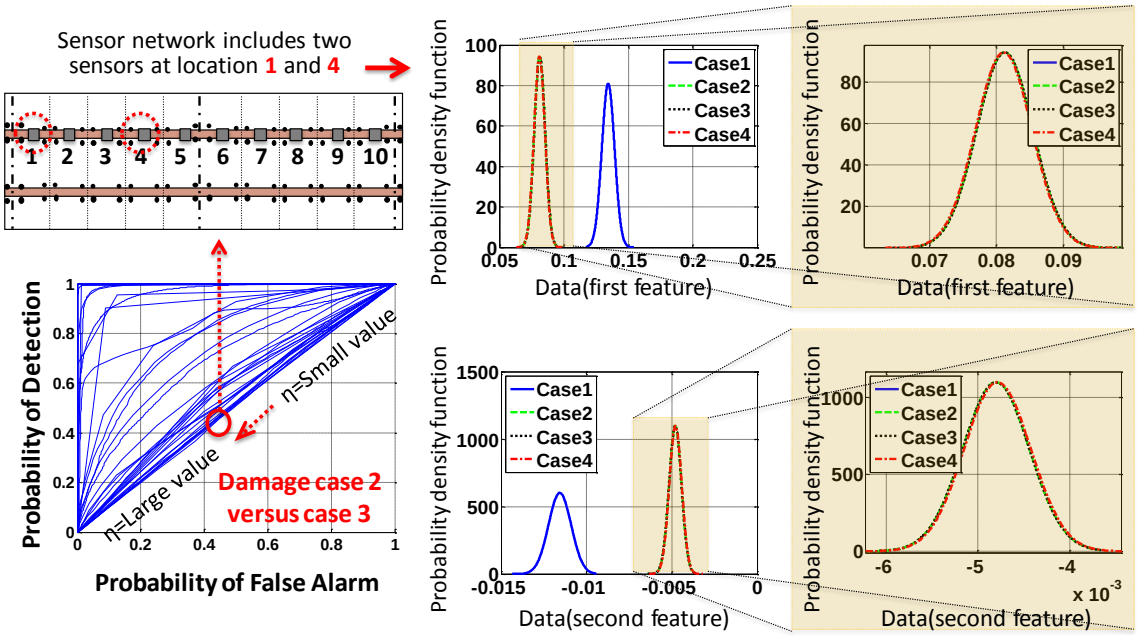

Figure 64: Unacceptable design of sensor network for the 4-Span Bridge

As shown in Figure 64 (right), the underlying distributions of the first and second performance-sensitive features for cases 2, 3 and 4 (shown in green, black and red, respectively) are indistinguishable. As mentioned earlier, this will lead to an unfavorable tradeoff curve which is almost diagonal as shown in Figure 64. The inseparability of the distributions is further shown in the zoomed plots (shown in yellow) in Figure 64 (right).

The second type of design is the one that is labeled as poor or unsatisfactory. The layouts as well as the related outcomes are shown in Figure 65. This design (one senor at location 3 and the other at location 7) is preferred over the first one (unacceptable type) because of having a better tradeoff curve, i.e., higher probability of detection for the same probability of false alarm. As it is clearly perceived from Figure 65, the underlying distributions for cases 1 and 4 are well

distinguishable in comparison to cases 2 and 3. This indicates that there is a significant risk of misclassification between cases 2 and 3 while the chance of misclassification is negligible when considering case 1 against case 4. Hence, it is concluded that while changing the arrangement of the sensors from the previous configuration could indeed lead to an improved tradeoff curve, it is still hard to distinguish between the underlying distributions of features for cases 2 and 3. The underlying distributions of the first and second performance-sensitive features for cases 1, 2, 3 and 4 are shown in Figure 65 in blue, green, black and red, respectively. The zoomed plots (highlighted in yellow) illustrate the corresponding distributions for cases 2 and 3. It is clear that it is quite impossible to distinguish between the distributions of the second feature for cases 2 and 3 while there is minor difference with respect to the distributions of the first feature.

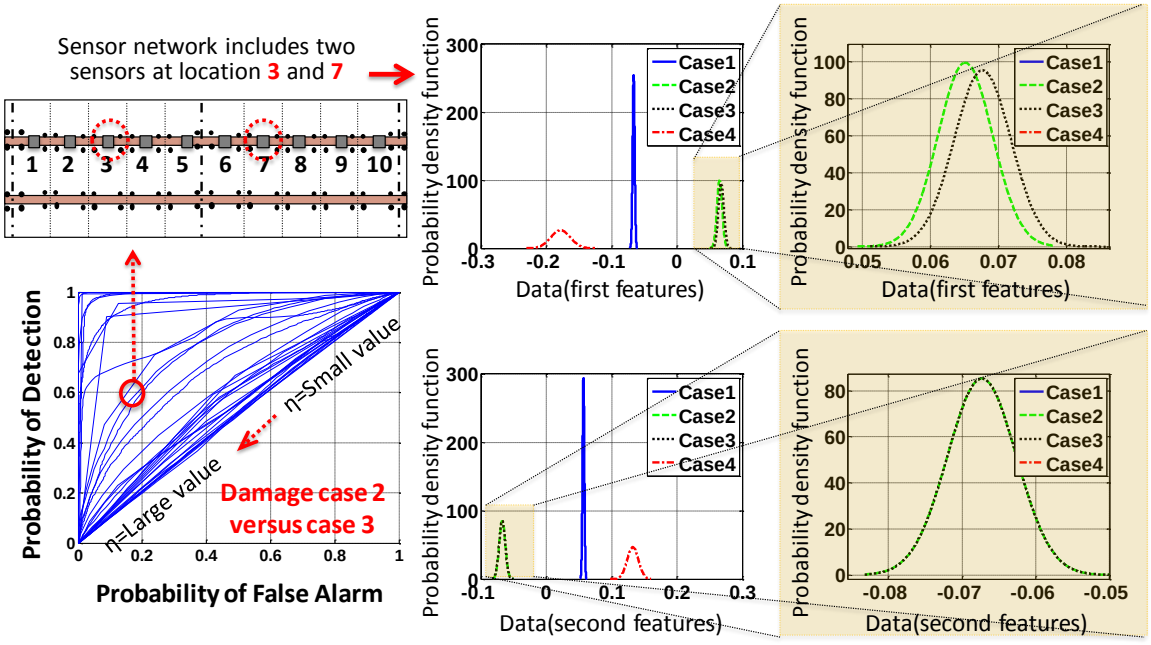

Figure 65: Poor or unsatisfactory design of sensor network for the 4-Span Bridge

Finally, an example of an optimized network, which includes two sensors at locations 2 and 8, is pictured in Figure 66. The associated ROC curve is almost similar to a right angle

curve, which demonstrates a favorable tradeoff between the detection and the false alarm probabilities. In this design, as shown in Figure 66, the underlying distributions of both features for cases 1, 2, 3 and 4 are well separated, which results in an almost perfect ROC curve. After discussing different examples of sensor network design, throughout the following sections, the ROC curves are studied with respect to their performance in classifying different binary combinations of the implemented damage scenarios.

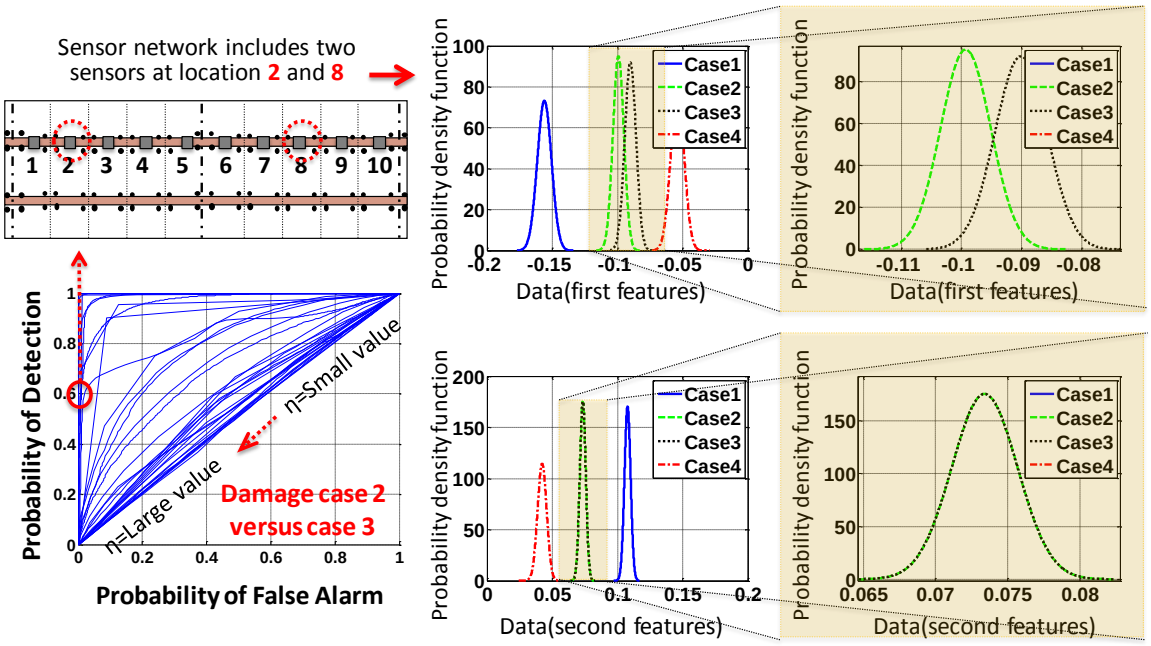

Figure 66: Optimized design of sensor network for the 4-Span Bridge

7.5.2.1. ROC curves for case 1 versus cases 2, 3 and 4

The underlying distributions of the performance-sensitive features associated with case 1 are clearly classifiable from the ones corresponding to case 2, case 3 and case 4. As a consequence, the relevant ROC curves, displayed in Figure 67, are all in right angle shape. This conveys the fact that as long as detecting and classifying case 1 from other cases is the only concern, no particular arrangement of sensors is required. Therefore, all the different sensor

configurations (45 arrangements) are acceptable because the associated probabilities of false alarm are insignificant. This can be also realized from column A in Table 4.

7.5.2.2. ROC curves for case 2 versus case 4

There are 17 individual configurations (17 out of 45) that can be implemented for detecting and differentiating between case 2 and case 4 (Figure 67). Column C in Table 4 shows the appropriate designs for this case.

7.5.2.3. ROC curves for case 3 versus case 4

Finally, there are 12 configurations, out of 45 possible designs, that are acceptable with respect to case 3 and case 4. These configurations are presented in Table 4 and column D. The difference of case 3 and 4 is in the number of the removed bolts where 4 bolts are removed for case 3 and 6 bolts for case 4.

7.5.3. Phase II: Optimized network of senor for the 4-Span Bridge

In previous sections the optimized networks of sensors were discussed for different binary combinations of damage scenarios. However, since the objective is to design a reliable network of sensors and a decision rule to distinguish among all damage scenarios, the selected sensor network should have a reliable performance in terms of all binary combinations of the implemented damages. In other words, the optimized network would be the one, which is common among all binary combinations in Table 4.

As concluded from Table 4, with respect to the 4-Span Bridge, there is only one optimized design or configuration (utilizing two sensors) that can meet this criterion.

Table 4: Performance of individual design of sensor networks with respect to different binary combinations of damage scenarios

NID: Network ID **NC**: Network Configuration **A**: Performance of network with respect to case 1 against all other cases **B**: Performance of network with respect to case 2 against 3 **C**: Performance of network with respect to case 2 against 4 **D**: Performance of network with respect to case 3 against 4 Configuration (a_1, a_2) indicates that one sensor is installed at location a_1 while the second one is installed at location a_2	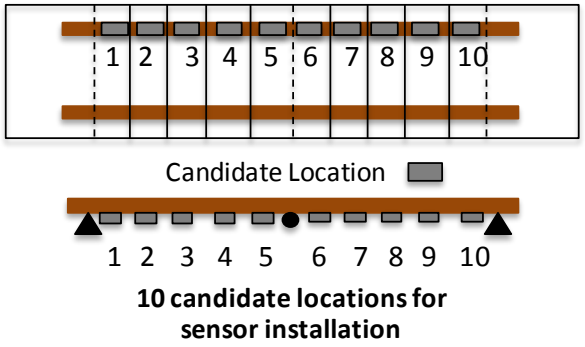

NID	NC	A	B	C	D	NID	NC	A	B	C	D
1	(1-2)	✓	×	×	×	24	(3-10)	✓	×	×	×
2	(1-3)	✓	×	×	×	25	(4-5)	✓	×	×	×
3	(1-4)	✓	×	×	×	26	(4-6)	✓	×	×	×
4	(1-5)	✓	×	×	×	27	(4-7)	✓	×	×	✓
5	(1-6)	✓	×	×	×	28	(4-8)	✓	×	×	×
6	(1-7)	✓	×	✓	✓	29	(4-9)	✓	×	×	×
7	(1-8)	✓	×	×	×	30	(4-10)	✓	×	×	×
8	(1-9)	✓	×	×	×	31	(5-6)	✓	×	×	×
9	(1-10)	✓	×	×	×	32	(5-7)	✓	×	✓	✓
10	(2-3)	✓	×	×	✓	33	(5-8)	✓	✓	✓	×
11	(2-4)	✓	×	✓	✓	34	(5-9)	✓	×	×	×
12	(2-5)	✓	×	✓	✓	35	(5-10)	✓	×	×	×
13	(2-6)	✓	×	✓	✓	36	(6-7)	✓	×	✓	✓
14	(2-7)	✓	×	✓	✓	37	(6-8)	✓	✓	✓	×
15	(2-8)	✓	✓	✓	✓	38	(6-9)	✓	×	×	×
16	(2-9)	✓	×	✓	✓	39	(6-10)	✓	×	×	×
17	(2-10)	✓	×	×	×	40	(7-8)	✓	×	×	×
18	(3-4)	✓	×	✓	×	41	(7-9)	✓	×	✓	✓
19	(3-5)	✓	×	✓	×	42	(7-10)	✓	×	×	×
20	(3-6)	✓	×	✓	×	43	(8-9)	✓	×	×	×
21	(3-7)	✓	×	✓	×	44	(8-10)	✓	×	×	×
22	(3-8)	✓	✓	✓	×	45	(9-10)	✓	×	×	×
23	(3-9)	✓	×	×	×	**(2-8) is the optimized network of sensor**					

The optimized design is achieved by positioning the first sensor at location 2 and the second sensor at location 8, as highlighted in Table 4. Thus, this arrangement is the only available option for a designer to distribute two sensors over the bridge in such a way that not only the critical and common abnormal behaviors are detected but also those can be classified appropriately. Other configurations will inevitably result in misclassification and may result in taking inappropriate maintenance actions. It is worth noting that since a reliable configuration for the studied damage scenarios was obtained using two sensors, we no longer need to consider a larger number of sensors.

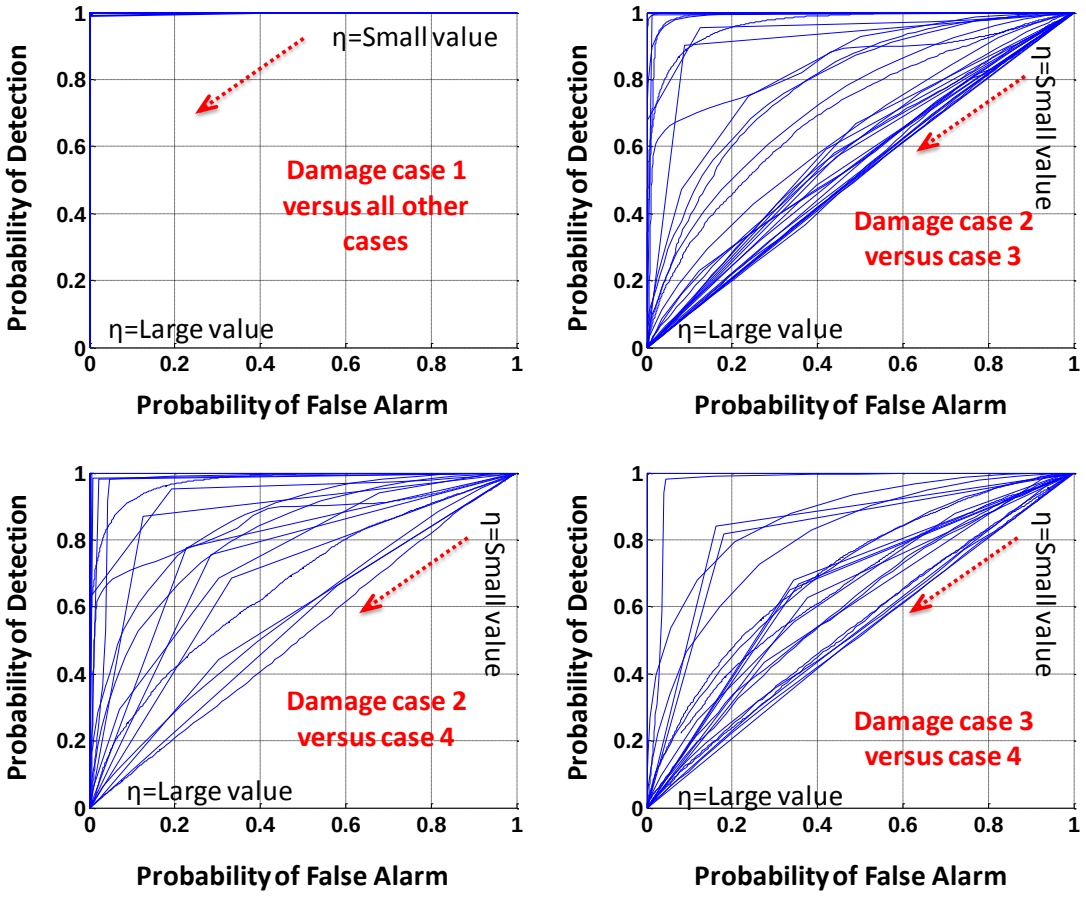

Figure 67: The corresponding ROC curves for individual binary combinations of implemented damages

7.5.4. Phase III: Real-time Interpretation of SHM Data

In the previous section (phase II of the algorithm) the optimized network configuration was designed. Implementing the optimized network and using the Monte-Carlo simulation, the underlying distributions of the performance-sensitive features under common damage scenarios are learnt. Once the distributions are learnt, new incoming live data can be effectively classified. Therefore, phase III is dedicated to real-time processing of the SHM data using statistical analysis and classifying the extracted features.

Having classified the new incoming features, the current status of the structure is revealed and subsequently the corresponding maintenance action can be taken in real-time. The proposed methodology is categorized as a supervised classification algorithm in the sense that initially the underlying distributions are learnt using a simulation study (phase I and II), then the new extracted features from live SHM data are classified using a statistical decision rule.

Therefore, for the training part (phase II and phase III), the FE model of the 4-span Bridge is utilized to simulate the selected damages. Monte-Carlo simulations are conducted to learn the responses of the 4-Span Bridge under common damages. In order to experimentally verify the proposed framework, in phase III an experimental study is designed and conducted to collect the SHM data from the 4-Span Bridge using the In-house developed FBG system. The data are captured under the same damage scenarios as were utilized in analytical phases I and II (training phase).

Moreover, in order to be consistent with the training phase, the 4-Span Bridge is instrumented with all possible design scenarios for the sensor network (45 different arrangements). The SHM data collected under different damages scenarios is then used in the

monitoring phase (phase III) in order to be interpret and classify the damage. The outcomes of the classifier (hypothesis testing) are presented in Figure 68 for individual scenarios. The horizontal axis indicates different designs of the sensor network (which were also shown in Table 4) and the vertical axis represents different damage scenarios.

It should be also noted that, the test was repeated 15 times for each configuration and damage scenario. However, since the outcomes of the classifier were very similar for all the repeated tests and also for visualization purpose, only the results corresponding to one of the test is presented in Figure 68.

The top left plot in Figure 68, presents the outcomes of the classification when the SHM data are captured under the first damage scenarios. As evidenced by this plot, regardless of the implemented network, there is not any misclassification in outcomes. The fact that there is no misclassification in this case is due to the difference in the level of the damage induced in this case compared to other scenarios.

As it was also shown in phase II (training phase), the underlying distribution of features extracted from this case is well separated from the ones associated with others cases, which ensures no misclassification. The experimental outcomes validate the analytical results presented in previous sections as both indicate negligible misclassification for case1.

However, the optimized network (2, 8), which was selected through phase II, exhibits faultless performance in the sense that there are no associated misclassifications. This shows that using the proposed methodology we are able to detect and classify the common damages and also design an optimized network of sensors with a minimum probability of misclassification.

7.6. Concluding Remarks

A hybrid framework is proposed in this study for continuous real-time performance assessment of a structure. The framework is hybrid in the sense that it integrates non-parametric and model-based data interpretation approaches. A supervised classification algorithm consisting of three phases, phase I (study phase), phase II (training phase) and finally phase III (monitoring phase) is proposed. During phase I, a comprehensive study is conducted on a given structure to decide the corresponding critical damage scenarios.

Upon identifying the corresponding damages scenarios, an FE model of the structure is developed to predict the relevant performance of the structure using Monte-Carlo simulations (phase II) under these different scenarios. In addition to detecting and classifying the damage, another objective is to optimize the number of sensors and their locations. Moving Principal Component Analysis (MPCA) is implemented to process and extract the corresponding performance-sensitive features for individual damage scenarios.

Then, we learn the underlying distributions of the extracted features to design a classifier based on multi-hypothesis testing. Throughout the third phase (the monitoring phase) features are extracted from live SHM data and fed into this classifier. The real-time classification of these features determines the current performance condition of the structure, which potentially leads to appropriate maintenance actions. The efficiency of the proposed methodology is verified through an experimental study on a 4-Span Bridge and the in-house developed FBG system.

The SHM data is generated under the same damage scenarios used in the analytical part, and fed into the third phase of the algorithm to study the classification performance of the proposed algorithm. The results are shown to be consistent with the results of the analytical

phase. The optimized sensor network configuration, which was designed through phase II, demonstrates perfect performance in terms for classifying the different damage scenarios.

CHAPTER EIGHT: CONCLUSIONS

8.1. Introduction

The main objective of this dissertation study is to investigate the utilization and efficiency of non-parametric data analysis methods for damage/change detection within the context of Structural Health Monitoring (SHM). In addition, a non-parametric data analysis method is extended in conjunction with a model-based method approach to alleviate some of the drawbacks of non-parametric data analysis methods. The main points covered in this study can be summarized as listed in the following:

1. Systematic comparison of selective non-parametric damage detection algorithms (RRA, MPCA, MCCA and CCA) utilizing in-house developed FBG sensing system along with the data analysis performance criteria by using experimental data from simulated damage scenarios.
2. Upon evaluation of the advantages and disadvantages of the selected algorithms, a new machine-learning based damage detection algorithm (MPCA-CCA) is designed and introduced in order to mitigate drawbacks associated with the existing algorithms. The efficiency of the proposed algorithm is subsequently evaluated and compared against the selected algorithms using both experimental and real-life SHM data.
3. Movable structures are a new class of structures with large scale mechanical and electrical component. In this study, an investigation is conducted in order to study the efficiency of the non-parametric techniques for long-term maintenance monitoring of mechanical components of a movable structure.

4. Finally a hybrid data interpretation framework is designed by integrating the non-parametric and parametric approaches for automated long-term performance assessment of structures and structural components.

In this context, a systematic comparison study is conducted between some of the most efficient non-parametric damage detection algorithms including CCA, RRA, MCCA and MPCA. The comparative study is conducted based on performance criteria including, detectability, time to detection, effect of noise and the required size of window. A unique experimental structure is used to generate the SHM data under different damage scenarios. This unique four span bridge model is phenomenologically representative of common highway bridges in terms of its static and dynamic response as well as its structural components and characteristics such as the deck, girders, composite action, boundary conditions etc. A number of damage conditions are simulated on the bridge model based on the feedback from bridge engineers. SHM data generated under operating traffic loading on the bridge model are analyzed to evaluate the efficiency of selected algorithms for the purpose of bridge monitoring implementations. Sensors and data acquisition are important and integral part of SHM. For the laboratory studies, Fiber Bragg Grating (FBG) sensors and a fiber optic interrogator developed in-house are employed for the experimental studies. Non-parametric and improved methods are discussed in a comparative fashion using the FBG data that are obtained from the study summarized above.

8.2. Conclusion

A new machine-learning based algorithm is designed in such a way that it can reduce some of the drawbacks associated with the existing non-parametric methods. The algorithm is developed by integrating the MPCA and MCCA techniques. The proposed algorithm is

evaluated utilizing the SHM data under common critical damage scenarios from both experimental and real-life study. The algorithm (MPCA-CCA) is compared with RRA, MCCA and MPCA with respect to the critical criteria. It is observed that MPCA-CCA (newly proposed algorithm) has the best performance in terms of detectability while the RRA algorithm outperforms other techniques with respect to time to detection. The MPCA-CCA is influenced by noise less than RRA, MCCA and MPCA. Also, MCCA and MPCA have almost the same performance regarding detectability and time to detection. However, when it comes to computational time, the MPCA-CCA has the highest required computational time while the RRA has the minimum required time. The noise has the most adverse effect on the RRA algorithm while MPCA-CCA has the least. It is also observed that, the MCCA requires less data set in order to establish the baseline condition in comparison to the MPCA algorithm.

As part of data analysis method evaluation, long-term SHM data from the Sunrise Bridge are used to further assess the performance of the newly developed algorithm. It is observed that while all the selected algorithm including RRA, MCCA, MPCA have failed to detect the common induced damages, MPCA-CCA algorithm could effectively detect all the critical damage scenarios. This emphasises the reliable performance of the newly designed algorithm (MPCA-CCA) for SHM applications.

In addition to the algorithms that have been studied and developed for structural health monitoring, a framework is introduced in order to facilitate the long-term maintenance condition monitoring of critical mechanical component of a movable bridge. A maintenance condition index is defined for identifying and tracking the critical maintenance issues. The efficiency of the maintenance condition index is then investigated and demonstrated against some of the

corresponding maintenance problems that have been visually and independently identified for the bridge.

It is realized that the developed condition index is reliable for detecting critical maintenance issues. It is also realized that the SHM system provides the opportunity to timely identify the abnormal behaviors which is very important for functionality of the movable bridge.

Finally, a hybrid data interpretation framework is designed and introduced for more effective long-term performance assessment of structures. The proposed framework is hybrid in the sense that it combines the benefits of both parametric and non-parametric approaches and attempts to mitigate their shortcomings. The proposed approach can then be employed not only to detect the damage but also to assess the identified abnormal behavior. As a side benefit with this approach, it is possible to determine the number of sensors and their corresponding locations required to effectively monitor a structure. In particular, the sensor network is optimized so that the collected information can be ultimately used in performance-based assessment.

The developed hybrid algorithm is a supervised classification algorithm consisting of three phases: Phase I (study phase), Phase II (training phase) and finally Phase III (monitoring phase). During Phase I, a comprehensive study is conducted on a given structure to decide the corresponding critical damage scenarios. Upon defining critical damages scenarios, FE models of the structure is developed to predict the relevant performance of the structure using Monte-Carlo simulations (Phase II) corresponding to these different damage scenarios. In addition to detecting and classifying the damage, the number of sensors and their locations are also optimized. Using the FE models, Moving Principal Component Analysis (MPCA) is

implemented to process and extract the corresponding performance-sensitive features for individual damage scenarios.

Consequently, the underlying distributions of the extracted features are established to design a classifier based on multi-hypothesis testing. Throughout the third phase (the monitoring phase), features are extracted from acquired SHM data and fed into this classifier. The real-time classification of these features determines the current performance condition of the structure, which potentially leads to appropriate maintenance actions as the non-parametric evaluation is linked to prior established damage conditions. The efficiency of the proposed methodology is verified with an experimental study on a 4-Span Bridge instrumented with in-house developed FBG system.

The SHM data is generated under the same damage scenarios used in the analytical study, and fed into the third phase of the algorithm to study the classification performance of the proposed algorithm. The results are shown to be consistent with the results of the analytical phase. The optimized sensor network configuration, which was designed in Phase II, demonstrates perfect performance in terms of classifying the different damage scenarios.

8.3. Recommendations

The newly introduced machine-learning-based algorithm (MPCA-CCA) is tested using both experimental and real-life SHM data; however, one immediate need for future research is to explore the efficiency of the algorithm in the presence of real life environmental effects. Although it can be expected that the additional correlation analysis on the time series of the eigenvectors can detect the abnormal behavior even in the presence of temperature effects, it

would have been an important to scientifically study such an influence. In addition, the new algorithm can be investigated for other types of infrastructure including pipeline, buildings, tunnel etc.

Moreover, the efficiency of the method can be improved by exploring the new nonparametric techniques to extract the damage indices as well as performance-sensitive features. Besides, nonlinear classification techniques can be implemented for classifying the extracted performance sensitive features in the case that the boundaries between feature clusters are not linearly separated.

LIST OF REFERENCES

[1].Aktan, A. E. Catbas, F. N., Grimmelsman, K. A. and Tsikos, C. J. (2000). "Issues in Infrastructure Health Monitoring for Management," *Journal of Engineering Mechanics*, ASCE, Vol. 126 (7), 711-724.

[2].Chang F. K. 1999 Structural Health Monitoring 2000 (Technomic)

[3].Puentes, R. (2008). "A Bridge to Somewhere: Rethinking American Transportation for the 21stCentury," Brookings Institute, Washington, DC.

[4].Glisic B. Inaudi D. and Casanova N. (2010) "SHM process as perceived through 350 projects," *in Smart Struct. Mater./NDE Symp*., San Diego, CA, p. 76480P.

[5].Brownjohn, J. M., S.-C. Tjin, G.-H. Tan and B.-L. Tan. (2004). "A Structural Health Monitoring Paradigm for Civil Infrastructure." *1st FIG International Symposium on Engineering Surveys for Construction Works and Structural Engineering*, Nottingham, UK.

[6].ISIS Canada, Guidelines for Structural Health Monitoring Canada, 2001.

[7].Sohn, H., C. R. Farrar, F. M. Hemez, D. D. Shunk, D. W. Stinemates and B. R. Nadler (2003). "A Review of Structural Health Monitoring Literature: 1996-2001", Los Alamos National Laboratory Report.

[8].Brownjohn, J. M., A. Zasso, G. A. Stephen and R. T. Severn (1995). "Analysis of Experimental Data from Wind-Induced Response of a Long Span Bridge." *Journal of Wind Engineering and Industrial Aerodynamics* 54/55: pp. 13-24.

[9].Aktan, A. E., D. N. Farhey, D. L. Brown, V. Dalal, A. J. Helmicki, V. J. Hunt and S. J. Shelley (1996). "Condition Assessment for Bridge Management." *Journal of Infrastructure Systems*, ASCE 2(3): 108-117.

[10].Enright, M. P. and D. M. Frangopol (1999). "Condition Prediction of Deteriorating Concrete Bridges Using Bayesian Updating." *Journal of Structural Engineering*, ASCE 125(10): 1118-1125.

[11].Federal Highway Administration (FHWA) (2008). "Deficient Bridges by State and Highway System."

[12].Hill KO, Fuji Y, Johnson DC, Kawasaki BS. (1978) "Photosensitivity in optical fiber waveguides: application to reflection fiber fabrication." *Appl Phys Lett* ;32(10):647–9.

[13].Meltz G, Morey W, Glenn W. (1989) "Formation of Bragg grating in optical fiber by the transverse holographic method." *Opt Lett*;14(15):823–5.

[14].Morey WW, Meltz G, GlennWH. (1989) "Fiber optic Bragg grating sensors." *SPIE*;1169:98–107.

[15].Melle S, Liu K, Measures RM. (1991) "Strain sensing using a fiber optic Bragg grating." *SPIE*;1588:255–63.

[16].Ferdinand P. Magne S. Marty-Dewynter V. Martinez C. Rougeault S. and Bugaud M. (1997) "Applications of Bragg grating sensors in Europe," *in Proc. 12th Int. Conf. Optical Fiber Sensors.*

[17].Vohra S.T., Todd M.D., Johnson G.A., Chang C.C. and Danver B.A. (1999) "Fiber Bragg grating sensor system for civil structure monitoring: applications and field tests." *Proc. 13th Int. Conf. Optical Fiber Sensors (Kyongju, Korea, 1999)* pp 32–7

[18].Todd M.D. Johnson G. A. Vohra S T. Chang C.C. Danver B. and Malsawma L. (1999) "Civil infrastructure monitoring with fiber Bragg grating sensor arrays." *2nd Int. Workshop on Structural Health Monitoring (Palo Alto, CA, 1999)*

[19].Todd M.D. Johnson G.A. and Chang C.C. (2000) "Real-time girder deflection reconstruction using a fiber Bragg grating system." *Proc. IMAC XVIII: a Conf. on Structural Dynamics.*

[20].Johnson G.A. Pran K. Wang G. Havsgård G.B. and Vohra S.T. (1999) "Structural monitoring of a composite hull air cushion catamaran with a multi-channel fiber Bragg grating sensor system." *Proc. 2nd Int. Workshop on Structural Health Monitoring (Palo Alto, CA, 1999)*

[21].E. Udd. (1995) "Fiber optic and smart structures", John Wiley & Sons, Wiley-Interscience, New-York .

[22].Inaudi D. (2002) "Photonic sensing technology in civil engineering applications" in "Handbook of optical fibre sensing technology", J. M. Lopez-Higuera editor, Wiley (2002).

[23].Worden K. (1997). "Structural fault detection using a novelty measure." *Journal of Sound and Vibration* 201(1): 85-101.

[24].Laory I. Trinh T. N. and Smith. I. F. C. (2011) "Evaluating two model-free data interpretation methods for measurements that are influenced by temperature." *Adv. Eng. Inform*. 25(3): 495-506.

[25].Robert-Nicoud Y., Raphael B., Smith I.F.C. (2005) "System Identification through model composition and stochastic search." *Journal of Computing in Civil Engineering* 19 (3) 239–247.

[26].Lanata F. (2005) "Damage detection algorithms for continuous static monitoring of structures" Ph.D. Thesis, Italy, University of Genoa DISEG .

[27].Worden K. and Dulieu-Barton J. M. (2004). "An Overview of Intelligent Fault Detection in Systems and Structures." *Structural Health Monitoring* 3(1): pp 85-98.

[27].Agbabian, M. S., Masri, S. F., Miller, R. K., and Caugher, T. K. (1990). "System identification approach to detection of structural changes." *ASCE Journal of Engineering Mechanics,* 117, 370-390.

[28].Aktan, A. E., Farhey, D. N., Helmicki, A. J., Brown, D. L., Hunt, V. J., Lee, K. L., and Levi, A. (1997). "Structural identification for condition assessment: Experimental arts." *Journal of Structural Engineering,* 123(12), 1674-1684.

[29].Aktan, A. E., Helmicki, A. J., and Hunt, V. J. (1998). "Issues in health-monitoring for intelligent infrastructure." *Smart Materials and Structures,* 7(5), 674-692.

[30].Biswas, M., Pandey, A. K., and Samman, M. M. (1989). "Diagnostic experimental spectral/Modal analysis of a highway bridge." *International Journal of Analytical and Experimental Modal Analysis,* 5(1), 33-42.

[31].Brownjohn, J. M. W., Dumanoglu, A. A., Sevem, R. T., and Taylor, C. (1987). "Ambient vibration measurements of the Humber suspension bridge and comparison with calculated characteristics." *Institution of Civil Engineers, Part 2,* 83, 561-600.

[32].Brownjohn, J. M. W. (2003). "Ambient vibration studies for system identification of tall buildings." *Earthquake Engineering and Structural Dynamics,* 32(1), 71- 95.

[33].Brownjohn, J. M. W., Moyo, P., Omenzetter, P., and Lu, Y. (2003). "Assessment of highway bridge upgrading by dynamic testing and finite element model updating." *ASCE Journal of Bridge Engineering,* 8(3), 162-172.

[34].Doebling, S. W., Farrar, C. R., and Prime, M. B. (1998). "A summary review of vibration-based damage identification methods." *Shock and Vibration Digest,* 30(2), 91-105.

[35].Douglas, B. M., and Reid, W. H. (1982). "Dynamic tests and system identification of bridges." *ASCE Journal of Structural Engineering,* 108(10), 2295-2312.

[36].Farrar, C. R., and Doebling, S. W. (1998). "Damage detection II: Field applications to large structures." *Proceedings of NATO Advanced Study Institute on Modal Analysis and Testing, Sesimbra, Portugal.*

[37].Fujino, Y., and Abe, M. (2002). "Vibration-based structural health monitoring of civil infrastructures." *First International Workshop on Structural Health Monitoring, ISIS, Winnipeg, Canada.*

[38].Hornbuckle, J., Mercurio, T., Howard, G., Ibanez, P., Smith, C. B., and Vasudevan, R. (1973). "Forced vibration tests and analyses of nuclear power plants." *Nuclear Engineering and Design,* 25(1), 51-93.

[39].Kou, J. W., and DeWolf, J. T. (1997). "Vibrational behavior of continuous span highway bridge - influencing variables." *ASCE Journal of Structural Engineering,* 123(3), 333-344.

[40].Maeck, J., and De Roeck, G. (2003). "Damage assessment using vibration analysis on the Z24-bridge." *Mechanical Systems and Signal Processing,* 17(1), 133-142.

[41].Natke, H. G., and Yao, J. T. P. (1986). "Research topics in structural identification." *3rd Conference on Dynamic Response of Structures, Los Angeles, CA.*

[42].Natke, H. G., and Yao, J. T. P. (1989). "System identification methods for fault detection and diagnosis." *Fifth International Conference on Structural Safety and Reliability, San Francisco, CA.*

[43].Stubbs, N., Kim, J. T., and Topole, K. (1992). "An efficient and robust algorithm for damage localization in offshore platforms." *10th ASCE Structures Congress, San Antonio, TX.*

[45].Teughels, A., and De Roeck, G. (2004). "Structural damage identification of the highway bridge Z24 by FE model updating." *Journal of Sound and Vibration,* 278(3), 589-610.

[46].Chang, C. C., Chang, T. Y. P., and Zhang, Q. W. (2001). "Ambient vibration of long-span cable-stayed bridge." *ASCE Journal of Bridge Engineering,* 6(1), 46- 53.

[47].Masri, S. F., Nakamura, M., Chassiakos, A. G., and Caughey, T. K. (1996). "Neural network approach to detection of changes in structural parameters." *Journal of Engineering Mechanics,* 122(4), 350-360.

[48].Nakamura, M., Masri, S. F., Chassiakos, A. G., and Caughey, T. K. (1998). "Method for nonparametric damage detection through the use of neural networks." *Earthquake Engineering and Structural Dynamics,* 27, 997-1010.

[49].Zapico, J. L., Gonzalez, M. P., and Worden, K. (2003). "Damage assessment using neural networks." *Mechanical Systems and Signal Processing,* 17(1), 119- 125.

[50].Al-Khalidy, A., Noori, M., Hou, Z., Yamamoto, S., Masuda, A., and Sone, A. (1997). "Health monitoring systems of linear structures using wavelet analysis." *International Workshop on Structural Health Monitoring,* Stanford University, Palo Alto, CA.

[51].Gurley, K., and Kareem, A. (1999). "Applications of wavelet transform in earthquake, wind and ocean engineering." *Engineering Structures,* 21(2), 149- 167.

[52].Hou, Z. K., Noori, M., and Amand, R. S. (2000). "Wavelet-based approach for structural damage detection." *ASCE Journal of Engineering Mechanics,* 126(7), 677-683.

[53].Kijewski, T., and Kareem, A. (2003). "Wavelet transforms for system identification in civil engineering." *Computer-Aided Civil and Infrastructure Engineering,* 18, 339-355.

[54].Andersen, P., and Kirkegaard, P. H. (1998). "Statistical damage detection of civil engineering structures using ARMAV models." *16th International Modal Analysis Conference,* Society of Experimental Mechanics, Santa Barbara, CA.

[55].Bodeux, J. B., and Golinval, J. C. (2001). "Application of ARMAV models to identification and damage detection of mechanical and civil engineering structures." *Smart Materials and Structures,* 10, 479-489.

[56].Shinozuka, M., and Ghanem, R. (1995). "Structural system identification II: Experimental validation." *ASCE Journal of Engineering Mechanics,* 121(2), 265- 273.

[57].Huang, N. E., and et al. (1998). "The empirical mode decomposition and the Hilbert spectrum for non-linear and non-stationary time series analysis." *Philosophical Transactions of the Royal Society of London, Series A, Mathematical and Physical Sciences,* 454, 903-995.

[58].Vincent, H. T., Hu, S. J., and Hou, Z. (1999). "Damage detection using empirical mode decomposition method and a comparison with wavelet analysis." *2nd International Workshop on Structural Health Monitoring,* Stanford University, Palo Alto, CA.

[59].Yang, J. N., Lei, Y., and Huang, N. E. (2001). "Damage identification of civil engineering structures using Hilbert-Huang transform." *3rd International Workshop on Structural Health Monitoring,* Stanford University, Palo Alto, CA.

[60].Berry, M. J. A. and G. Linoff (2000). "*Mastering data mining: the art and science of customer relationship management*." New York, *Wiley Computer Pub*.

[61].Ide, T., S. Papadimitriou and M. Vlachos (2007). "Computing correlation anomaly scores using stochastic nearest neighbors." *The 2007 Seventh IEEE International Conference on Data Mining*. Omaha NE, USA, IEEE**:** 523-528.

[62].Posenato, D., F. Lanata, D. Inaudi and I. F. C. Smith (2008). "Model-free data interpretation for continuous monitoring of complex structures." *Advanced Engineering Informatics* 22(1): 135-144.

[63].Laory, I., Trinh, T.N. and Smith, I.F.C. (2011) "Evaluating two model-free data interpretation methods for measurements that are influenced by temperature, *Advanced Engineering Informatics*, 25(3), 495-506.

[64].Posenato, D., P. Kripakaran, D. Inaudi and I. F. C. Smith (2010). "Methodologies for model-free data interpretation of civil engineering structures." *Computers & Structures* 88(7-8): 467-482.

[64].Bisby L.A. (2005) "An introduction to structural health monitoring." ISIS Educational Module 5.

[65].Cawley P. Adams R.D. (1979) "The location defects in structures from measurements natural frequencies." *Journal of Strain Analysis* 14 . 49–57.

[66].Douka, E. Doutridis E. Trochidis A. (2004) "Crack identification in plates using wavelet analysis." *Journal of Sound and Vibration* 270.279–295.

[67].Kim J.T. Ryu Y.S. Cho H.M. Strubbs N. (2003) "Damage identification in beam-type structures: frequency based method vs mode-shape method." *Engineering Structures* 25 .57–67.

[68].Hong J.C. Kim Y.Y. Lee H.C. Lee Y.W. (2002) "Damage detection using Lipschitz exponent estimated by wavelet transform: applications to vibration modes of beam,." *International Journal of Solid and Structures* 39.1803–1846.

[69].Messina A. (2004) "Detecting damage in beams through digital differentiator filters and continuous wavelet transform." *Journal of Sound and Vibration* 272.385–412.

[70].Rucka M. Wilde K. (2006) “Crack identification using wavelets on experimental static deflection profiles” *Engineering Structures* 28.279–288.

[71].Gentile A. Messina A. (2003) “On the continuous wavelet transforms applied to discrete vibration data for detecting open cracks in damaged beams.” *International Journal of Solid and Structures* 40.295–315.

[72].Lanata F. “Damage detection algorithms for continuous static monitoring of structures” Ph.D. Thesis, Italy, University of Genoa DISEG (2005).

[73].Saitta S. , Raphael B. Smith I.F.C. (2003), “Data mining techniques for improving the reliability of system identification.” *Advanced Engineering Informatics* 19 .289–298.

[74].Giles, I., Mondanos, M., Badcock, R., and Lloyd, P. (1999) “Distributed Optical Fibre Based Damage Detection in Composites,” *Sensory Phenomena and Measurement Instrumentation for Smart Structures and Materials, Proceedings of SPIE,* Vol. 3,670, pp. 311–321.

[75].Seim, J., Udd, E., Schulz, W., and Laylor, H. (1999) “Health Monitoring of an Oregon Historical Bridge with Fiber Grating Strain Sensors,” *Smart Structures and Materials 1999: Smart Systems for Bridges, Structures, and Highways, Proceedings of SPIE,* Vol. 3,671, pp. 128–134.

[76].Austin, T., Singh, M., Gregson, P., Dakin, J., and Powell, P. (1999) “Damage Assessment in Hybrid Laminates Using an Array of Embedded Fibre Optic Sensors,” *Smart Structures and Materials 1999: Smart Systems for Bridges, Structures, and Highways, Proceedings of SPIE,* Vol. 3,671, pp. 281–288.

[77].Takeda, N., Kosaka, T., and Ichiyama, T. (1999) “Detection of Transverse Cracks by Embedded Plastic Optical Fiber in FRP Laminates,” *Smart Structures and Materials 1999: Sensory Phenomena and Measurement Instrumentation for Smart Structures and Materials, Proceedings of SPIE,* Vol. 3,670, pp. 248–255.

[78].Gregory, O., Euler, W., Crisman, E., Mogawer, H., and Thomas, K. (1999) “Smart Optical Waveguide Sensors for Cumulative Damage Assessment,” *Smart Structures and Materials 1999: Smart Systems for Bridges, Structures, and Highways, Proceedings of SPIE,* Vol. 3,671, pp. 100–108.

[79].Furrow, P.C., Brown, R.T., and Mott, D.B. (2000) "Fiber Optic Health Monitoring System for Composite Bridge Decks," *Smart Structures and Materials 2000: Smart Systems for Bridges, Structures, and Highways, Proceedings of SPIE, Vol. 3,988, Newport Beach, California*, pp. 380–391.

[80].Kwon, I.B., Park, P., Huh, Y.H., Kim, D.J., Hong, S.H., Lee, D.C., Titin, C., and Moon, H. (2000) "Failure Detection of Reinforced Concrete Beams with Embedded Fiber Optic Michelson Sensors," *Smart Structures and Materials 2000: Smart Systems for Bridges, Structures, and Highways, Proceedings of SPIE*, Vol. 3,988, Newport Beach, California, pp. 400–411.

[81].Lloret, S., Inaudi, D., Glisic, B., Kronenberg, P., and Vurpillot, S. (2000) "Optical Set-Up Development for the Monitoring of Structural Dynamic Behavior Using SOFO Sensors," *Smart Structures and Materials 2000: Sensory Phenomena and Measurement Instrumentation, Proceedings of SPIE*, Vol. 3,986, pp. 199–205.

[82].Ansari,F.(2009) "Structural Health Monitoring with Fiber Optic Sensors." *Frontiers of Mechanical Engineering in China*, Vol.4, No.2, pp. 103-110.

[83].Kwon Il.B. Choi K.S. (2012) "Fiber optic sensors and their applications on structural health *monitoring* in South Korea." *International Conference on Optical Fiber Sensors.* Proceedings of SPIE Vol. 8421 (SPIE, Bellingham, WA 2012), 84210I.

[84].Lienhart, W. (2005) "Experimental investigation of the performance of the SOFO measurement system." *In Proc. 5 th International Workshop on Structural Health Monitoring* (pp. 1131-1138)

[85].Rytter, A. (1993) "Vibration based inspection of civil engineering structures." Ph.D. thesis, Department of Building Technology and Structural Engineering, University of Aalborg, Denmark.

[86].Balan, R. Daubechies I. and Vaishampayan V. (2000). "The analysis and design of windowed Fourier frame based multiple description source coding schemes." *IEEE Transactions on Information Theory* 46(7): 2491-2536.

[87].Moyo, P. and J. M. W. Brownjohn (2002). "Detection of anomalous structural behaviour using wavelet analysis." *Mechanical Systems and Signal Processing* 16(2-3): 429-445.

[88].Catbas, F. N., Gokce, H. B., Gul, M. (2011) "Non-parametric Analysis of Structural Health Monitoring Data for Identification and Localization of Changes: Concept, Lab and Real Life Studies." *Structural Health Monitoring*, 11(5)- 613-629.

[89].Andersen R. (2008) "Modern Methods for Robust Regression." *SAGE Publications, Inc*.

[90].Jajo N. (2005) "A review of robust regression and diagnostic procedures in linear regression." *Acta Mathematicae Applicatae Sinica (English Series)* 21 (2005) 209–224.

[91]. Kwon, I. B., Malekzadeh, M., Ma, Q., Gokce, H., Terrell, T. K., Fedotov, A., & Catbas, F. N. (2011). Fiber optic sensor installation for monitoring of 4 span model bridge in UCF. In *Rotating Machinery, Structural Health Monitoring, Shock and Vibration, Volume 5* (pp. 383-388). Springer New York.

[92]. Catbas, F. N., Malekzadeh, M., & Khuc, T. (2013). Movable Bridge Maintenance Monitoring.

[93]. Malekzadeh, M., Gul, M., & Catbas, F. N. (2012). Use of FBG Sensors to Detect Damage from Large Amount of Dynamic Measurements. In *Topics on the Dynamics of Civil Structures, Volume 1* (pp. 273-281). Springer New York.

[94]. Malekzadeh, M., Gul, M., & Catbas, F. N. (2013). Application of Multivariate Statistically Based Algorithms for Civil Structures Anomaly Detection. In *Topics in Dynamics of Civil Structures, Volume 4* (pp. 289-298). Springer New York.